INFORMATION TO USERS

This material was produced from a microfilm copy of the original document. While the most advanced technological means to photograph and reproduce this document have been used, the quality is heavily dependent upon the quality of the original submitted.

The following explanation of techniques is provided to help you understand markings or patterns which may appear on this reproduction.

1. The sign or "target" for pages apparently lacking from the document photographed is "Missing Page(s)". If it was possible to obtain the missing page(s) or section, they are spliced into the film along with adjacent pages. This may have necessitated cutting thru an image and duplicating adjacent pages to insure you complete continuity.

2. When an image on the film is obliterated with a large round black mark, it is an indication that the photographer suspected that the copy may have moved during exposure and thus cause a blurred image. You will find a good image of the page in the adjacent frame.

3. When a map, drawing or chart, etc., was part of the material being photographed the photographer followed a definite method in "sectioning" the material. It is customary to begin photoing at the upper left hand corner of a large sheet and to continue photoing from left to right in equal sections with a small overlap. If necessary, sectioning is continued again — beginning below the first row and continuing on until complete.

4. The majority of users indicate that the textual content is of greatest value, however, a somewhat higher quality reproduction could be made from "photographs" if essential to the understanding of the dissertation. Silver prints of "photographs" may be ordered at additional charge by writing the Order Department, giving the catalog number, title, author and specific pages you wish reproduced.

5. PLEASE NOTE: Some pages may have indistinct print. Filmed as received.

Xerox University Microfilms
300 North Zeeb Road
Ann Arbor, Michigan 48106

73-24,562

FINK, David Jordan, 1943-
THE KINETICS OF ENZYMES IMMOBILIZED IN SEMI-PERMEABLE MICROCAPSULES.

The University of Michigan, Ph.D., 1973
Engineering, chemical

University Microfilms, A XEROX Company, Ann Arbor, Michigan

THIS DISSERTATION HAS BEEN MICROFILMED EXACTLY AS RECEIVED.

THE KINETICS OF ENZYMES IMMOBILIZED IN SEMI-PERMEABLE MICROCAPSULES

by

David Jordan Fink

A dissertation submitted in partial fulfillment
of the requirements for the degree of
Doctor of Philosophy
(Chemical Engineering)
in The University of Michigan
1973

Doctoral Committee:

Professor Jerome S. Schultz, Chairman
Professor Minor J. Coon
Professor Rane L. Curl
Associate Professor Joe D. Goddard
Professor William I. Higuchi

To Karen Ann Fink

ACKNOWLEDGMENTS

The author gratefully acknowledges the contributions of many persons who have contributed to this investigation.

The guidance of Professor Jerome S. Schultz, chairman of the doctoral committee, was especially helpful. His wide range of experience and interests serve as an appropriate model for his students. The other members of the doctoral committee, Professors Minor J. Coon, Rane L. Curl, Joe D. Goddard, and William I. Higuchi, have also shown an active interest in this study.

The help of the author's many friends among the faculty, staff, and students of The Department of Chemical Engineering has always been appreciated. The many discussions with Dr. George T. S. Chen, Dr. Shyam R. Suchdeo, and Mr. William H. Talbott have been particularly useful. The patient assistance of Miss Sandee Thomson in the preparation of the manuscript was also most helpful.

The financial assistance given by the National Science Foundation and the Shell Oil Company and the reagents supplied by the Phillips Petroleum Company were significant contributions to this effort.

Finally, the understanding and encouragement of the author's wife and parents can never be repaid.

TABLE OF CONTENTS

		Page
DEDICATION		ii
ACKNOWLEDGMENTS		iii
LIST OF TABLES		viii
LIST OF FIGURES		ix
NOMENCLAUTRE		xi
ABSTRACT		xv
I.	INTRODUCTION	1
II.	OBJECTIVES AND SCOPE OF THIS STUDY	4
III.	LITERATURE REVIEW	7
	1. The Production and Behavior of Immobilized Enzymes	7
	A. Production Techniques	8
	B. The Stability of Immobilized Enzymes	10
	C. Factors Affecting The Kinetic Behavior of Immobilized Enzymes	11
	2. The Properties of Trypsin and Trypsin Derivatives	13
	A. Soluble Trypsin	13
	B. Tryptic Assays	15
	C. Insoluble Trypsin -- Preparation	20
	D. Insoluble Trypsin -- Behavior	25
	3. Microencapsulated Enzymes	33
	A. Microencapsulated Enzymes -- Preparation and Applications	34
	B. Microencapsulated Enzymes -- Kinetic Properties	37
	4. Immobilized Enzyme Reactor Kinetics	44
	A. Batch Reactor	44
	B. Continuous-feed, Stirred Tank Reactor	47
	C. Fixed-bed Reactor	48

Page

5. Interpretation of Kinetic Data -- Nonlinear Regression Analysis 49

IV. THE KINETICS OF SUBSTRATE CONVERSION BY IMMOBILIZED ENZYME SOLUTIONS 51

1. Problem Description 52

2. Numerical Solution of the Steady-state Kinetic Equations 59

A. Numerical Computation Procedure 59

B. Generalized Effectiveness Factor Charts 61

3. Semi-analytical Solutions of the Steady-state Kinetic Equations 66

A. First-Order Reaction Rate Approximation 66

B. Zero-Order Reaction Rate Approximation 67

C. Constant Average Reaction Rate Approximation 68

D. Approximate Solution For Constant Average Reaction Rate 70

4. Perturbation Solutions for Low and High Steady-state Reaction Rates 71

A. Regular Perturbation Solution for Large ϵ 71

B. Singular Perturbation Solution for Small ϵ 76

5. Discussion of the Steady-state Models 80

A. Comparison of the Models 80

B. Generalization to Other Geometries 93

C. Effect of Electrostatic Membrane Charges on the Kinetics of Substrate Conversion 93

6. Unsteady-state Kinetics 96

Page

V. EXPERIMENTAL METHODS 100

1. Preparation of Microcapsules 100

2. Assay of Tryptic Esterase Activity 101

A. Continuous (Steady-state) Assay Procedure 102

B. Batch Assay Procedure 103

C. Determination of Microcapsule Size Distributions 106

3. Properties of the Capsules 107

4. Performance of the Batch Assay Procedure 107

VI. EXPERIMENTAL RESULTS AND DISCUSSION 118

1. Thermal Stability 118

2. Adsorption of Trypsin onto Microcapsule Membranes 126

3. Temperature Effects 131

4. pH Effects 133

5. Microcapsule Membrane Permeability Studies 135

6. Capsule Diameter and Enzyme Loading Effects 140

7. Estimation of Effectiveness Factors by Breaking Capsules 145

8. Prediction of Kinetic Parameters From Batch Reaction Rates 148

9. General Discussion 160

VII. SUMMARY AND CONCLUSIONS 164

APPENDIX A. GENERALIZED INTERNAL EFFECTIVENESS FACTOR CHARTS FOR PLANAR AND CYLINDRICALLY ENCAPSULATED ENZYMES 170

APPENDIX B. GENERALIZED OVERALL EFFECTIVENESS FACTOR CHARTS FOR PLANAR AND CYLINDRICALLY ENCAPSULATED ENZYMES 173

Page

APPENDIX C. REGULAR PERTURBATION SOLUTIONS FOR STEADY-STATE KINETICS 176

APPENDIX D. SINGULAR PERTURBATION SOLUTIONS FOR STEADY-STATE KINETICS 182

BIBLIOGRAPHY 187

LIST OF TABLES

Table		Page
1	Specificity and Kinetic Constants for BAEE and TAME.	18
2	Light Absorption Data for BAEE and TAME.	18
3	Values of K_m for BAEE.	19
4	Values of K'_m for Trypsin Immobilized on the Inner Wall of Hollow Nylon Tubes [74].	26
5	Steric Hindrance of Immobilized Trypsin Reactions.	28
6	Approximate Half-life, $t_{1/2}$, of Active MEC-Catalase As Calculated From Chang's Data [29].	36
7	Nylon Microcapsules: Permeability Data.	38
8	Kinetic Data of Boguslaski and Janik [19] for Nylon-MEC-Bovine Carbonic Anhydrase (BCA).	40
9	"Effect of Concentration of Asparaginase on Microencapsulation" as Reported by Mori et al. [104].	40
10	Summary of Substrate Conversion Models For Encapsulated Enzymes.	81
11	Estimated Time to Reach 99% Of The Steady-State $\overline{c_{is}}$.	99
12	Properties Of The Batches Of Microcapsules.	108
13	Calibration Of The Thrombocytocrit Measurement Of V_c.	112
14	Comparison Of BAEE Assays For Water-Equilibrated Microcapsules.	117
15	Summary Of Results For Adsorption Of Trypsin Onto The Outside Of Nylon Microcapsules.	128
16	Effectiveness Factors From Assays Of Ultrasonically Broken And Whole Capsules.	148

LIST OF FIGURES

Figure		Page
1	Schematic Representation of a Micro-encapsulated Enzyme Reaction.	2
2	Typical Substrate Concentration Profile In Model Capsule.	53
3	Generalized Internal Effectiveness Factor Chart, Spherically Encapsulated Enzymes.	62
4	Generalized Overall Effectiveness Factor Chart, Spherically Encapsulated Enzymes.	63
5	Schematic Interpretation of Reaction Rate Approximations For Models 1, 2, 3, and 4.	83
6	Locus Of Points For Which Model 1 Is Within 5% Of The Michaelis-Menten Kinetics Reaction Rate.	85
7	Average Reaction Rate Interpretation For Model 3.	86
8	Illustration Of The Regions Of Validity For The Substrate Conversion Models Given In Table 10.	92
9	Continuous Assay System.	103
10	Photographs Of Typical Batches Of Nylon-MEC Trypsin.	109
11	Typical Batch Reaction Assay.	110
12	Capsule Volume-Activity Dependence For Batch Assay Technique.	115
13	Storage Stability Of Free-Solution Trypsin.	120
14	Storage Stability Of Microencapsulated Trypsin, 100% = Initial Encapsulated Activity.	121
15	Storage Stability Of Microencapsulated Trypsin, 100% = Initial Apparent Activity.	122
16	Storage Stability Of Broken Capsule Membrane Enzyme Activity.	124

Figure		Page
17	Effect Of Temperature On Free-Trypsin And MEC-Trypsin Reaction Rates.	132
18	Effect Of pH On Free-Trypsin And MEC-Trypsin Reaction Rates.	134
19	Efflux Of BAEE From Trypsin-Free Microcapsules.	137
20	Effects Of Capsule Diameter And Enzyme Loading On "Apparent" Microencapsulated Activity.	141
21	Retention Of Activity Of Ultrasonically Irradiated Trypsin Solution.	147
22.	Typical Batch Reaction Data For Complete Conversion Of 1mM Substrate Solution In 3 ml Reactor.	150
23.	Concentration-Reaction Rate and Lineweaver-Burk Plots For Batch 10 MEC-Trypsin Reaction.	153
24.	Concentration-Reaction Rate and Lineweaver-Burk Plots For Batch 13-1 MEC-Trypsin Reaction.	154
25.	"Best Fit" Kinetic Parameters Computed From Batch Reactions Using Batch 13-1 Capsules.	157
A-1.	Generalized Internal Effectiveness Factor Chart For Enzymes Encapsulated In Planar Membranes.	171
A-2.	Generalized Internal Effectiveness Factor Chart For Enzymes Encapsulated in Cylindrical Membranes.	172
B-1.	Generalized Overall Effectiveness Factor Chart For Enzymes Encapsulated In Planar Membranes.	174
B-2.	Generalized Overall Effectiveness Factor Chart For Enzymes Encapsulated in Cylindrical Membranes.	175

NOMENCLATURE

a	Substrate activity
A	Transformation parameter
A_{r_o}	Capsule area at r_o, [cm^2]
c	Dimensionless substrate concentration
c^*	Transformed dimensionless substrate concentration
c'	Dimensionless concentration at $r = r_o$
c_{is}	Internal substrate concentration, [mM]
$\overline{c_{is}}$	Average internal substrate concentration, [mM]
c'_{is}	Substrate concentration at $r = r_o$, [mM]
c_{iI}	Inhibitor substrate concentration, [mM]
c'_{es}	Substrate concentration at $r = R_o$, [mM]
c_{so}	Bulk substrate concentration, [mM]
d	Average batch capsule diameter, [μ]
d_{32}	Sauter mean diameter, [μ]
D_{is}	Substrate diffusivity coefficient inside capsule, [cm^2/sec]
e	Electronic charge
E_t	Total enzyme concentration, [μM]
F	Faraday constant
h_e, h_i	External and internal partition coefficient
H	Product of h_e and h_i
k_e	External film mass transfer coefficient, [cm/sec]
k_{cat}	Substrate turnover number for enzyme, [μmoles substrate/min/unit enzyme]

k_1, k_{-1}, k_2	Reaction rate constants in Michaelis-Menten mechanism
k_v	Intrinsic reaction rate constant defined by Satterfield [122]
K	System Michaelis-Menten constant, [mM]
K_m	Enzyme Michaelis-Menten constant, [mM]
K'_m	Apparent enzyme Michaelis-Menten constant, [mM]
K_I	Equilibrium constant for inhibitor-enzyme complex
L	Length of reactor bed, [cm]
m	Order of reaction
N_s	Flux of substrate into the cell, defined at $r = r_o$ [μmoles/cm^2/sec]
p	Geometric factor indicating planar, cylindrical, or spherical coordinates
P	Combined external film and membrane mass transfer (permeability) coefficient, [cm/sec]
P_s	Membrane permeability coefficient, [cm/sec]
q	Average reaction rate, [μmoles/cm^3/min]
Q	Flow rate of substrate solution through reactor, [ml/min]
r	Radial distance, [cm]
r_o, R_o, R_∞	Radii of inner membrane surface, outer membrane surface, and "bulk" solution from center of capsule, [cm]
R	Universal gas constant
t	Time of reaction, [min]
$t_{1/2}$	Activity half-life of enzyme, [days]
T	Absolute temperature
v_s	Local reaction rate, [μmoles/cm^3/min]

v_{es}	Externally observed reaction rate (from outside of capsule), [μmoles/cm^3/min]
V	Volume of reactor excluding capsules, [cm^3]
V_c	Volume of capsules in reactor, [cm^3]
V_{max}	Maximum possible rate of enzyme-catalyzed reaction, [μmoles/cm^3/min]
x	Dimensionless radial coordinate
z	Ionic valence
α	Sherwood Number for membrane transport
β	Damköhler Number for enzyme phase
γ	Reciprocal Damköhler Number for membrane transport
δ	Thickness of external unstirred layer
$\Delta\epsilon$	Extinction coefficient difference, product minus substrate
$\Delta\rho$	Density difference, particle minus liquid
ϵ	Perturbation parameter
η_E	External (diffusion only) effectiveness factor
η_I	Internal (reaction) effectiveness factor
η_o	Overall effectiveness factor
κ	Dimensionless Michaelis-Menten constant
λ	Perturbation solution reaction rate term
Λ	Dimensionless reciprocal mass transfer coefficient, model 3
Λ_s	Reciprocal mass transfer coefficient, model 3

ξ	"Stretched" radial coordinate, singular perturbation solution
ρ	Reaction rate expressed as fraction of V_{max}
σ	Standard deviation of capsule diameters, normal distribution
ϕ	Thiele Modulus
ψ	Electrostatic potential in charged carrier

ABSTRACT

THE KINETICS OF ENZYMES IMMOBILIZED IN SEMI-PERMEABLE MICROCAPSULES

by

David Jordan Fink

Chairman: Jerome S. Schultz

In recent years, the production of enzymes immobilized on or in solid matrices has led to catalysts which are better suited for many applications than the corresponding free enzymes. The properties and kinetic behavior of enzymes rendered insoluble by microencapsulation are investigated in this report.

The microencapsulation process involves the entrapment of enzyme solutions inside hollow, semi-permeable, spherical membranes. Small substrate molecules can diffuse into the capsules to react with the enzyme but the larger enzyme molecules cannot escape.

The microencapsulated enzyme system was mathematically modelled as a homogeneous, catalytic inner phase surrounded by a semipermeable membrane and external unstirred liquid layer. Analytical solutions of the general diffusion-reaction equations could not be obtained for the case of Michaelis-Menten enzyme kinetics. Numerical solutions were generated for the general steady-state equations and used in the preparation of generalized effectiveness factor charts for this system. Semi-analytical solutions were derived by assuming the limiting conditions for the reaction kinetics, by assuming an average reaction rate, and by regular and singular perturbation techniques. The range of kinetic parameters for which these solutions are valid was determined by comparison with numerical computations.

Nylon-microencapsulated-enzyme solutions were prepared by the interfacial polymerization method of Chang et al. [Can. J. Physiol. Pharmacol. 44, 115 (1966)]. Trypsin was used as the model enzyme and two esters of arginine were the model substrates.

Microcapsules prepared by the interfacial polymerization technique were found to be easily broken when assayed in continuous stirred tank reactors. A simple batch assay was therefore employed in which the capsules were stirred only occasionally in the spectrophotometer cell.

Microencapsulated trypsin was more stable upon storage in distilled water than the free enzyme. At 37° C, the microencapsulated enzyme denatured at two rates: an initial rate similar to the free enzyme denaturation rate and a much lower long-term rate. At 4°C, microencapsulated trypsin lost little activity over several months of storage.

The microencapsulated enzyme had a higher apparent energy of activation (11.8 - 13.0 kcal/gmole) than free trypsin (9.5kcal/gmole) for the ester hydrolysis reaction and the pH optimum was shifted about 1/2 pH unit to higher pH for microencapsulated trypsin.

It was concluded that the differences in stability, activation energy, and pH optimum are due to the adsorption of the enzyme to the capsule membrane. Studies using microcapsule ghosts and the adsorption of enzyme to the outside of enzyme-free capsules support this conclusion.

The combined membrane-external film mass transfer coefficient for the substrate was estimated to be: $2\text{-}5 \times 10^{-5}$ cm/sec from mass transport studies in the absence of reaction; $1\text{-}7 \times 10^{-4}$ cm/sec from attempts to fit semi-analytical models to experimentally observed initial reaction rate data assuming 100% of the original

enzyme remained active; and 3×10^{-3} cm/sec from batch reaction studies in which an "apparent" Michaelis constant, estimated from the integrated Michaelis-Menten kinetics, was related to the free enzyme Michaelis constant by one of the semi-analytical models. The cause of the disparity in the estimates of the mass transfer coefficient, also observed by other investigators, is not known.

The overall effectiveness factor for the microencapsulated enzyme system was generally greater than 0.4, based on ultrasonic breakage of the capsules, which is consistent with a membrane-external film permeability greater than 1×10^{-4} cm/sec. The yield of active encapsulated enzyme was from 60-100%.

I. INTRODUCTION

In the last decade, many different procedures have been developed for producing immobilized enzymes. These protein molecules which serve as biological catalysts have been covalently attached, adsorbed, and cross-linked to organic and inorganic supports, entrapped in gel matrices, and encapsulated in hollow cylinders and spheres. Enzyme derivatives produced by the above processes are referred to as "immobilized" or "insolubilized" since the enzyme is physically constrained to move with the solid material with which it is associated.

Generally speaking, insolubilized enzymes are desired to permit reuse of high-priced, purified enzymes, to increase their storage stability, and to change the apparent enzymatic properties. Furthermore, enzymes which are in the vicinity of solid surfaces are thought to give a better model of the manner in which many enzymes actually behave in vivo than do the enzymes in free solution. Unfortunately, the immobilization techniques available at this time often lead to significant losses of enzymatic activity. At the same time, the rate of substrate conversion by the catalyst can be greatly reduced by mass transfer limitations outside or inside the solid matrix. All of these factors are important considerations when an immobilized enzyme system is characterized.

The system to be discussed in this study is that of nylon microencapsulated trypsin solutions (abbreviated hereafter as nylon-MEC-trypsin [130]). As indicated in Figure 1, thin, spherical, semi-permeable nylon membranes enclose aqueous trypsin solutions. The membranes have small enough pore structures to effectively block passage of the enzyme out of the capsules. Smaller substrate molecules (S), however, are able to enter the capsules to react with the enzyme and product (P) can leave the cells.

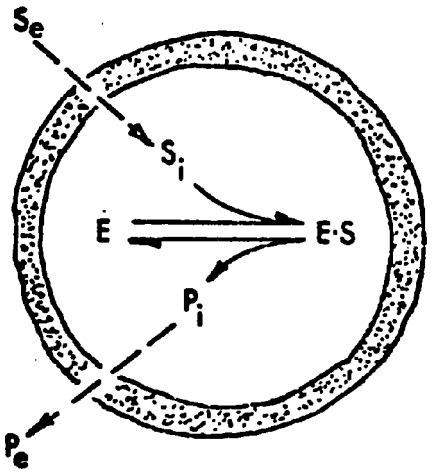

Figure 1. Schematic Representation Of A Microencapsulated Enzyme Reaction

From an engineering point of view, this system can be thought of as a heterogeneous catalyst particle possessing a localized mass transfer barrier (the membrane) and a catalytic inner phase. From a biological viewpoint, this is perhaps the simplest model of a living cell. The "cell" draws substrate molecules across the simple membrane, utilizes the substrate in a one-reaction step, and then expels the reaction products, without the complicating factors of reproduction or growth.

When considered as possible industrial or pharmaceutical catalysts, MEC enzymes appear to possess the following desirable attributes:

1. High catalyst loading capacity - the solubility of the enzyme is the theoretical upper limit;
2. Reduced diffusion resistance inside the catalyst particle;
3. High membrane area/catalyst volume ratio;
4. Possibility of encapsulating other materials along with the enzyme(s);

5. Ability to produce thin, high-flux membranes;
6. Ability to vary the properties of the membrane and the size of the capsules;
7. Improved economics of immobilization since fewer materials are required than for many other techniques.

On the other hand, the following possibilities tend to limit the utility of MEC-enzymes:

1. Activity loss during encapsulation;
2. Capsule breakage during use;
3. Thick, strong membranes reduce breakage but increase diffusion resistance;
4. Membrane porosity may limit reactions to small substrates;
5. Possibility of enzyme leakage from capsule;
6. Interaction of the membrane with the external solution.

Trypsin was selected for this study for many reasons. The enzyme is well characterized as it exists in solution and has been successfully immobilized by more procedures than perhaps any other enzyme. Denaturation of the enzyme can proceed by autodigestion; increases in stability due to the process of immobilization should be easily recognized. The proteolytic enzymes are useful analytical and industrial catalysts. Finally, several small substrates for trypsin are known which obey the classic Michaelis-Menten reaction kinetics, thus serving as good model substrates.

This study was undertaken in an attempt to characterize the MEC-trypsin system with consideration given to many of the factors discussed above. The results of this work should not only add to the knowledge of the behavior of immobilized trypsin and MEC-enzymes, but also prove generally useful in analyzing complex immobilized enzyme kinetics.

II. OBJECTIVES AND SCOPE OF THIS STUDY

The original objectives of this work were stated to be: (1) to determine the effect of the encapsulation process on trypsin; (2) to determine the catalytic behavior of trypsin in the MEC form and show how this differs from the free-solution enzyme; and (3) to develop and verify mathematical models for this simple system that might be applicable to more complex biological systems.

Consideration of the extent to which mass transfer rates can "diguise" (as Wei [143] terms it) the true enzyme kinetics leads to the realization that objective (3) above must be completed before objectives (1) and (2) can be answered. That is to say, one must be able to correct the "apparent" kinetic rates he observes experimentally for mass transfer effects before he can draw any conclusions regarding the "true" kinetic behavior of the catalyst. Many attempts have been made in the literature to model systems similar to the MEC-enzyme system described above. None have been completely successful in describing the case of a Michaelis-Menten enzyme in a spherical capsule over the entire range of possible kinetic parameters.

As a consequence of the above observations, the different aspects of this study can be conveniently separated into three phases; experimental, mathematical modelling, and data analysis.

A. Experimental

The technique described by Chang [24] was perfected for reproducibly encapsulating trypsin solutions inside nylon membranes. An assay was then developed to quickly give a "characteristic" reaction rate for a batch of capsules. This assay was used in a series of experiments to determine several important properties of MEC-trypsin prepared by the same technique. The areas investigated were the storage stability of the enzyme at several temperatures,

the pH and temperature dependence of the reaction rate, the effects of capsule size and initial enzyme loading on the retained enzymatic activity, and the relationship between the external concentration and the observed reaction rate. Attempts were also made to break the capsules in order to assay the internal solution activity, to independently measure the membrane permeability for the substrate in the absence of reaction, and to determine whether the enzyme tends to adsorb onto the nylon membrane.

B. Mathematical Modelling

The most convenient experimental measures of the substrate conversion rate are the rate of substrate disappearance or the rate of product appearance in the liquid outside the capsules. Mathematical models relating either of these rates to the parameters which characterize the kinetic behavior of the MEC-enzyme are necessary therefore to permit prediction of these parameters from experimental data. For the MEC Michaelis-Menten enzyme system, the general equations describing combined diffusion and reaction can be solved analytically only when certain simplifying assumptions are made. Models resulting from a variety of assumptions and limiting conditions are presented below. The models are also compared with numerical computations to determine the regime of parameter values for which each model applies.

C. Data Analysis

Given mathematical relationships which predict the externally observed rate of substrate disappearance as a function of the external substrate concentration and the system kinetic parameters, and given experimental data relating the reaction rate to the external concentration, it is possible in theory to statistically predict the

system kinetic parameters. Since the substrate conversion models tend to be highly non-linear, sophisticated, non-linear regression analysis is required for this purpose. This treatment leads to reliable selection of the "best" model to predict the data and the "best-fit" parameter values for this model. Ideally then, these "best-fit" parameter values should be used to characterize the behavior of the system.

This type of analysis was attempted for the MEC-trypsin system with results which were not completely satisfactory. The attempt to perform the analysis however led to added insight into the behavior of the system.

III. LITERATURE REVIEW

This chapter is intended to place the kinetic analysis of MEC-trypsin into historical perspective with respect to previous investigations of insolubilized enzyme systems. Fortunately, many recent and quite adequate reviews of different aspects of the literature are available. Wherever possible, therefore, the conclusions and insights presented by these reviewers are discussed below and no attempts are made to rigorously describe these portions of the literature.

III-1. The Production and Behavior of Immobilized Enzymes

Many excellent papers will serve as introductions to the general topic of insolubilized enzymes. Mosbach [106], Wiseman and Gould [147], and Kay [82] offer particularly readable discussions of the capabilities of immobilized enzyme technology. The review of Carbonell and Kostin [22], and the symposium by Wingard [146] give an overview of all of the aspects of the emerging field of "enzyme engineering". The most comprehensive discussions of the techniques of insolubilization and the interpretation of enzyme behavior, however are available from the articles by Melrose [97], Goldman, et al. [58], and McLaren and Packer [96].

Melrose summarizes the insolubilization techniques reported in the literature along with the resulting retention of catalytic activity, enzyme-by-enzyme. Industrial and analytical applications of many insolubilized enzymes are itemized along with a concise presentation of the equations most frequently used to describe the kinetics of immobilized derivatives. Goldman et al. list the insolubilized enzymes by method of preparation and then by

enzyme, including a particularly useful discussion of covalent-bounding techniques. Sections concerning the stability of water-insoluble enzyme derivatives, the kinetic behavior of particulate-immobilized enzymes, enzyme columns, and enzyme-bearing membranes, and the applications of insoluble enzymes give perhaps the best single discussion of this field available to date. McLaren and Packer's review is particularly oriented towards the behavior of naturally-occurring enzymes. Artificially insolubilized enzymes are considered here as useful analogs of enzymes which are found in vivo associated with membranes, gels, or surfaces.

III-1-A. Production Techniques

Goldman et al. [58] list four techniques that have been used to produce immobilized enzyme derivatives: adsorption (17,39); occlusion in cross-linked polymeric matrices (16, 23); covalent binding to water-insoluble carriers (42, 80); and intermolecular cross-linking (7 ,15). The numbers in the parentheses following each technique represent the number of enzymes successfully immobilized and total number of publications, respectively, arising from each process up to 1970, as reviewed by Goldman et al. These statistics, although probably incomplete, indicate the relative emphasis recently placed on each method.

The adsorption of proteins onto solid supports, arising from oppositely signed charges on the two, was the earliest procedure described for producing immobilized enzymes. Owing to the reversible nature of this process, however, other methods are probably better suited for use where complete insolubilization is required [97]. Desorption of the enzyme is especially pronounced in the presence of high salt or substrate concentrations [58].

Enzymes can be mechanically trapped in gel matrices in the following manner: A monomer (typically acrylamide) residing in solution with the enzyme is cross-linked to form a solid (polyacrylamide) matrix with the enzyme held in the interstitial pores. The solid can then be broken into particles of smaller size to reduce the mass transfer resistance. This procedure is considered "mild" with respect to the enzyme since the protein does not play an active role in the formation of the matrix. Interaction of the monomer with the enzyme can cause loss of activity, however. An apparent decrease in the reaction rate is anticipated since the substrate must penetrate the gel to interact with the enzyme. Reaction of large substrates may be impossible, therefore, depending on the porosity of the matrix [58,97].

Immobilization techniques which covalently link the enzyme to the solid support take advantage of certain polyfunctional amino acids in the protein which do not play an active role in the catalytic properties of the molecule. These non-critical groups serve as the point of construction of a bridge between the enzyme and the solid support. Denaturation of the enzyme during immobilization may result to a greater or lesser degree depending on the extent to which side reactions with the "active" portion of the molecule are blocked during the process. Loss of catalytic activity may also result when the "bridge" is in the proximity of the active center, causing some local distortion of the protein configuration.

Enzymes have been covalently attached to many types of solids including porous and non-porous glass beads, silica gels, polymeric membranes, tubes, and spheres. These materials range from rigid particles to flexible, swollen polymeric gels, and possess anionic, neutral, and cationic surface charges.

Cross-linked enzyme derivatives can be prepared by precipitating the protein into aggregates or adsorbing the enzyme onto the surface of a solid and then cross-linking the molecules in place by treatment with a difunctional agent such as glutaraldehyde. The insolubilized enzyme in the latter case forms a secondary matrix over the surface or throughout the interior of the solid support. Denaturation of the enzyme can again occur if the cross-linking tends to interfere with the local structure of the enzyme near the active center [58].

III-1-B. The Stability of Immobilized Enzymes

One of the more important consequences of the insolubilization of the enzymes is the increased period of time that many of these derivatives retain enzymatic activity when compared with the enzyme in solution. It is not always possible, however, to predict with certainty whether a given method of insolubilition will yield a more stable form of a particular enzyme.

Melrose [97] notes that of the 50 cases he found in which the stability of soluble and insoluble forms of enzymes were compared directly, the insoluble form was more stable 30 times, the soluble form 8 times, and little difference was observed 12 times. For the 11 cases of proteolytic enzymes reported in the above figures, the insoluble form was more stable 6 times, the soluble form 3, and the two forms were about the same twice. Melrose concludes that, given the variety of insolubilition techniques available, it is likely that suitable conditions can be found to stablize nearly all enzymes.

Goldman, Goldstein, and Katchalski [58] offer a more detailed discussion of the stability characteristics of insolubilized enzymes. They find that most insoluble enzyme derivatives, particularly of

proteolytic enzymes, can be successfully stored in the cold ($4^{o}C$) for several months without much loss of activity. Upon storage at higher temperatures, however, the soluble form seems to be more active in most cases. They conclude in general that adsorbed or covalently bound enzymes have decreased thermal stability due, perhaps, to "a decrease in the probability of the recovery of the native enzyme conformation following thermal perturbation". These authors also note that the stability of many enzymes has been increased towards storage in pH conditions unfavorable to the native enzyme. This modification is attributed to both the local microenvironment of the enzyme created by the presence of the carrier and also to chemical modifications in the enzyme caused by the insolubilization process.

III-1-C. Factors Affecting the Kinetic Behavior of Immobilized Enzymes

Goldman et al. [58] have discussed four factors which may influence the rate of substrate conversion in immobilized enzyme systems: diffusion limitations; steric effects; chemical modification of the enzyme; and microenvironmental effects.

When electrically-neutral, enzyme-bearing particles or membranes are suspended in a substrate solution, the substrate must be transported to the location of the enzyme before the reaction can proceed. The transport of the substrate by diffusive processes to the catalytic site will, in general, result in a substrate concentration gradient throughout the particle and the "unstirred" liquid film surrounding it. The substrate concentration will be everywhere lower than that in the bulk liquid resulting in a slower reaction rate than expected for an

equivalent amount of the soluble enzyme at the bulk conditions. Prediction of the extent of reaction limitation owing to low mass transport rates is the subject of extensive discussion in Chapter IV of this report.

For carriers bearing enzymes immobilized on the outer surface of the particle only, differences in the conversion rate of small and large substrates should result only from differences in diffusion rates across the external unstirred film. If the catalyst is distributed throughout the interior of the particle, however, larger substrates may be greatly hindered or even prohibited from approaching the site of the enzyme, depending upon the size of the pores in the carrier. Thus, steric effects produced by the nature of the carrier can result in apparent differences in the activity of a given enzyme for small and large substrates.

Chemical modification of the enzyme moiety during the insolubilization step should probably be expected to a certain degree, except perhaps for the case of enzymes trapped in gels. If a functional group on one of the amino acids is used for covalent bonding purposes, a change in the net charge of the enzyme might result, possibly causing a slightly altered molecular configuration. As Goldman et al. [58] note, however, these effects are normally small compared to the microenvironmental effects which can be caused by highly charged carriers. Studies to investigate modifications in the enzyme structure are more easily performed using neutral carriers in order to make identification of the modification as easy as possible.

The local electrostatic field produced by fixed charges on the carrier can greatly effect the apparent behavior of the enzyme [58]. For example, the local pH inside an enzyme-polyanionic carrier

is somewhat lower than the pH which is measured in the solution surrounding the catalyst particle. The pH optimum of the enzyme derivative will therefore appear to be displaced towards higher pH values when based on the measured bulk properties. The opposite effect has also been observed for polycationic enzyme derivatives. This effect has even been used to estimate the local electrostatic field produced by the carrier with reasonable results [58].

Fixed charges on the support can also affect the rate at which charged substrates are transported into the enzyme phase. Thus, substrates having the same charge as the support will tend to be repelled while substrates having oppositely-signed charges will be attracted. A lower or higher rate, respectively, of substrate converstion will be observed. The mathematical description of this phenomenon is considered in Chapter IV.

III-2. The Properties of Trypsin and Trypsin Derivatives

Trypsin (E. C. 3. 4. 4. 4) one of the earliest identified and best characterized of the proteolytic enzymes, has been discussed in recent reviews [41,83]. In this section, a brief description of the properties of soluble trypsin and the most commonly used tryptic assays will be given. Developments in the production and characterization of insoluble trypsin derivatives are then reviewed.

III-2-A. Soluble Trypsin

Trypsin selectively hydrolyses peptide, amide, and ester bonds at the C-terminal ends of lysine and arginine residues with the hydrolysis rate increasing in the order given. The inactive precursor, trypsinogen, is produced in the pancreas and converted

to active trypsin by the enzyme enterokinase or autocatalytically by trypsin itself [118]. The production of an inert protein formed during the activation step can be blocked by the presence of Ca^{++}. This ion has been shown to stabilize the active enzyme by preventing aggregation of the trypsin molecules and therefore limiting the rate of autodigestion [40]. Commercial preparations of trypsin are normally produced by activation of bovine trypsinogen from acid extracts of the pancreas [83]. The isoionic point of bovine trypsin is 10.8 [118] and the molecular weight is approximately 23,300 [118]. Trypsin shares many common properties with the other pancreatic proteolytic enzymes, especially chymotrypsin [110].

Trypsinogen is stable in acid pH but is activated to trypsin under neutral or alkaline conditions [83].

Trypsin exists in solution in equilibrium between an inactive denatured form and the active native protein. Irreversible inactivation can proceed by autohydrolysis resulting from digestion of the denatured form by the native enzyme. The equilibrium favors the formation of the reversibly denatured protein as the pH decreases but the rate of autohydrolysis increases with pH in the range of 2 to 10. Thus, below pH 2 the enzyme is found as the reversibly denatured protein which can be irreversibly denatured by exposures to elevated temperatures [92]. The enzyme is most stable at pH 2-3 in the cold (4°C) where only minor inactivation is observed in several months [40]. In the pH range 5-10, the enzyme is generally denaturing rapidly due to autodigestion with the protein split into fragments and losing all activity [40]. Above pH 11, a reversibly inactive protein is observed if exposures to this condition are short [92].

III-2-B. Tryptic Assays

Two types of assays have been used to determine the "activity" of typsin solutions. The more frequently employed procedure measures the initial rate of conversion of substrate to product per unit of "active" enzyme present under conditions where the substrate is in excess. The second technique utilizes a specific inhibitor for the enzyme to stoichiometrically "titrate" the number of active sites present per unit of enzyme present.

Bender et al. [9] have shown that the rate assays suffer from many difficulties: 1) the problem of defining the standard of 100% active enzyme; 2) the necessity of controlling many variables such as temperature, ionic strength, cofactors, inhibitors, activators and pH in the assay; 3) the requirement that the substrate concentration be high enough to "saturate" the enzyme; and 4) the inability in many cases to adequately determine the initial rate. Direct titration of the active site would appear to overcome these difficulties, if an appropriately specific titrant could be found.

The general mechanism for tryptic reactions is [9] :

$$E + S \underset{k_{-1}}{\overset{k_1}{\rightleftharpoons}} E\cdot S \overset{k_2'}{\rightarrow} E\cdot S' + P_1$$
$$E\cdot S' \overset{k_2}{\rightarrow} E + P_2 \qquad (3.1)$$

where E represents the active enzyme, S the substrate, E· S the enzyme-substrate complex, E· S' the acyl-enzyme intermediate, P_1 the group split from the substrate, and P_2 the "product". The reaction rate, v, for production of P_2 for this mechanism in the pseudo-steady state is [9]:

$$v = \frac{k'_{cat}\,[E][S]}{[S] + K'_m} \tag{3.2}$$

where

$$k'_{cat} = \frac{k'_2\,k_2}{k'_2 + k_2} \quad \text{and} \quad K'_m = \frac{(k_{-1}+k'_2)}{k_1}\;\frac{k_2}{(k'_2 + k_2)}$$

Generally speaking, the breakdown of E·S in Eq. 3.1 is much more rapid than the corresponding reaction for E·S′ with the result that most mechanisms for tryptic reactions appear to follow the classic Michaelis-Menten sequence [77]:

$$E + S \underset{k_{-1}}{\overset{k_1}{\rightleftharpoons}} E \cdot S \overset{k_2}{\rightarrow} E + P_1 + P_2 \tag{3.3}$$

with rate expression

$$v = \frac{k_{cat}\,E_t\,[S]}{[S] + K_m} \tag{3.4}$$

where

$$k_{cat} = k_2\,, \qquad K_m = \frac{k_{-1} + k_2}{k_1}\,,$$

and E_t is the concentration of active enzyme in all possible forms. Note that k'_{cat} degenerates to k_{cat} for $k'_2 >> k_2$ but that K'_m does not reduce to K_m in the same limit.

Tryptic assays based upon measurement of the "maximum" turnover rate are carried out at conditions such that $[S] >> K_m$ so that, from Eq. 3.4,

$$v = V_{max} = k_2\,E_t \tag{3.5}$$

Active site titrations generally attempt to interrupt the sequence of Eq. 3.1 after the formation of E·S' by binding a molecule to stabilize this intermediate [9]. A stoichiometric measure for the enzyme thus results from the amount of P_1 produced.

Rick [118] describes several commonly employed rate assays for trypsin. Proteolytic activity is usually measured by the rate of hydrolysis of denatured hemoglobin or denatured casein; hydrolysis of undenatured protein proceeds very slowly. Amidase or esterase activity is determined by the hydrolysis of amides or esters of lysine or arginine. Common substrates are α-N-benzoyl-L-arginine amide (BAA) [11], α-N-benzoyl-L-arginine ethyl ester (BAEE) [123], α-N-benzoyl-L-arginine-β-naphthylamide (BANA) [119], and p-toluenesulfonyl-L-arginine methyl ester (TAME) [76]. BAEE is perhaps the most frequently used "small" substrate for trypsin and was used for most of the rate assays in the work described below. Some of the earlier studies were made using TAME.

For BAEE, Eq. 3.1 becomes

$$\begin{aligned} E + BAEE &\underset{k_{-1}}{\overset{k_1}{\rightleftharpoons}} E\cdot BAEE \overset{k_2'}{\rightarrow} E\cdot BA + C_2H_5OH \\ E\cdot BA &\overset{k_2}{\rightarrow} E + BA \end{aligned} \qquad (3.6)$$

where BA is the carboxylic acid α-N-benzoyl-L-arginine. This reaction has been observed to follow Michaelis-Menten kinetics, Eq. 3.4 , under most assay conditions [77]. The corresponding reaction for TAME has been shown to diverge from Eq. 3.4 at high substrate concentrations (above about 2mM), the effect being that of substrate activation of the reaction [137]. At concentrations below about 1mM, Michaelis-Menten kinetics were obeyed [5].

Schwert and Takenaka [124] and Hummel [76] describe procedures for the spectrophotometric assay of trypsin using BAEE and TAME, respectively. Both suggest the use of 1mM substrate solutions in tris-hydroxymethyl-aminomethane buffer solutions. The Worthington Biochemical Corporation [149] gives a similar assay for BAEE using TAME in 0.04 M tris solution.

Barman [8] gives data for the specificity and kinetic contracts and light absorption characteristics for BAEE and TAME as shown in Tables 1 and 2.

Table 1*

Specificity and Kinetic Constants for BAEE and TAME

Substrate	k_{cat}, (sec^{-1})	K_m, (M)	Conditions
TAME	147	5×10^{-5}	pH 7.8-8.0, 25°C
BAEE	22	5×10^{-5}	pH 7.8-8.0, 25°C

Table 2*

Light Absorption Data for BAEE and TAME

Substrate	λ	$\Delta\epsilon$ (P - S)
BAEE	255 mμ	800 $M^{-1} cm^{-1}$ (pH 5-10)
TAME	247 mμ	540 $M^{-1} cm^{-1}$ (pH 8.1)

* as given by Barman [8], entry (3.4.4.4)

BAEE -- benzoyl-L-arginine ethylester

TAME -- p-toluenesulphonyl-L-arginine methylester

k_{cat} in Table 1 represents the number of molecules of substrate transformed per molecule of enzyme per second. $\Delta\epsilon$ in Table 2 is the difference in the absorption of one molar solutions of product (e.g., BA) and substrate (BAEE) in a one centimeter cell at wavelength λ.

The value for the Michaelis-Menten constant, K_m, for BAEE in Table 1 does not represent a consensus of those provided in the literature. Other estimates previously presented are summarized in Table 3.

Table 3

Values of K_m for BAEE

Reference	K_m, (M)	Conditions
Gutfreund [63]	1×10^{-5}	0.1M NaCl, 0.01M phosphate, 25°C, pH 7.5
Schwert & Eisenberg [123]	8×10^{-5}	0.1M phosphate, 25°C, pH 8.0
Ignagami & Sturtevant [77]	3.4×10^{-6}	0.025M $CaCl_2$, 25°C, pH 8
Bender et al. [9]	2×10^{-5}	25°C, pH 8.0
Barman [8]	5×10^{-5}	25°C, pH 7.8 - 8.0
Li [92]	8×10^{-5}	27°C, pH 7.0, 0.1M phosphate

The wide range of values for K_m for the tryptic hydrolysis of BAEE in Table 3 probably reflects the effects of pH, ionic strength, and, especially, Ca^{++} concentration. Green and Neurath [62] have found that Ca^{++} increases the esterase activity of trypsin to a maximum of about 28% at $\sim [Ca^{++}] = 5 \times 10^{-4}$ M. Above this concentration the activity drops slowly to about 18% enhancement at 0.1M then drops rapidly with increasing concentration above this point [77].

Gutfreund [63] has found the apparent energy of activation for the tryptic hydrolysis of BAEE to be 11 kcal/gmole at pH 7.5 in 0.1M NaCl and 0.01M phosphate buffer. Ignagami and Sturtevant [77] estimated the activation energy to be 9.3 kcal/gmole at pH 8 in 0.01M phosphate buffer and 9.1 kcal/gmole in the phosphate buffer with 0.05M NaCl. The

difference between the latter observations and the value obtained by Gutfreund was attributed to the decreased ionic strength [77]. Li has recently observed that the energy of activation for hydrolytic reactions by trypsin ($E_a \sim 9$-15 kcal/gmole) appears to be substantially lower than for the reversible denaturation reaction of the denatured trypsin - native trypsin equilibrium ($E_a \sim 67$ kcal/gmole).

Keil [83] suggests that the two best titrants for use in the active site titration procedures are p-nitrophenyl N^2-benzyl-oxycarbonyl-L-lysinate HCl [10] and p-nitrophenyl-p'-guanidino-benzoate HCl [37]. The release of p-nitrophenol is determined spectrophotometrically as P_1 in Eq. 3.1 for both substrates.

III-2-C. Insoluble Trypsin-Preparation

Each of the methods discussed in Section III-1-A has been successfully used to immobilize trypsin. In this section, many of the recent publications concerning insoluble trypsin derivatives will be reviewed. A more complete compendium of the literature has recently become available [78].

Adsorbed Trypsin

Mitz and Schleuter [99] describe stable derivatives prepared by adsorption of trypsin to the acidic cellulosic ion exchangers carboxymethyl cellulose, cellulose citrate and cellulose phosphate. Typical amounts of trypsin sorbed were 5% by weight protein for carboxymethyl cellulose and 1.5% for cellulose citrate. The samples could be freeze dried or air dried and the enzyme could be reversibly desorbed by proper selection of the pH. Recovered activity following freeze drying and desorption ranged from 80% to 99%.

Kobamoto et al. [86] have shown that trypsin will also adsorb to cellulose dialysis membrane, glass, and quartz. For trypsin adsorbing onto cellulose, two or three exponential components of the rate of adsorption suggested that several trypsin conformers may have been present and adsorbing at different rates. Chemisorption was considered to be the primary mode of attachment since the amount adsorbed increased with temperature, showed an optimum at pH 6.3 and increasing ionic strength decreased the quantity of adsorbed protein. It was also observed that all tryptic activity was lost at 4°C after 48 hours when a membrane was placed in a 1μM trypsin solution and after 72 hours for a membrane in a 3μM solution. Negligible loss of activity was observed in control solutions containing no membrane. They conclude that "a dynamic process of adsorption, unfolding, and desorption accounts for the continual loss of activity in the supernatant". Adsorption onto glass varied with the surface preparation and properties of the glass. Rapid adsorption of primarily the inactive protein followed by slower adsorption of the active protein was observed for one batch of glass. Active protein could be desorbed by raising the pH. The amount of protein adsorbed onto quartz was somewhat less than for glass. pH optima for glass and quartz adsorption occurred at 6 and 7-9, respectively.

Goldberg, Campbell and Roy [57] found that trypsin and chymotrypsin adsorbed to particulate matter from human ileal material (intestinal debris) and to discrete human intestinal epithelial cells to about the same degree and with only small losses in activity. The protein could not be made to desorb by repeated freezing and thawing, incubation at 37°C for periods

up to 4 hours, pH ranging from 1.6 - 4.5, or addition of protein, nucleic acid or polysaccharides. Two pH optima were observed for the amount of adsorbed protein at about pH 5 and pH 8.5 for both trypsin and chymotrypsin when either TAME or casein were used as substrates.

Haynes and Walsh [67] have adsorbed a monolayer of trypsin onto the surface of silica particles. The trypsin was then cross-linked by treatment with glutaraldhyde to form an "enzyme envelop" around the surface of the particle. 99% yield of immobilized enzyme was obtained with 80% retention of esterase (BAEE) activity and 17% retention of proteolytic (casein) activity. pH-activity behavior with BAEE was nearly the same as for the native enzyme. It was observed that maximum retained activity of the "envelop" was obtained only when sufficient amounts of the silica particles were present to permit monolayer coverage of the surface. In the absence of silica, a 55% loss in initial activity was observed following cross-linking due to the formation of large polymerized protein aggregates.

Gel-Entrapped Trypsin

Polyacrylamide gels have been successfully employed to trap trypsin [12,107,144] with resulting "apparent" enzymatic activity ranging from 2% [144] to 11% [12] of the initial activity. It is likely that diffusion inside the gel is responsible for a major portion of the reduced activity [58]. Brown, Patel, and Chattopadhyay [21] have found that trypsin can be entrapped in a hydrophobic Silastic matrix. Esterase activity (TAME and BAEE) of thin discs (0.1 mm. thickness) of the lattice were about 60% for TAME and 40% for BAEE of the soluble enzyme activity,

measured at 25°C in phosphate buffers. O'Driscoll, Izu, and Korus [112] report the entrapment of trypsin in gels of 2-hydroxyethyl-methacrylate (HEMA). Crushed gels have been used in enzyme columns to hydrolyze TAME at pH 8.0 and 25°C with only 5% loss of activity in 50 days of continuous operation. pH optima for two batches of trypsin-HEMA were observed at ~pH 8.0. The TAME/BAEE activity ratio as determined by batch assay was 1.1 - 1.5 for the HEMA entrapped trypsin but about 7 for the soluble trypsin (see k_{cat} TAME/k_{cat} BAEE in Table 1). The authors conclude that the rate of diffusion of substrate to the enzyme in the gel is probably controlling the reaction rate.

Covalently-Bound Trypsin

A great variety of carriers have been employed to support covalently bound trypsin derivatives. Active insoluble trypsin has been obtained from binding to many cellulosic derivatives [39, 43, 54, 65, 99, 132, 135]; Sepadex and Sepharose [4, 50, 51]; ethylene-maleic anhydride copolymers [2, 91, 113]; polystyrene [136]; polyacrylamide beads [79]; acrylamide-acrylic acid and acrylamide-hydroxyethyl methacrylate copolymers [105]; diazo-DL-phenylalanine-L-leucine copolymers and poly (diazo-DL-phenylalanine) [7]; alanine-glutamic acid copolymers [138]; reaction with N-carboxy-L-tyrosine anhydride [55] and then with poly (p-diazo-DL-phenylalanine-L-leucine) [6, 7]; a diazo derivative from "dialdelyde" starch [59], or p-aminobenzyl cellulose [61]; nylon tubes [72, 74]; and porous glass [45, 92, 141, 142].

Generally speaking, 20-60% of the initial activity will be retained after binding the enzyme [97] and storage stability will be improved in the cold when compared to the native enzyme [58]. Weetall [142] has concluded that trypsin coupled to inorganic

carriers tends to have greater stability than commercially available organic polymer-trypsin derivatives when stored at 5°C and 23°C in lyophilized form or in distilled water. Trypsin coupled to porous glass by azo linkage retained 79% and 89% of the original activity after 72 days in water at 5° and 23°C, respectively. Trypsin-glass derivatives prepared by sulfonamide linkage lost all activity after 30 days at either temperature while the corresponding silica derivative was 58% as active as the initial preparation after 42 days at 23°C. Freeze-dried cellulose derivatives retained 60% of the original activity after 42 days at 5°C or 63 days at 23°C. Ethylene-maleic acid (EMA) copolymer derivatives were 100% active after 22 days at 5°C and 42 days at 23°C if lyophilized but lost all activity in water at 5°C after 30 days. Levin et al. [91] reported, however, that EMA-trypsin derivatives were nearly 100% stable at 4°C after 4 months, wet or dry. These immobilized enzymes also displayed improved stability in adverse (alkaline) pH conditions, presumably due to the polyanionic nature of the carrier as discussed below.

Cross-linked Trypsin

Habeeb [65] has prepared cross-linked trypsin via glutaraldehyde by a procedure similar to the one employed by Haynes and Walsh [67] as described above except that the enzyme was not adsorbed to any carrier. Cross-linked trypsin aggregates were formed which possessed 70-86% of the activity of the original soluble enzyme by proteolytic (casein) assay.

III-2-D. Insoluble Trypsin-Behavior

In this section, the factors affecting the behavior of immobilized trypsin are reviewed within the framework of Section III-1-C.

Diffusion Limitation of the Reaction Kinetics

This aspect of immobilized trypsin systems has been relatively neglected in the studies recently reported, owing in part, at least, to the difficulties in defining quantitatively the effects of the mass transport process on the kinetics. A common method of reporting the diffusion effect is to estimate the "apparent" Michaelis constant, K'_m, for the system and attribute the change from the soluble enzyme K_m to diffusion effects. The Michaelis constant as defined in Eq. 3.4 is that substrate concentration at which one half the maximum possible reaction rate is observed. Since the local substrate concentration inside the enzyme phase will normally be lower than in the bulk solution, then "apparent" values of K_m based on measurement of the bulk concentration will generally be higher than the K_m for the soluble enzyme. Thus, for other proteolytic enzymes bound to the surface of rigid, unchanged particles, the external "unstirred" liquid layer has been observed to increase the apparent K_m by two to three times that of the soluble enzyme [61,73]. For chymotrypsin bound throughout a swollen Sepharose matrix, Axén et al. [3] report a K'_m about ten times greater than for the soluble protein. In a recent study employing trypsin immobilized on the inner wall of hollow nylon tubes, Horvath and Solomon [74] found the values of K'_m for BAEE hydrolysis in 0.1M phosphate buffer at pH 8 given in Table 4. Substrate solution was passed through the center of the tubes and the extent of conversion of BAEE to BA was based on entering and exiting concentrations. Two graphical

Table 4

Values of K'_m for Trypsin Immobilized on the Inner Wall of Hollow Nylon Tubes [74]

Reactor	Binding Procedure	Tube I.D. (mm)	K_m (M)
Tube A	Surface-bound (via phosgene)	0.5	8.4×10^{-5}
Tube B	Surface-bound (via glutaraldehyde)	0.1	8.5×10^{-4}, 6.0×10^{-4}
Tube E	Enzyme bound in polyanionic gel coated onto tube wall	0.5	6.2×10^{-3}
Tube F		0.25	7.4×10^{-3}

techniques were employed to extract K'_m. Surface-bound trypsin was thought to be unaffected by diffusion limitations. The somewhat higher K'_m values, when compared to the values of K_m reported in Table 3, resulted from "chemical modification of trypsin by crosslinking and by steric hindrances with respect to the accessibility of the active sites". The authors conclude, however, that the gel-coated tube reactions (E and F) were significantly effected by diffusional resistance.

Ford et al. [45] describe three simple, conventional tests for determining if diffusion effects are affecting reactions catalyzed by trypsin bound to porous glass in a recirculation reactor. The hydrodynamic boundary layer can generally be reduced by increasing the flow rate of the liquid with respect to the solid surface. The authors found that, by increasing the recirculation flow rate through the reactor, a sufficiently high flow rate could be attained such that the conversion was no longer flow-dependent. The "external" mass transfer resistance was therefore rendered insignificant. Since the effects of diffusion inside the carrier

will be accentuated by increasing the particle size, determination of K'_m as a function of the particle diameter should give an indication of internal diffusion limitations. Ford et al. found that the K'_m for trypsin bound to glass particles of 10μ and 35μ diameters, when assayed with α-N-acetyl-L-lysine methyl ester (ALME) in 1.0M phosphate buffer at pH6 and 25°C, were essentially the same as the K_m of the soluble enzyme (2.9×10^{-4}M). Internal diffusion, therefore, was not considered to be an important factor in the kinetics. As an alternative to changing the size of the carrier particles, these authors suggest increasing the catalyst loading. Assuming the amount of active, immobilized enzyme can be accurately determined, then the reaction rate in the presence of excess substrate will be directly proportional to the enzyme loading if negligible mass transport resistances are encountered. Ford et al. successfully employed this test to demonstrate the absence of diffusion limitation for glass-bound trypsin. The basis for these tests will be considered in quantitative terms in Chapter IV.

The assay procedure suggested by O'Driscoll et al. [112], as discussed in Section III-2-C, wherein the rates of hydrolysis of two substrates (BAEE and TAME, in this case) have different turnover numbers, will also serve as an indicator of significant mass transfer intrusion on the kinetics.

Steric Effects

The evidence for steric hindrance of the reactions of immobilized trypsin comes from three types of experiments: (1) hydrolysis of small substrates (e.g., amino acid esters)

vs. large substrates (e.g., proteins); (2) modified catalytic behavior of the enzyme; and (3) inhibition of the enzyme by small and large inhibitor molecules.

The studies summarized in Table 5 give quantitative evidence of the steric exclusion of large substrates.

Table 5

Steric Hindrance of Immobilized Trypsin Reactions

Immobilized Trypsin System	Reference	Esterase Activity (Substrate)	Proteolytic Activity (Substrate)
adsorbed on silica and cross-linked via glutaraldehyde	Haynes and Walsh [67]	80% (BAEE)	17% (casein)
trapped in nylon micro-capsules	Chang [23]	active	inactive
reaction with activated esters of Sephadex	Axén and Porath [4]	17-24% (BAEE)	4% (casein)
poly-tyrosyl trypsin coupled to poly(phenyl-alanineleucine)	Bar-Eli and Katchalski [6]	28% (BAME)	5% (casein)
amino-ethyl-cellulose trypsin	Glassmeyer and Ogle [54]	75-97% (BAPA)	11-24% (casein)

Insoluble trypsin has been observed to digest fibrinogen [2] and to activate chymotrypsinogen to chymotrypsin [91, 100] in a manner similar to the soluble native enzyme.

Alexander et al. [2] have shown that polytyrosyl-trypsin (P-T) and ethylene-maleic anhydride-trypsin (EMA-T) derivatives both convert prothrombin to thrombin. However, native trypsin and the P-T derivative will not digest the product thrombin but the EMA-T derivative will. Lowey et al. [93] have shown that the pattern of digestion of myosin and of the meromyosins by EMA-trypsin differs from that of the native protein. Ong et al. [113] have also found that EMA-trypsin will hydrolyze only 10 lysyl-peptide bonds in pepsinogen while the soluble enzyme will hydrolyze 15. While it is true that the polyanionic nature of the EMA carrier may also contribute to the modified enzyme behavior in these cases, steric influences must also be considered [58].

Levin et al. [91] have also observed that the esterase activity of EMA-trypsin derivatives can be blocked by a comparatively low-molecular weight inhibitor (pancreatic trypsin inhibitor, M. W. ~ 9000). A high-molecular weight inhibitor (soybean trypsin inhibitor, M. W. ~ 21, 500) has no significant effect on the esterase activity but does block the caseinolytic activity of the bound enzyme. Thus, the inhibitor can also be subject to steric exclusion in the same manner as the substrate.

Chemical Modification

Several studies have shown that the pH-activity curves for trypsin-neutral carrier derivatives are displaced from that of the native enzyme [7 ,59 ,61]. Since the displacement was essentially independent of the ionic strength, it was concluded that the pH-activity behavior can be attributed to modifications near the active site of the enzyme rather than to a change in the net charge on the molecule [58].

Gabel, Steinberg, and Katchalski [51] have recently described a method for observing via a fluorometric technique the change in conformation of chymotrypsin bound to Sephadex. This analysis revealed subtle changes in the conformation of the enzyme which were attributed to the presence of the carrier.

Microenvironmental Effects

The studies in which the microenvironment of bound enzymes has been considered deal primarily with the effect of fixed surface charges on the reaction kinetics. For example, Goldman et al. [58] describe in detail the displacement of pH-activity profiles at low ionic strength for trypsin and chymotrypsin bound to charged carriers. The polyanionic ethylene-maleic anhydride-trypsin (EMA-T) derivative pH-activity profile was displaced from a pK(apparent) of about 6. 0 for soluble trypsin to a pK(apparent) of about 8. 5 for EMA-T at low ionic strength. Increasing the ionic strength reduced the difference between the two pK's. Similar behavior was reported for EMA-chymotrypsin derivatives but for polycationic (polyornithyl) chymotrypsin derivatives a displacement in the opposite direction was observed. An explantion of this behavior, as given by Goldman et al.[58], follows.

The relationship between the activities of hydrogen ions in the bulk solution ($a^{o}_{H^+}$) and in the polyelectrolyte phase ($a^{i}_{H^+}$), assuming a Maxwell-Boltzmann distribution, is given by

$$a^{i}_{H^+} = a^{o}_{H^+} \exp(ze\psi/kT) \tag{3.7}$$

where z is the ionic valance (= +1 for H^+), e is the electronic charge, ψ is the electrostatic potential in the charged carrier (assumed uniform), k is the Boltzmann constant, and T is the absolute temperature. The pH difference between the bulk and carrier phases is found directly from Eq. 3.7 as

$$\Delta pH = pH^{i} - pH^{o} = 0.43\, ze\psi/kT \tag{3.8}$$

Therefore, for the polyanionic EMA-T derivatives discussed above, z = +1 and ψ is negative, so $pH^{o} > pH^{i}$. If the enzyme displays the same pH-activity behavior under the local carrier conditions as it does in the bulk, then the apparent pH-activity profile based on the bulk pH will be shifted to more alkaline conditions. Goldman et al. found the values of ψ for the EMA matrix, calculated from Eq. 3.8 based on the observed pH-activity shifts for trypsin and chymotrypsin derivatives, was in the range of 50-150 mV. These values were considered to be in good agreement with polyelectrolyte theory for the correspondingly ionized polymers [58].

Another effect of the surface charge on the carrier is to influence the flux of charged substrate. Using the positively charged benzoyl-L-arginine amide (BAA) as substrate, Goldman et al. [58] found that K'_m for EMA-trypsin derivatives was 2×10^{-4}M, much lower than for the native enzyme ($K_m = 6.9 \times 10^{-3}$M). Increasing the ionic strength served to raise K'_m for the EMA-T to

5.2×10^{-3} M but had little effect on K_m for the soluble enzyme. Using an expression similar to Eq. 3.7, but written for the substrate (BAA), Goldman et al. arrived at Eq. 3.9.

$$a^{i}_{BAA^+} = a^{o}_{BAA^+} \exp(ze\psi/kT) \tag{3.9}$$

If the concentration is assumed equal to the activity, then the Michaelis-Menten expression, in terms of conditions inside the carrier, can be rewritten in terms of the bulk conditions as Eq. 3.10.

$$v = \frac{k_2 E_t [BAA] \exp(ze\psi/kT)}{[BAA] \exp(ze\psi/kT) + K_m} \tag{3.10}$$

or, upon rearrangement of Eq. 3.10,

$$v = \frac{k_2 E_t [BAA]}{[BAA] + K'_m} \tag{3.11}$$

where $K'_m = K_m \exp(-ze\psi/kT)$. (3.12)

Goldman et al. [58] have shown that the difference between K'_m for EMA-T and K_m for the soluble enzyme lead, via Eq. 3.12, to a value of $\psi = 92$ mV which is in good agreement with the reported values, based on the shift in the pH-activity profiles.

The effects of other aspects of local electrostatic charges are treated in more detail in Section IV-5-C.

Taylor and Swaisgood [136] have examined the effect of the distance between trypsin and the surface of neutral hydrophobic polystyrene by a solid-phase peptide synthesis technique. Chains of amino acid residues were attached to polystyrene and trypsin molecules were attached to the ends of the chains. One to ten amino acids made up the links, which were composed entirely of

glycine except for an initial alanine residue for chains of two to ten residues. The polystyrene beads were then placed in columns and the esterase (TAME) activity determined by flowing substrate solution through the column (0.46M Tris buffer, 0.1M $CaCl_2$, pH 8.1). k_{cat}, as defined in Eq. 3.4, was found to be relatively insensitive to the chain length ($\sim$ 11-12 sec^{-1}); it was concluded that some inactive enzyme had been bound during preparation of the insoluble derivatives. K_m (apparent), however, was observed to increase from about 0.1mM for chains of one amino acid to about 0.4mM for 10-residue chains, and were slightly lower when the substrate solution flow rate was increased. The authors conclude that the decrease in K_m (apparent) as the flow rate was increased was due to the reduction in the thickness of the unstirred liquid layer surrounding the bead. The increase in K_m (apparent) with increasing chain length probably resulted from microenvironmental influences on the substrate binding constant, k_1, of the enzyme (see Eq. 3.1). k_2' and k_2 were thought to be unaffected by chain length since k_{cat} was not sensitive to this treatment.

III-3. Microencapsulated Enzymes

When the meaning of the term "capsule" as used, say, in the pharmaceutical sense is considered, one finds that the term implies a small container formed by an impermeable membrane which is intended to keep some substance "locked" inside. Webster [140], for example, defines a capsule as "a small rounded container, often of gelatin, in which nauseous or acrid doses are enclosed to be swallowed". Presumably, the capsule wall can be ruptured, perhaps by mechanical means or dissolution, at a later time to permit the application of the "encapsulated" substance

in its properly-administered location. Encapsulation technology has been developed in the last decade or so to permit the preparation of very small capsules (hence "microcapsules") for a wide variety of uses in the pharmaceutical industry and many others [94]. A new dimension was given to this technology by the findings by Chang that microcapsules can be prepared having "semi-permeable" or, perhaps, "perm-selective" membranes to allow the selective interaction of the fluids inside and outside of the membrane [24, 29]. The preparation, applications, and kinetic behavior of microencapsulated (MEC) enzymes as discussed in the literature are the subjects of this section.

III-3-A. Microencapsulated Enzymes-Preparation and Applications

In his early studies in which he was attempting to produce "artificial" red blood cells, Chang [24] developed two techniques for producing hemoglobin-containing, hollow membrane spheres; these processes involve the formation of membranes in situ via "interfacial polycondensation" or "interfacial coacervation" processes. Chang's polycondensation technique was adapted from processes originally proposed by Wittbecker and Morgan and their associates for the production of polymeric films [102,148]. Briefly stated, this process involves the contacting of two immiscible liquid phases, one distributed as small droplets suspended in the other, in which reside two monomers that polymerize by condensation, one monomer in each phase. A polymerization reaction is initiated spontaneously at the interface of the phases and proceeds, under the proper conditions, until a thin, viable membrane completely surrounds the suspended (inner) phase. Coacervation or phase separation techniques utilize the selective deposition

of the membrane-forming material from solution in the continuous phase of a suspension. This deposition occurs preferentially at the continuous phase-suspended phase interface and can be brought about by any perturbation to the system which results in a decreased solubility of the dissolved polymer. For example, the slow evaporation of the continuous phase solvent or the addition of a soluble compound to the continuous-phase solution which acts as a "non-solvent" for the polymer will often cause the selective deposition desired.

Chang found that, by including some enzyme in the hemoglobin during preparation of the microcapsules, he was able to produce MEC-enzyme solutions which catalyzed reactions involving relatively small substrates [24]. Recipes have been given by Chang et al. [34] for producing nylon microcapsules by means of the "condensation" technique and collodion (cellulose nitrate) microcapsules via the "coacervation" route. The successful preparation of membranes formed from cross-linked protein from the inner phase [24], of lipid-coated [27] and negatively charged microcapsule membranes, and of microencapsulated suspensions of yet smaller capsules or intact cells was also demonstrated [24].

Other procedures which have been described for the preparation of microcapsules by interfacial polymerization result in polyurethane and polyphenolester [133], polyphthalamide [89], and sulfonated polyphthalamide [134] membranes. Boguslaski and Janik [19] have prepared nylon-MEC-carbonic anhydrase wherein bovine serum albumin was substituted for the hemoglobin in Chang's recipe. Mori et al. [104] have found that nylon-MEC-asparaginase retains more activity when encapsulated along with casein than with either albumin or hemoglobin. L-aspartic

acid, a product of the enzyme degradation of asparagine, also stabilized the enzyme if added to the enzyme solution during preparation.

In a study of the storage stability of MEC-enzymes, Chang [29] found that enzymes such as catalase, asparaginase, and urease are more stable when encapsulated in concentrated hemoglobin solutions than were the enzymes in free solution. MEC-enzymes which were treated with glutaraldehyde to further immobilize the enzymes by cross-linking were nearly as stable as the MEC-enzymes at 4°C but much more stable at 37°C. About 2/3 of the original MEC activity was lost following cross-linking, however.

Approximate values for the half-life, $t_{1/2}$, of collodion-MEC-catalase in the free solution, MEC, and cross-linked-MEC forms are given in Table 6. A small aliquot of penicillin (50 mg/100 ml solution or suspension) was added to each sample to retard bacterial growth during the tests.

Table 6

Approximate Half-life, $t_{1/2}$, of Active Catalase

As Calculated From Chang's Data [29]

Form of Enzyme	Approximate $t_{1/2}$, days	
	4°C	37°C
free solution	15	1
collodion-MEC	~ 600 (95% after 40 days)	2
collodion-MEC cross-linked via glutaraldehyde	~ 260 (90% after 40 days)	6

Chang has been at the forefront of the research to find new clinical applications for encapsulated enzymes or absorbents. Nonthrombogenic microcapsules have been prepared with heparin-complexed membranes [31]. Intraperitoneally injected MEC-enzymes have been demonstrated to have clinical uses: MEC-urease reduced body urea levels in dogs [33]; MEC-catalase effectively replaced the lack of the enzyme in acatalasemic mice [36]; and MEC-asparaginase suppressed the growth of asparagine-dependent tumors [28]. In extracorporeal shunt systems, MEC-enzymes have been used to reduce the level of blood-borne substrates [25]. MEC-urease has also been administered orally in conjunction with ammonium adsorbents to lower blood urea levels [32 ,53 ,129].

III-3-B. Microencapsulated Enzymes-Kinetic Properties

The in vivo experiments with MEC-enzymes mentioned above have been of a qualitative nature owing to the difficulties in quantitatively describing the conditions under which the reactions were conducted. Several authors have described in vitro kinetic studies wherein the conditions were more easily controlled. These experiments, however, must be considered of limited value, except for the recent study by Morgensen [103], since the authors were unable to adequately interpret their results.

Chang [30], for example, concludes that ". . . . the enclosed enzymes remain unchanged; but the kinetics of reaction are governed by a large number of factors: concentration of enzymes in the microcapsules, permeability of membrane to the substrates and products, charge of membrane, composition of membranes, and other factors." One of his principal pieces of evidence for this conclusion is from the in vitro assay of free-solution and

MEC-catalase acting on $NaBO_3$, which resulted in the following kinetic constants [115]: enzyme in free solution, k_2E_t = 0.72 mM/min., K_m = 0.15M; MEC-enzyme, k_2E_t = 0.31 mM/min., K'_m = 0.15M.

In another experiment, intended to determine permeability constants for nylon microcapsule membranes in the absence of chemical reaction the results presented in Table 7 were obtained [35]. The experiment was conducted by measuring the rate of accumulation of radioactive solutes in microcapsules based on the rate of loss of radioactivity of the bulk solution. In addition, the equivalent pore radius for these capsules was estimated to be 18 Å. Membrane permeabilities of the magnitude presented in Table 7, when considered in view of the theoretical analysis given in Chapter IV of this report, would result in k_2E_t being much lower and K'_m being much higher than those reported for MEC-catalase above, if ". . . . the enclosed enzymes remain unchanged. . . . " !

Table 7*

Nylon Microcapsules: Permeability Data

Solute	Mol. Wt.	Half-Time for Equilibration (sec.)	Permeability Constant (cm/sec)x10^4
urea	60.1	4.3	2.01
creatinine	113.1	17.5	0.61
uric acid	168.1	42.5	0.19
creatine	131.1	16.6	0.75
glucose	180.2	26.2	0.54
sucrose	342.3	35.5	0.37
acetal salicylic acid	180.2	39.0	0.32
tritiated water		<1.0	

*as given by Chang and Poznansky [35] for 207μ diameter microcapsules.

Shigeri and Kondo [127] estimated that the permeability coefficients of newly formed, polyurethane microcapsule membranes ranged from 3×10^{-8} to 5×10^{-8} cm/sec for inorganic electrolytes. The measurements were made by following the rate of change of the conductance of a capsule suspension as the electrolytes passed from outside to inside the capsules. It was found that the permeability of the membrane increased for chloride salts in the order $Cs^+ > Na^+ > Li^+$ and for sodium salts in the order $Br^- > Cl^- > SO_4^= > CrO_4^=$.

Boguslaski and Janik [19] have used a batch assay technique for measuring the activity of nylon-MEC-bovine carbonic anhydrase (in serum albumin) using p-nitrophenyl acetate as the hydrolysis substrate. K_m' and k_2E_t values for three batches of capsules and for the enzyme in free solution were determined from Lineweaver-Burk plots (see Section III-4) with initial reaction rates measured at c_{so} = 3.15, 2.33, 1.55, 0.94, and 0.78 mM. The results are summarized in Table 8 ($k_{cat}=k_2E_t/c_{BCA}$). Microcapsules used in these studies were from 70-110μ in diameter. Dye molecules (M. W. ~ 1000) were observed to diffuse rapidly from these capsules. The authors concluded that since K_m' for the MEC-enzyme was "close" to the native enzyme while k_{cat} was an order of magnitude lower, it is likely that much of the active enzyme was lost during encapsulation. "Adverse effects of diffusion, partition, conformational changes or interaction of the substrate with the support" were not considered to significantly influence the system kinetics. Further support for this claim was rendered by an independent study in which ^{125}I-labeled BCA was encapsulated. Measurement of the microencapsulated radioactivity indicated that only about 10% of the labeled BCA was incorporated into the microcapsules. Capsule ghosts displayed no activity.

Table 8

Kinetic Data of Boguslaski and Janik [19]
for Nylon-MEC-Bovine Carbonic Anhydrase (BCA)

Capsule Batch #	BCA Concentration* c_{BCA}, (M)	K_m (mM)	k_2E_t (μM/min)	k_{cat} min^{-1}
1	4.0	5.8	7.7	1.9
2	9.4	36.0	196.0	21.0
3	12.5	59.0	380.0	30.3
BCA in free	0.052	13.0	10.0	193.0
solution	0.26	12.8	80.0	308.0

* For encapsulated BCA, all enzyme in the preparation was assumed to be encapsulated and remain active.

Mori et al. [104] presented the results in Table 9 to illustrate what they term the "effect of concentration of asparaginase on microencapsulation". The asparaginase activity was estimated from the initial rate of conversion of L-asparagine to aspartic acid and ammonia in batch assay. No attempt was made to estimate the possible effects of diffusion on the measured activity of the MEC-asparaginase. One International Unit (I. U.) is the quantity of active enzyme which will catalyse the liberation of one μmole of ammonia in one minute. The size of the capsules used in these experiments was not reported.

Table 9

"Effect of Concentration of Asparaginase on Microencapsulation"
as Reported by Mori et al. [104]

Asparaginase Added		MEC-Activity	
mg	IU	IU	Yield, % of Initial Activity
1	70	24.5	35.0
5	350	116.9	33.4
20	1400	222.6	15.9
50	3500	392.0	11.2

Morgensen [103] has recently completed a detailed study of the in vitro reaction kinetics of the collodion-MEC-enzymes catalase and urease. He observed that when capsules were packed into fixed-bed columns they tended to "slump" (sic) together resulting in an increased bed pressure drop. This problem was overcome by distributing the capsules throughout a column packed with glass wool batting which served to keep the capsules separated. In tests in which the capsules were assayed in stirred suspensions, breakage of the capsules was considered "unacceptably high"; the breakage rate increased with the stirring rate. Morgensen suggested assaying the capsules under conditions wherein the agitation was just sufficient to keep the capsules suspended in order to minimize breakage.

Morgensen found that under suitable conditions, mass transfer across the "unstirred" boundary layer surrounding the particle, mass transfer through the membrane, or the combined diffusion-reaction rate inside the cell could control the system kinetics. From well-established engineering correlations [122], the external mass transfer coefficient, k_e, for capsules falling in liquid at terminal velocity ($\Delta\rho = 0.1$) was estimated to be about 0.01 cm/sec for $\sim 100\mu$ diameter capsules with a solute diffusivity of 10^{-5} cm/sec. Solutions to the unsteady-state diffusion-reaction equations were presented (see Sec. IV-5) for reactions conducted in suspensions of limited volume and for the cases of no reaction and first-order internal reaction. The first-order reaction solution was valid for the kinetics of one of the enzymes he studied but is generally the low-substrate limiting case for Michaelis-Menten kinetics. Measurement of the rate of substrate conversion by intact microcapsules and of the capsule

contents (obtained by crushing the capsules by mortar-and-pestle) thus led to an estimate of the membrane permeability from the difference of the encapsulated and crushed-capsule reaction rates.

From measurements of the rate of hydrolysis of H_2O_2 by catalase, Morgensen found that the "overall transport coefficient" for combined external and membrane transport resistance was approximately 0.015 cm/sec. Therefore, it was concluded that the membrane permeability >> 0.01 since the "combined" coefficient was very close to the "external film" coefficient of 0.01 cm/sec. This, he concludes, would also agree with the findings of Chang and Poznansky (Table 7) that water is very rapidly transported across the membrane. From the urease-catalyzed decomposition of urea, the membrane permeability was estimated to be $\sim$ 0.001 cm/sec. Chang and Poznansky report a value of 2.33×10^{-4} for collodion microcapsules which was corrected by Morgensen using his more suitably derived diffusion-only equations to be about 3.2×10^{-4} cm/sec, or approximately 1/3 of the value predicted from his measurements. All of this evidence suggests that the membrane permeability is much lower than the value which might be expected from simple extrapolation of the values for conventional semipermeable dialysis membranes, based on thickness considerations only. Morgensen [103] had estimated that the permeability might be as high as 0.34 cm/sec for 500 Å thick membranes using this technique. It would appear, however, that it is unreasonable to expect a decrease in the membrane permeability of over tenfold when the size of the solute has merely doubled, based on the molecular weight, as Morgensen suggests for H_2O_2 and urea.

Morgensen found that encapsulation of catalase by Chang's collodion technique reduced the active enzyme to 1/10 or 1/20 of that initially charged. Tests of the sensitivity of the enzyme to each of the chemicals used in the encapsulation process, except for the collodion and the detergent, Tween 20, used to wash the capsules, showed no effect on the enzyme activity. He therefore concluded that the activity loss resulted from either denaturation by Tween 20 or the collodion, or by failure to encapsulate all of the enzyme. Successive capsule washes with saline solution gave a steady loss of activity, however. It was also found that assays of crushed capsules were very reproducible for a given batch of capsules but a wide variation was observed between batches when the same quantity of enzyme was initially charged. In typical experiments using MEC-catalase the intact-capsule activity was about half that of the crushed-capsule activity. For MEC-urease in batch assay, however, ". . . . in two out of three cases the intact capsules acted as fast as or faster than the crushed capsules. . . . " . This statement would seem to be in conflict with the fact that ". . . . surprisingly. . . the activity of the enzyme [urease] after encapsulation and subsequent release is the same as that of the original enzyme [never encapsulated]. . . . " , unless the enzyme was somehow more active in the encapsulated environment. Unfortunately, Morgensen offers no evidence to prove that the process of crushing the capsules does not cause a change in the encapsulated enzyme.

In summary, Morgensen has presented expressions for describing the expected reaction rates in stirred tank reactors of limited volume for no reaction or first-order internal reaction. The expected substrate conversion for fixed-bed reactors was obtained analytically for first-order reactions and an approximate method

was given for Michaelis-Menten kinetics. Thus, Morgensen provides a method for predicting the permeability of the capsule membrane if one has reliable estimates of the encapsulated and crushed-capsule enzymatic activities and the external film mass transfer coefficient. A healthy scepticism would appear to be in order, however, regarding the reliability of his experimental measurements since a) it seems that the process of crushing the capsules may cause some denaturation of the released enzyme, b) significant quantities of enzyme may have been on the outside of the capsules during the assays, and c) the estimates of the membrane permeabilities for H_2O_2 and urea do not seem to be of reasonable relative magnitude.

III-4. Immobilized Enzyme Reactor Kinetics

Three types of reactors have been utilized for the determination of immobilized enzyme activity: batch reactors, continuous-feed, stirred tank reactors (CSTR), and fixed-bed reactors (FBR) [97, 146]. The equations commonly employed to extract kinetic constants from these reactor configurations with Michaelis-Menten enzyme catalysts are discussed briefly below. (See Satterfield [122] or any recent text on heterogeneous catalysis for a more complete discussion of the factors influencing the design of these reactors.)

III-4-A. Batch Reactor

In the pseudo-steady state, for reactors which have catalyst particles (e.g. capsules) suspended in a homogeneous substrate solution,

$$- V \frac{dc_{so}}{dt} = V_c v_{es} \qquad (3.13)$$

where, in the notation used hereafter for MEC-enzyme catalysts, V is the volume of the reactor not occupied by the capsules, V_c is the volume of the capsules in the reactor, c_{so} is the concentration of the substrate in the bulk solution outside of the capsules, v_{es} is the apparent, externally-observed rate of reaction per unit volume of capsule present, and t is time. Thus the number of moles of substrate leaving the bulk solution equals the number of moles converted to products in the catalyst. If it is assumed that the catalyst particle obeys "apparent" Michaelis-Menten kinetics (Eq. 3.4), then

$$- V \frac{dc_{so}}{dt} = V_c \frac{k_2 E_t c_{so}}{K'_m + c_{so}} \tag{3.14}$$

where K'_m is the "apparent" Michaelis constant. If $v = - V \frac{dc_{so}}{dt}$ and $V_{max} = k_2 E_t V_c$, then Eq. 3.14 can be rewritten as

$$v = \frac{V_{max} c_{so}}{K'_m + c_{so}} \tag{3.15}$$

or, taking the reciprocals of both sides of Eq. 3.15,

$$\frac{1}{v} = \frac{K'_m}{V_{max}} \frac{1}{c_{so}} + \frac{1}{V_{max}} \tag{3.16}$$

A plot of $\frac{1}{v}$ vs. $\frac{1}{c_{so}}$ leads to the estimation of V_{max} and K'_m from the intercept and slope of the best straight line through the data points as in the commonly used Lineweaver-Burk analysis for homogeneous enzyme solutions [9].

Eq. 3.14 can also be integrated upon rearrangement, as

$$- \int_{c^o_{so}}^{c^t_{so}} \left(1 + \frac{K'_m}{c_{so}}\right) dc_{so} = \frac{k_2 E_t V_c}{V} \int_o^t dt \qquad (3.17)$$

where c^o_{so} and c^t_{so} are the bulk substrate concentrations at t = o and t = t respectively. Proceeding with the integration,

$$(c^o_{so} - c^t_{so}) + K'_m \log_e \left(\frac{c^o_{so}}{c^t_{so}}\right) = \frac{k_2 E_t V_c}{V} t \qquad (3.18)$$

or, rearranging Eq. 3.18,

$$K'_m \frac{\log_e (c^o_{so}/c^t_{so})}{t} = \frac{c^t_{so} - c^o_{so}}{t} + \frac{k_2 E_t V_c}{V} \qquad (3.19)$$

and a plot of $\frac{\log_e (c^o_{so}/c^t_{so})}{t}$ vs. $\frac{c^o_{so} - c^t_{so}}{t}$ leads to the estimation of the kinetic constants.

Moo-Young and Kobayashi [101] have shown how Eq. 3.14 can be integrated for more complex kinetic expressions such as those with terms for product inhibition or substrate activation.

It should be kept in mind in this analysis that the assumption of the pseudo-steady state in this application may not be valid for any particular system and so further analysis should be considered to confirm the applicability of the reactor equations presented here. For example, if the rate of diffusion into the catalyst is slow when compared to the reaction rates involved, the penetration of substrate into the central region of the particle may require extended periods of time, thus rendering the "batch" steady-state assumption invalid.

In the event that the "apparent" Michaelis-Menten kinetics as used in Eq. 3.14 are not applicable, this equation can be more generally written as

$$- V \frac{dc_{so}}{dt} = V_c \eta_o \frac{k_2 E_t c_{so}}{K_m + c_{so}} \qquad (3.20)$$

where η_o is the overall effectiveness factor for the system as defined by Satterfield [122] and discussed in Chapter IV of this report. η_o is normally a complex function of all of the system parameters and, therefore, the analytical integration of Eq. 3.20 is not generally possible.

III-4-B. Continuous-feed, Stirred Tank Reactor

The ideal reactor of this type is one wherein a stream of substrate solution flows through a well-mixed vessel in which the catalyst particles are uniformly distributed. The resulting design equation is found by equating, in the steady-state, the number of moles of substrate lost due to reaction to the difference in the moles in the incoming and outgoing streams.

$$V_c v_{es} = Q (c_{s,in} - c_{so}) \qquad (3.21)$$

where Q is the volumetric flow rate of solution through the reactor and $c_{s,in}$ is the concentration of substrate in the inlet stream. As above, v_{es} can be approximated in an "apparent" Michaelis-Menten expression to give

$$V_c \frac{k_2 E_t c_{so}}{K'_m + c_{so}} = Q (c_{s,in} - c_{so}) \qquad (3.22)$$

or written in more general terms as

$$V_c \eta_o \frac{k_2 E_t c_{so}}{K_m + c_{so}} = Q(c_{s,in} - c_{so}) \qquad (3.23)$$

This reactor would appear to be the most desirable type for use in the estimation of kinetic parameters since the system can be assayed under steady-state conditions (assuming the rate of the catalyst denaturation is much slower than the rate at which the steady state is achieved) and all of the enzyme particles reside in a solution of uniform concentration. Hydrodynamic conditions may result, however, in higher agitation rates in some parts of the vessel than in others; this condition could be important if the external mass transfer resistance is a major factor in the overall reaction kinetics.

III-4-C. Fixed Bed Reactor

A mass balance on a differential cross-sectional element of a fixed-bed reactor taken perpendicular to the axis of the reactor results in the following expression in the steady state:

$$\frac{VQ}{V_c A} \frac{dc_{so}}{dz} = v_{es} \qquad (3.24)$$

where A is the cross-sectional area of the bed and z is the distance in the axial direction. For pseudo-Michaelis-Menten kinetics, Eq. 3.24 becomes

$$\frac{VQ}{V_c A} \frac{dc_{so}}{dz} = \frac{k_2 E_t c_{so}}{K'_m + c_{so}} \qquad (3.25)$$

Rearranging and integrating between the reactor inlet (z=0, $c_{so}=c_{so}^{o}$) and outlet (z=L, $c_{so}=c_{so}^{L}$) conditions,

$$\int_{c_{so}^{o}}^{c_{so}^{L}} \left(\frac{K_m'}{c_{so}} + 1 \right) dc_{so} = \frac{k_2 E_t V_c A}{VQ} \cdot \int_{o}^{L} dz \qquad (3.26)$$

or

$$\left(c_{so}^{L} - c_{so}^{o} \right) + K_m' \log_e \left(\frac{c_{so}^{L}}{c_{so}^{o}} \right) = \frac{k_2 E_t V_c}{Q} \qquad (3.27)$$

from which K_m' and $k_2 E_t$ can be found following rearrangement of Eq. 3.27 in a manner analogous to the procedure used for the batch reactor above. As for the batch reactor, the more general formulation of Eq. 3.24 as

$$\frac{VQ}{V_c A} \frac{dc_{so}}{dz} = \eta_o \frac{k_2 E_t c_{so}}{K_m + c_{so}} \qquad (3.28)$$

is typically impossible to solve analytically owing to the complexity of the algebra involved.

III-5. Interpretation of Kinetic Data - Nonlinear Regression Analysis

Recent advances in the methods of interpreting kinetic data should be of great importance in the analysis of immobilized-enzyme kinetics. Cleland [38], for example, has made available statistical algorithms for fitting relatively simple kinetic models to enzyme reaction data. Heineken et al. [70] have also discussed the estimation of parameter values for Michaelis-Menten-type models and have indicated the type of

statistical analysis which will lead to the maximum confidence in the parameter estimates with the fewest experimental measurements. Several other examples of the use of computers for the estimation of kinetic constants in complex enzymatic systems are also available [64, 90, 117].

The use of nonlinear estimation theory in the chemical engineering literature is much more extensive, as the review by Seinfeld [126] attests. Good examples of the application and interpretation of this analysis are given by Kittrell and Mezaki [85, 98]. Several texts [42, 71, 145] will also provide an understandable introduction to this field. Marquardt [95] has developed a flexible computer program for calculating parameter values in nonlinear models; this program, with slight modifications, was used in the present study.

IV. THE KINETICS OF SUBSTRATE CONVERSION BY IMMOBILIZED ENZYME SOLUTIONS

The equations which describe the transport and reaction of substrates in particles containing immobilized enzymes are usually nonlinear and therefore difficult, if not impossible, to solve analytically. In the event that analytical solutions are formidable, numerical methods or the solution of the equations in certain "practical" limiting conditions may provide an adequate description of the problem. This chapter treats the mathematical description of an idealized enzyme-containing particle, approximate solutions for certain limiting conditions, and the comparison of these solutions with numerical computations and the other models.

The equations relating substrate transport and reaction rates in the model MEC enzyme system are presented in Section IV-1. A numerical computation procedure for integration of the steady-state equations and several generalized correlations which are useful for quickly predicting the approximate behavior of immobilized enzyme catalysts are described in Section IV-2. Several steady-state derivations from the literature (Sec. IV-3) and four solutions based on regular and singular perturbation analysis (Sec. IV-4) are then given. Comparison of the classical and perturbation solutions, some comments on the use of other geometries, and a discussion of electrostatic effects are also included as Section IV-5. Treatment of the unsteady-state equations concludes this Chapter in Section IV-6.

IV-1. Problem Description

The idealized system to be discussed here consists of a homogeneous enzyme solution entrapped within a permeable, spherical membrane as shown in Figure 1. The sphere is located within an infinite substrate solution. The membrane is permeable to small substrate molecules but impermeable to larger enzymes; all reaction is therefore confined to the region bounded by the membrane ($r < r_o$). External substrate molecules (S_e) diffuse through the external liquid film ($R_o < r < R_\infty$) and the membrane ($r_o < r < R_o$). The internal substrate (S_i) couples with the enzyme and reacts to form product (P_i). The product then diffuses out of the membrane-bounded region.

A typical substrate concentration profile is shown in Figure 2. Changes in c_s which occur at r_o and R_o indicate the possibility of partitioning of the substrate at the membrane-liquid interfaces. Note that by setting $r_o = R_o$, the model system described above can also be used to represent matrix-bound enzyme systems in which the enzyme is homogeneously distributed in the matrix phase and an "apparent diffusivity" is defined for the substrate in the catalyst particle.

Experimental measurement of the substrate concentration inside such cells cannot normally be made without disruption of the cell integrity. For this reason, the mathematical model of the kinetics which is of greatest utility relates the externally observable rate of substrate uptake to the measured bulk external substrate concentration, physical cell properties, and enzyme kinetic parameters. "Closed-form" analytical solutions are of special interest if non-linear parameter estimation techniques are to be employed. Modelling procedures based on the numerical

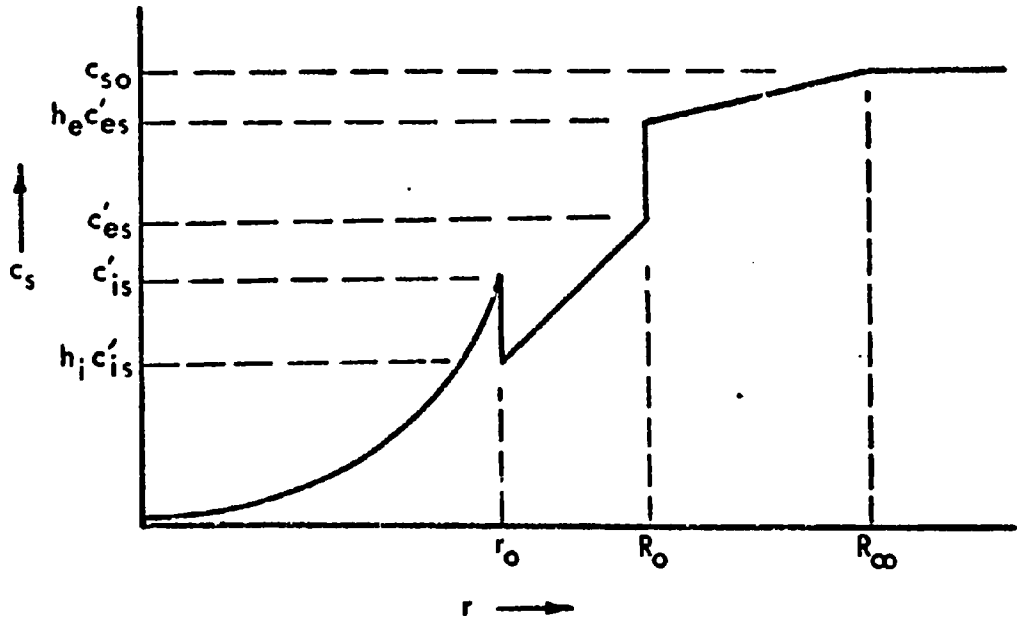

Figure 2. Typical Substrate Concentration Profile In Model Capsule

integration of the internal substrate concentration equations [84,109] are likely to be less informative and more expensive in application to the problem of parameter estimation from experimental data.

Since the capsule membrane can be expected to present a finite and, perhaps, quite high resistance to substrate transfer, the analysis of this system is more complicated than for solid particulate systems. If the resistance to substrate transport to the boundary of the enzyme phase is due only to a hydrodynamic boundary ("unstirred") liquid layer, then one might consider the design of an experiment in which the bulk agitation is high enough to render the film resistance insignificant (this may not prove to be practical in many situations, however). In this case, the kinetics of the reaction would be complicated only by diffusion inside the particle. For the encapsulated enzyme, however, highly agitated conditions will not reduce the membrane resistance except if the membrane were ruptured. Reaction kinetics will always reflect combined diffusion rates outside and inside the enzyme region. The encapsulated enzyme model reduces, of course, to the particulate model if the membrane thickness is set equal to zero.

The following assumptions will be made in the problem development:

1. The enzyme is homogeneously distributed throughout the interior of the cell - for enzymes existing in a liquid, this is equivalent to requiring that the diffusivities of all possible forms of the enzyme are equal;
2. Enzyme reaction kinetics can be represented by an expression of the Michaelis-Menten type with respect to the substrate

concentration, i.e., the volumetric rate of disappearance of S_i is

$$v_s = \frac{k_2 E_t c_{is}}{K + c_{is}} \tag{4.1}$$

where c_{is} is the local substrate concentration and E_t is the concentration of enzyme in all forms. If the reaction kinetics follow the Michaelis-Menten mechanism

$$E + S \underset{k_{-1}}{\overset{k_1}{\rightleftharpoons}} E \cdot S \overset{k_2}{\rightarrow} E + P \tag{4.2}$$

then $K = K_m = (k_2 + k_{-1})/k_1$. Other mechanisms exist which produce kinetic expressions of the type given in Eq. 1. For example, if competitive inhibition occurs,

$$E + I \rightarrow E \cdot I$$

while the inhibitor is homogeneously distributed, then the net effect on the kinetics is to add a constant to K_m, $K = K_m(1+c_{iI}/K_I)$ and the treatment to follow is still valid. An expression similar to Eq. 4.1 can also be used to describe the simplest type of adsorption-reaction kinetics (c.f. Satterfield, [122], p. 176).

3. The internal substrate diffusivity, D_{is}, is the same for all $r<r_o$;
4. The presence of reaction products does not affect the rate of substrate reaction.

A differential mass balance for the substrate leads to the following governing equation in the region where the enzyme is distributed ($r<r_o$):

$$D_{is} \nabla^2 c_{is} - v_s = \frac{\partial c_{is}}{\partial t} \tag{4.3}$$

For steady-state reactions of spherically encapsulated enzymes, Eq. 4.3 reduces to

$$D_{is} \frac{d^2 c_{is}}{dr^2} + \frac{2}{r} \frac{dc_{is}}{dr} = \frac{k_2 E_t c_{is}}{K + c_{is}} \tag{4.4}$$

The boundary conditions which apply are:

$$\begin{aligned} r = r_o: \quad N_s &= D_{is} \frac{dc_{is}}{dr} \\ &= P_s (c'_{es} - h_i c'_{is}) \\ &= k_e \frac{A_{R_o}}{A_{r_o}} (c_{so} - h_e c'_{es}) \\ &= P \left(\frac{c_{so}}{h_e} - h_i c'_{is} \right) \end{aligned} \tag{4.4a}$$

where $$\frac{1}{P} = \frac{A_{r_o}}{A_{R_o}} \frac{1}{h_e k_e} + \frac{1}{P_s}$$

$$r = 0: \quad \frac{dc_{is}}{dr} = 0 \text{ and } 0 < c_{is} < c_{so} \tag{4.4b}$$

N_s is the flux of substrate <u>into</u> the enzyme region, evaluated at $r = r_o$. The factor A_{r_o} / A_{R_o} is the ratio of the membrane area at $r = r_o$ to the area at $r = R_o$. Values for k_e, the external mass transfer coefficient, can be estimated from correlations such as those presented by Satterfield [122].

The apparent externally-observed, volumetric rate of reaction within the confined enzyme phase, v_{es}, is given by Eq. (4.5).

$$v_{es} = \frac{A_{r_o}}{V_{r_o}} N_s = \frac{3}{r_o} N_s \qquad (4.5)$$

where V_{r_o} is the volume of the enzyme phase confined by the membrane.

The following quantities will be used to generalize the analysis to follow:

$$\kappa = K/c_{so} \qquad (4.6a)$$

$$\beta = k_2 E_t r_o^2 / D_{is} K \qquad (4.6b)$$

$$\alpha = P r_o / D_{is} \qquad (4.6c)$$

$$H = h_e h_i \qquad (4.6d)$$

$$\eta_o = v_{es} / (k_2 E_t c_{so} / (K + c_{so})) \qquad (4.6e)$$

$$\rho = v_{es} / k_2 E_t = \eta_o / (1 + \kappa) \qquad (4.6f)$$

β is a Damköhler Number for the enzyme phase with K used as the characteristic concentration. The Sherwood Number, α, is defined for combined membrane and external film mass transfer. η_o, the "overall effectiveness factor" as defined by Satterfield [122] is the ratio of the actual reaction rate to the uniform rate that would be observed at the external substrate concentration, i.e., in the absence of diffusional resistances. This quantity is, therefore, a direct measure of the extent of mass transfer limitation

of the reaction kinetics. Comparison of the mathematical models to be developed below will be based upon the predicted values of ρ, the uptake rate normalized by the maximum possible enzyme catalysis rate.

Eq. 4.4 can now be cast in dimensionless form as

$$\frac{d^2c}{dx^2} + \frac{2}{x}\frac{dc}{dx} = \beta\kappa\frac{c}{c+\kappa} \tag{4.7}$$

where the dimensionless variables are $x=r/r_o$ and $c=c_{is}/c_{so}$. The boundary conditions become, with $c'=c(1)$:

$$x = 1: \quad \frac{dc}{dx} = \alpha\left(\frac{1}{h_e} - h_i c'\right) \tag{4.7a}$$

$$x = 0: \quad \frac{dc}{dx} = 0 \text{ and } 0 < c < 1 \tag{4.7b}$$

ρ is found by combining Eqs. 4.4a, 4.5, and 4.6f to give:

$$\rho = \frac{3}{\beta\kappa}\left.\frac{dc}{dx}\right|_{x=1} \tag{4.8}$$

The normal procedure for treating a system where either "external" or "internal" transport rates may influence the kinetics is to consider the processes separately [122]. "Regimes" of parameter values are defined in which each mode of transport can be expected to be the predominant factor in the net reaction rate. This type of analysis, however, is not sufficient when, for the real system to be considered, neither rate "controls" the kinetics. The derivations presented below are attempts to describe both aspects of the kinetics in a single expression.

IV-2. Numerical Solution Of The Steady-state Kinetic Equations

IV-2-A. Numerical Computation Procedure

The transformation proposed by Na and Na [109] permits the rewriting of the two-point, boundary value problem of Eqs. 4.7 into an initial value problem. The transformation amounts to stretching the concentration coordinate by defining

$$c = Ac^* \text{ or } c^* = c/A \tag{4.9}$$

where A is the transformation parameter. When c^* at $x = 0$ is set equal to 1, resulting in $A = c(x=0)$, Eq. 4.7 is transformed to

$$\frac{d^2c^*}{dx^2} + \frac{2}{x}\frac{dc^*}{dx} = \beta \kappa^* \frac{c^*}{c^* + \kappa^*} \tag{4.10}$$

where $\kappa^* = \kappa/A$. The transformed boundary conditions are:

$$x = 1: \quad \frac{dc^*}{dx} = \alpha(1/Ah_e - h_i c^*(1)) \tag{4.10a}$$

$$x = 0: \quad \frac{dc^*}{dx} = 0 \text{ and } c^* = 1 \tag{4.10b}$$

The numerical integration of Eq. 4.7 then proceeds in the following manner:

1. Values for β, and κ^* are selected;

2. Eq. 4.10 is integrated as an initial value problem from $x = 0$ to $x = 1$ to determine c^* and $\frac{dc^*}{dx}$ at $x = 1$. Intermediate values of c^* are saved as desired;

3. A range of values of α can be chosen and then the corresponding values of A are calculated from Eq. 4.10a as

$$A = 1/(h_i c^*(1) + \frac{1}{\alpha}\frac{dc^*}{dx}\Big|_{x=1}) h_e \tag{4.11}$$

4. The variables can then be retransformed by Eq. 4.9 to the unstretched coordinates to determine the actual concentration profiles and the values of κ. In this way, η_o can be calculated from Eqs. 4.8 and 4.6f for a given β, and a range of values of α and κ.

An alternate calculation algorithm would be the following:

1. Values for c(0), β, and κ are selected;

2. Eq. 4.7 is integrated from x = 0 to x = 1 to find c and $\frac{dc}{dx}$ at x = 1;

3. The value of α corresponding to the assumed set of parameter values can then be calculated from Eq. 4.7a:

$$\alpha = \left.\frac{dc}{dx}\right|_{x=1} \Big/ \left(\frac{1}{h_e} - h_i c(1)\right) \tag{4.12}$$

This procedure then gives η_o vs. α for fixed values of β and κ.

The latter algorithm requires many more computations than the former one to produce the same information, since Eq. 4.7 must be integrated for each set of parameter values.

Application of l'Hospital's rule to Eq. 4.10 leads to the following relationship for $\frac{d^2c^*}{dx^2}$ at x = 0, needed to start the numerical integration:

$$\left.\frac{d^2c^*}{dx^2}\right|_{x=0} = \frac{\beta\kappa^*}{2} \quad \frac{c^*}{c^* + \kappa^*} \tag{4.13}$$

Integration of Eq. 4.7 subject to boundary conditions (4.7a) and (4.7b) has been carried out for many values of β and α. A double precision, four-point Runge-Kutta integration routine with grid spacing of $\Delta x = 0.01$ was used in all cases.

IV-2-B. Generalized Effectiveness Factor Charts

The generalized effectiveness factor charts presented in Figures 3 and 4 are intended to permit rapid estimation of effectiveness factors in immobilized enzyme reactors when h_i and h_e are unity. This information should enable the reactor designer to quickly decide which parameters are important in a specific application and possibly simplify the design analysis.

ϕ, as defined by Eq. 4.14, is a modified form of the Thiele

$$\phi = [r_o^2 k_2 E_t / D_{is}(K + c_{so})]^{1/2} \qquad (4.14)$$

$$= [\beta\varkappa/(1+\varkappa)]^{1/2}$$

Modulus defined by Satterfield [122] as,

$$= \left[\frac{k'_v c_{so}^{m-1} r_o^2}{D_{is}}\right]^{1/2} \qquad (4.15)$$

where k'_v is the "intrinsic reaction-rate constant per unit of gross volume of catalyst pellet" and m is the order of the reaction. Therefore,

$$\text{for } m = 0, \quad \phi_o = [k'_v r_o^2 / D_{is} c_{so}]^{1/2} \qquad (4.15a)$$

$$\text{and} \quad \text{for } m = 1, \quad \phi_1 = [k'_v r_o^2 / D_{is}]^{1/2} \qquad (4.15b)$$

Referring to Eq. 4.1, we see that for enzyme kinetics, in the limits of high and low substrate concentration, v_s approaches zero- and first-order kinetics, with the following intrinsic reaction rate constants.

$$\text{for } K << c_{is}, \; k'_v = k_2 E_t \qquad (4.16a)$$

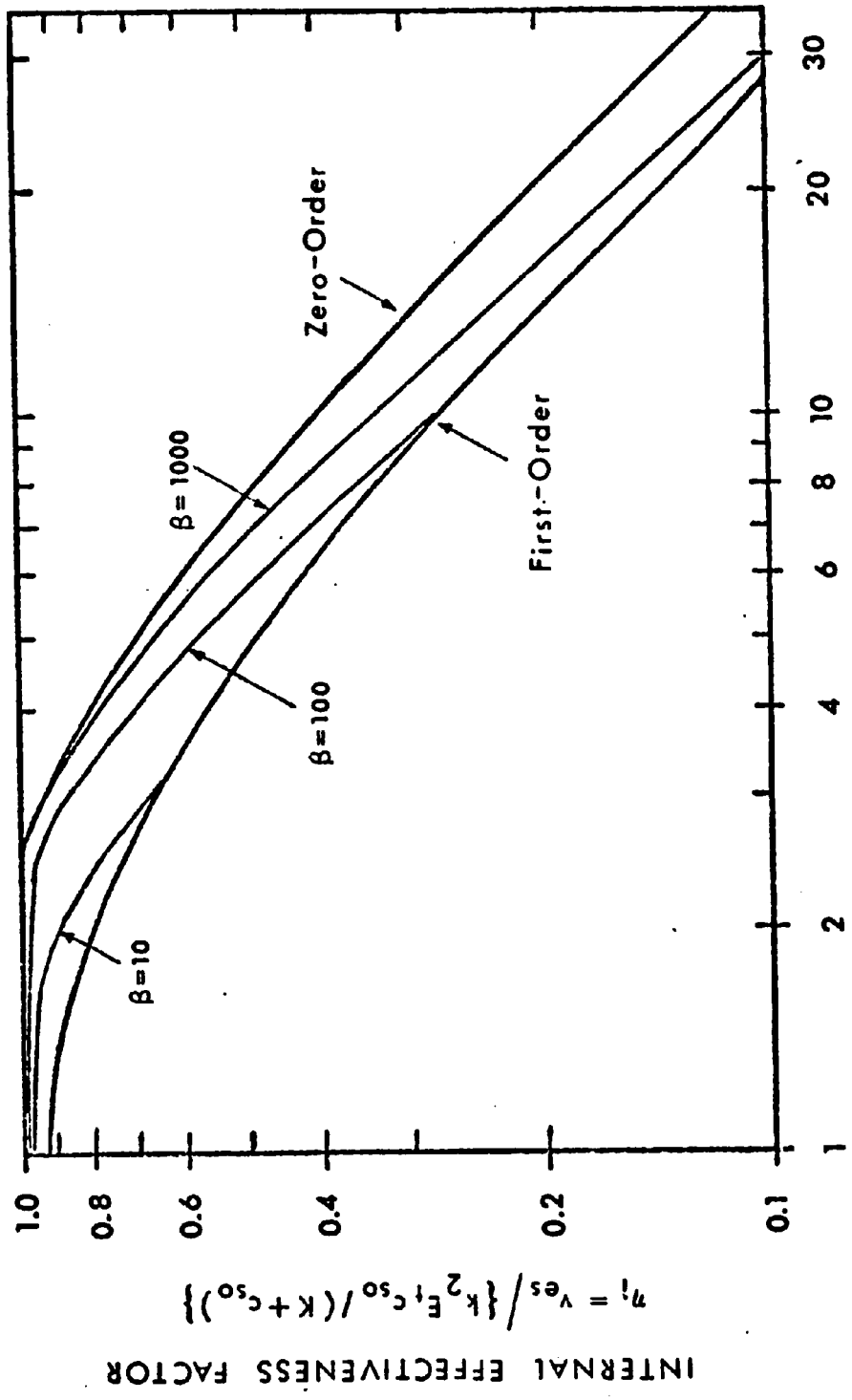

Figure 3. Generalized Internal Effectiveness Factor Chart, Spherically Encapsulated Enzymes. $\beta = (k_2 E_t r_o^2)/(KD_{is})$ and $\kappa = K/c_{so}$. The effect of the external film and membrane resistances has been neglected ($\alpha = Pr_o/D_{is} = \infty$).

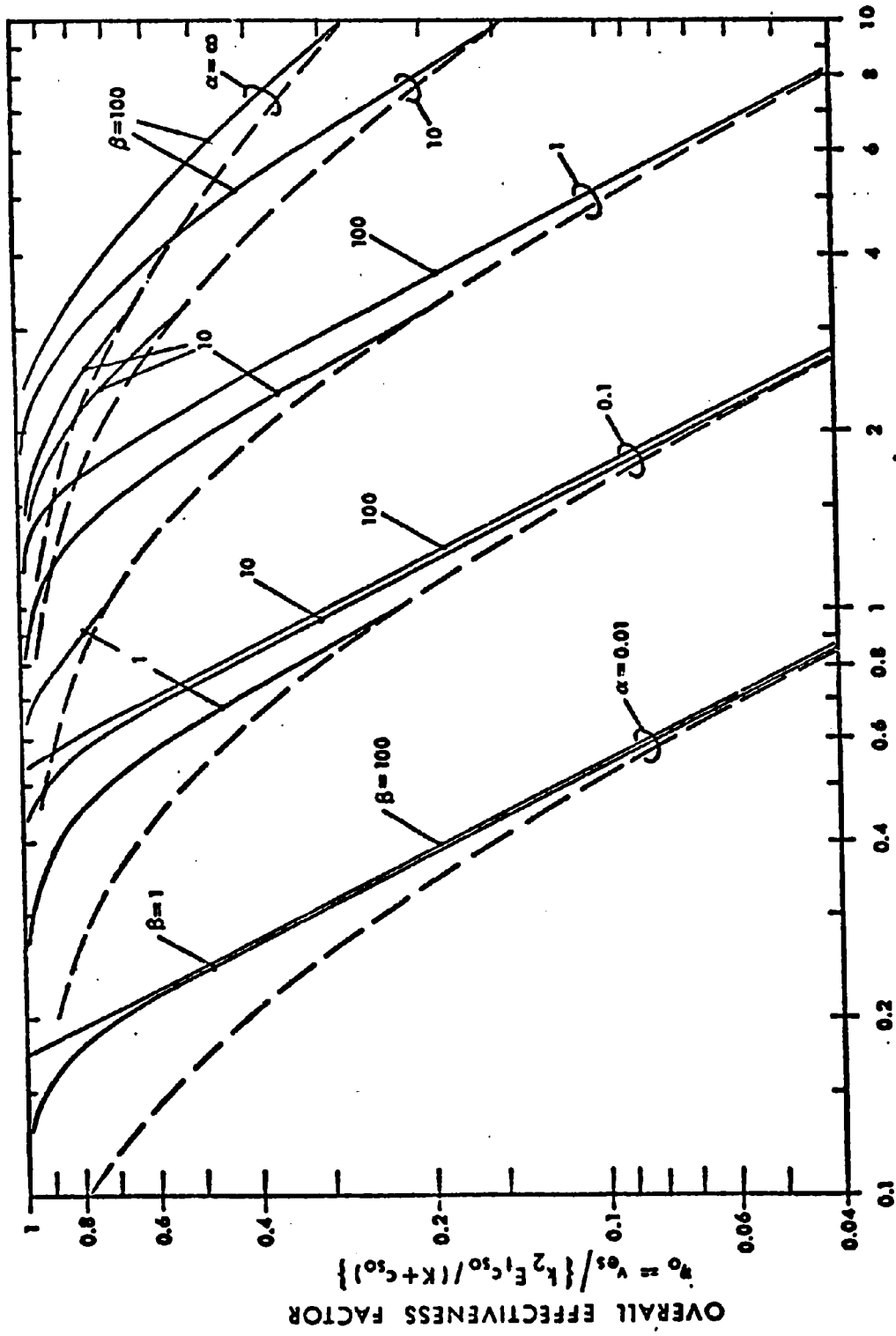

Figure 4. Generalized Overall Effectiveness Factor Chart, Spherically Encapsulated Enzymes. Dashed Lines Are For Analytical Solution Of First-order Reaction Kinetics.

and for $K >> c_{is}$, $k'_v = k_2 E_t / K$ (4.16b)

Therefore, $$\phi_0 = [k_2 E_t r_o^2 / D_{is} c_{so}]^{1/2} \quad (4.17a)$$

$$\phi_1 = [k_2 E_t r_o^2 / D_{is} K]^{1/2} \quad (4.17b)$$

where ϕ_0 and ϕ_1 refer to the zero- and first-order limits of enzyme kinetics.* The Thiele Modulus as defined in Eq. 4.14 conveniently includes the transition from first- to zero-order kinetics as c_{so} is increased. The author tends to agree with Satterfield [122, p. 202] that the use of more complicated "asymptotic" moduli [15, 101] results in a loss of simplicity and physical meaning in defining the system kinetics.

The chart presented in Figure 3 gives the effectiveness factor, η_I, for the internal, enzyme-containing phase only. The computations were made by setting $\alpha = 10^{30}$ (effectively ∞ for these calculations) and proceeding as outlined above.

The upper and lower bounds for η_I as shown in Figures 3 and 4 are provided by assuming zero- and first-order kinetics in Eq. 4.7, respectively.

The definition of ϕ as given in Eq. 4.14 permits one to follow the effect of external substrate concentration in Figure 3 as lines of constant β since a given encapsulated enzyme will have a characteristic value of β. If β is held constant, then a change in the external substrate concentration will be reflected in a change in the Thiele Modulus since $\chi = K/c_{so}$. In Figure 3, for example, with $\beta = 100$ and low substrate concentration

---

*The most commonly used definition for the Thiele Modulus in the enzyme literature appears to be ϕ_1 as used, for example, by Kasche et al. [81], Selegny et al. [125], and Rony [120].

(large κ, first-order kinetics), the effectiveness factor approaches a limit of 0.27 at $\phi = \beta^{1/2} = 10$. For high c_{so} (low κ, zero-order kinetics), η_I is greater than 0.98 for $\phi < 2$. For this particular enzyme system, $\beta = 100$, the internal effectiveness factor varies with external concentration by a range of over threefold between the limits of first- and zero-order kinetics.

Overall effectiveness factors, η_o, which include internal and external diffusion resistances calculated by the algorithm presented above are given in Figure 4. The parameter α gives the relative magnitude of internal to external diffusion resistances. The presence of mass transfer resistances surrounding the enzyme zone can greatly affect the efficiency of the catalyst. For example, considering the same enzyme particle as above ($\beta = 100$) and $\alpha = 1$, the overall effectiveness factor for spheres can vary from 0.98 to 0.027, or over a range of thirty-fold, as the external substrate concentration is changed. The need for the exact numerical solutions for estimating the performance of immobilized enzyme catalysts is evident, therefore, when β as defined here becomes greater than about 10 for spherical particles. When the overall effectiveness factor drops below about 0.1, however, the curves in Figure 4 suggest that little error will be incurred by using first-order kinetics to approximate Michaelis-Menten kinetics.

Generalized effectiveness factor charts comparable to Figures 3 and 4 for immobilized enzymes in planar and cylindrical configurations are presented in Appendices A and B of this report.

IV-3. Semi-analytical Solutions Of The Steady-state Kinetic Equations

IV-3-A. First-Order Reaction Rate Approximation

The most frequently applied approximation in the literature [17, 81, 103, 116, 120, 131] to solve Eq. 4.7 is for $c_{is} << K$ or $c << \mathcal{K}$, where Eq. 4.7 becomes

$$x < 1: \quad \frac{d^2c}{dx^2} + \frac{2}{x}\frac{dc}{dx} = \beta c \tag{4.20}$$

with the boundary conditions as in Eqs. 4.7a and 4.7b. The solution for this case is [120]:

$$\rho = \frac{3\alpha}{h_e \beta \mathcal{K}} \left(\frac{\sqrt{\beta} \coth\sqrt{\beta} - 1}{\sqrt{\beta} \coth\sqrt{\beta} - 1 + \alpha h_i} \right) \tag{4.21}$$

$$\text{or} \qquad \frac{1}{\rho} = \left[\frac{\beta h_e}{3\alpha} + \frac{\beta H}{3(\sqrt{\beta} \coth\sqrt{\beta} - 1)} \right] \mathcal{K} \tag{4.22}$$

If the following definitions are made,

$$\eta_E = \frac{3\alpha}{\beta h_e} \quad \text{and} \quad \eta_I = \frac{3(\sqrt{\beta} \coth\sqrt{\beta} - 1)}{\beta H} \tag{4.23}$$

then, from Eq. 4.22,

$$\rho = \eta_o \frac{1}{\mathcal{K}} \tag{4.24}$$

where

$$\frac{1}{\eta_o} = \frac{1}{\eta_E} + \frac{1}{\eta_I} \tag{4.25}$$

η_E and η_I are effectiveness factors for the external (diffusion only) and internal (enzyme) phases, respectively. The relationship given by Eq. 4.25 has been discussed by many authors [120]. For first-order kinetics, the reciprocals of the effectiveness

factors for the different regions of the system are additive, i.e., the effectiveness factors can be considered the "resistances" to mass transfer. This relationship does not generally carry over to models employing reaction rate expressions other than first-order. Note that the overall effectiveness factor for the first-order approximation is independent of the external bulk substrate concentration.

IV-3-B. Zero-Order Reaction Rate Approximation

When $c_{is} >> K$ or $c >> \kappa$, Eq. 4.7 becomes

$$x < 1: \quad \frac{d^2c}{dx^2} + \frac{2}{x}\frac{dc}{dx} = \frac{1}{x}\frac{d^2}{dx^2}(cx) = \beta\kappa \qquad (4.26)$$

For this case, the local rate of consumption of substrate is a constant. The possibility exists, therefore, that for sufficiently low bulk substrate concentrations, the internal substrate may be depleted in the central region of the cell. The appropriate boundary conditions for this case are, then,

$$x = 1: \quad \frac{dc}{dx} = \alpha\left(\frac{1}{h_e} - h_i c'\right) \qquad (4.26a)$$

$$x = x_o: \quad \frac{dc}{dx} = 0 \quad \text{and} \quad c = 0 \qquad (4.26b)$$

where x_o is the dimensionless radius at which the substrate concentration becomes zero.

Integration of Eq. 4.26 gives

$$c = \frac{\beta\kappa}{6}x^2 + A_o + \frac{B_o}{x} \qquad (4.27)$$

where A_o and B_o are constants of integration. Application of Eqs. 4.26a and 4.26b to Eq. 4.27 leads to the solution presented below:

$$\text{for} \quad \beta\kappa \leq \frac{6h_i\alpha}{h_e(2h_i+\alpha)}, \qquad x_o = 0 \text{ and } \rho = 1 \tag{4.28a}$$

$$\text{for} \quad \beta\kappa > \frac{6h_i\alpha}{h_e(2h_i+\alpha)}, \qquad \rho = 1 - x_o^3 \tag{4.28b}$$

$$\text{and} \quad \beta\kappa = \frac{6/h_e}{\frac{2}{\alpha}(1-x_o^3) + \frac{1}{h_i}(1-3x_o^2+2x_o^3)}$$

The solution for zero-order kinetics therefore consists of two regimes. For values of $\beta\kappa$ smaller than the critical value, substrate exists throughout the cell and the predicted reaction rate is $v_{es} = k_2 E_t$, the maximum possible rate. For $\beta\kappa$ greater than the critical value, the substrate is depleted at $x = x_o$ and an iterative solution for ρ is required.

IV-3-C. Constant Average Reaction Rate Approximation

Rashevsky [116] has presented a detailed solution to Eq. 4.4 for the case of a "constant average" reaction rate throughout the cell. For this case, boundary conditions Eqs. 4.4a and 4.4b still apply but Eq. 4.4 becomes,

$$r < r_o: \quad D_{is}\frac{dc_{is}}{dr^2} + \frac{2}{r}\frac{dc_{is}}{dr} = q \tag{4.29}$$

where q is a constant. Integrating Eq. 4.29 yields

$$c_{is} = \frac{q}{6D_{is}} r^2 + A_1 + \frac{B_1}{r} \tag{4.30}$$

Since c_{is} is finite at $r = 0$, $B_1 = 0$. Substitution of Eq. 4.30 into Eq. 4.4a leads to the expression for c_{is}:

$$c_{is} = \frac{c_{so}}{H} + \frac{q}{6D_{is}} r^2 - q\left(\frac{r_o}{3Ph_i} + \frac{r_o^2}{6D_{is}}\right) \qquad (4.31)$$

Rashevsky [116] defines q as the rate of consumption of substrate calculated from Eq. 4.32,

$$q = \frac{k_2 E_t \overline{c_{is}}}{K + \overline{c_{is}}} \qquad (4.32)$$

where $\overline{c_{is}}$ is the average concentration of substrate inside the cell, i.e.,

$$\overline{c_{is}} = \frac{\int_o^{r_o} c_{is} \cdot 4\pi r^2 dr}{\frac{4}{3}\pi r_o^3} \qquad (4.33)$$

Substituting Eq. 4.31 into Eq. 4.33 and performing the indicated integration gives

$$\overline{c_{is}} = \frac{c_{so}}{H} - \Lambda_s q \qquad (4.34)$$

where

$$\Lambda_s = \frac{r_o}{3Ph_i} + \frac{r_o^2}{15D_{is}} \qquad (4.35)$$

From Eqs. 4.34 and 4.32 then,

$$\overline{c_{is}} = \frac{c_{so}}{H} - \Lambda_s q = \frac{Kq}{k_2 E_t - q} \qquad (4.36)$$

Application of the quadratic formula to Eq. 4.36 gives the expression for q,

$$q = \frac{1}{2}\left\{ \left(k_2 E_t + \frac{c_{so}}{\Lambda_s H} + \frac{K}{\Lambda_s}\right) \pm \left[\left(k_2 E_t + \frac{c_{so}}{\Lambda_s H} + \frac{K}{\Lambda_s}\right)^2 - \frac{4k_2 E_t c_{so}}{\Lambda_s H} \right]^{1/2} \right\} \qquad (4.37)$$

The negatively-signed term in Eq. 4.37 is selected since $q \to 0$ as $c_{so} \to 0$. Factoring Eq. 4.37,

$$q = \frac{1}{2}\left(k_2 E_t + \frac{1}{\Lambda_s}\left(\frac{c_{so}}{H} + K\right)\right) \left\{1 - \left[1 - \frac{4k_2 E_t c_{so}}{\Lambda_s H\left(k_2 E_t + \frac{1}{\Lambda_s}\left(\frac{c_{so}}{H} + K\right)\right)^2}\right]^{1/2}\right\} \quad (4.38)$$

The constant average consumption rate, q, is equivalent to v_{es}, the externally observed volumetric consumption rate. Eq. 4.38 can therefore be rewritten in dimensionless form as:

$$\rho = \frac{1}{2}\left(1+\frac{1}{\Lambda}\left(\frac{1}{H} + \kappa\right)\right) \left\{1 - \left[1 - \frac{4}{\Lambda H\left(1+\frac{1}{\Lambda}\left(\frac{1}{H} + \kappa\right)\right)^2}\right]^{1/2}\right\} \quad (4.39)$$

where

$$\Lambda = \frac{\beta \kappa}{3\alpha h_i} + \frac{\beta \kappa}{15} \quad (4.40)$$

IV-3-D. Approximate Solution For Constant Average Reaction Rate

From the binomial expansion, for small y,

$$(1 - y)^{1/2} \doteq 1 - \frac{1}{2} y \quad (4.41)$$

Therefore, for small $y = 4/\Lambda H\left(1 + \frac{1}{\Lambda}(1+\kappa)\right)^2$, Eq. 4.39 can be approximated as

$$\rho = \frac{1}{1 + H(\kappa + \Lambda)} \quad (4.42)$$

IV-4. Perturbation Solutions For Low And High Steady-state Reaction Rates

Perturbation or matched asymptotic expansion methods have been described in general by many authors (see Acrivos [1] for a particularly simplified introduction) and also applied to several biological diffusion-reaction problems [56,108]. We will not attempt to generally discuss the method of solution here but will describe each step carefully to make comprehension as simple as possible.

If a new dimensionless parameter is defined as $\epsilon = \frac{1}{\beta \kappa}$, Eq. 4.7 can be written in two forms

$$\epsilon \left(\frac{d^2c}{dx^2} + \frac{2}{x} \frac{dc}{dx} \right) = \frac{c}{c+\kappa} = \lambda(c) \tag{4.43}$$

or

$$\frac{d^2c}{dx^2} + \frac{2}{x} \frac{dc}{dx} = \frac{1}{\epsilon} \left(\frac{c}{c+\kappa} \right) = \frac{1}{\epsilon} \lambda(c) \tag{4.44}$$

For small ϵ, the solution to Eq. 4.43 is of singular perturbation type, while for large ϵ, the solution to Eq. 4.44 is of regular perturbation type.

Murray [108] has discussed the singular perturbation solution of Eq. 4.43 in some detail. However, the effect of the membrane on the reaction rate is not completely considered.

IV-4-A. Regular Perturbation Solution For Large ϵ

We will consider first the solution of Eq. 4.44 when ϵ is large. The concentration c is expanded in a power series in arbitrary powers of the perturbation parameter, $1/\epsilon$,

$$c = c_o + \left(\frac{1}{\epsilon}\right)^n c_1 + \left(\frac{1}{\epsilon}\right)^{2n} c_2 + \left(\frac{1}{\epsilon}\right)^{3n} c_3 + \ldots\ldots \qquad (4.45)$$

where n is a positive number but not necessarily an integer.

$\lambda(c)$ is expanded in a Taylor Series around c_o, the "zero-order" concentration from Eq. 4.45,

$$\lambda(c) = \lambda_o + \left.\frac{d\lambda}{dc}\right|_{c_o} (c - c_o) + \frac{1}{2}\left.\frac{d^2\lambda}{dc^2}\right|_{c_o} (c - c_o) + \ldots. \qquad (4.46)$$

or $$\lambda(c) = \lambda_o + \lambda_1 (c - c_o) + \lambda_2 (c - c_o)^2 + \ldots. \qquad (4.47)$$

where $$\lambda_p = \frac{1}{p!}\left.\frac{d^p\lambda}{dc^p}\right|_{c_o}, \quad p = 1, 2, 3, \ldots. \qquad (4.48)$$

From Eq. 4.45, following algebraic rearrangement,

$$\left.\begin{aligned} (c - c_o) &= \left(\frac{1}{\epsilon}\right)^n c_1 + \left(\frac{1}{\epsilon}\right)^{2n} c_2 + \left(\frac{1}{\epsilon}\right)^{3n} c_3 + \ldots. \\ (c - c_o)^2 &= \left(\frac{1}{\epsilon}\right)^{2n} c_1^2 + 2\left(\frac{1}{\epsilon}\right)^{3n} c_1 c_2 + \left(\frac{1}{\epsilon}\right)^{4n} (c_2^2 + 2c_1 c_2) + \ldots. \end{aligned}\right\} \qquad (4.49)$$

Substituting Eqs. 4.49 into Eq. 4.47 and collecting terms,

$$\begin{aligned} \lambda(c) = \lambda_o &+ \left(\frac{1}{\epsilon}\right)^n \lambda_1 c_1 + \left(\frac{1}{\epsilon}\right)^{2n} (\lambda_1 c_2 + \lambda_2 c_1^2) \\ &+ \left(\frac{1}{\epsilon}\right)^{3n} (\lambda_1 c_3 + 2\lambda_2 c_1 c_2 + \lambda_3 c_1^3) + \ldots. \end{aligned} \qquad (4.50)$$

Substituting Eqs. 4.45 and 4.50 into Eq. 4.44,

$$\begin{aligned} &\left[\frac{d^2 c_o}{dx^2} + \left(\frac{1}{\epsilon}\right)^n \frac{d^2 c_1}{dx^2} + \left(\frac{1}{\epsilon}\right)^{2n} \frac{d^2 c_2}{dx^2} + \ldots.\right] + \frac{2}{x}\left[\frac{dc_o}{dx} + \left(\frac{1}{\epsilon}\right)^n \frac{dc_1}{dx} + \ldots.\right] \\ &= \left(\frac{1}{\epsilon}\right) \lambda_o + \left(\frac{1}{\epsilon}\right)^{n+1} \lambda_1 c_1 + \left(\frac{1}{\epsilon}\right)^{2n+1} (\lambda_1 c_2 + \lambda_2 c_1^2) + \ldots. \end{aligned} \qquad (4.51)$$

It can be shown that $n > 1$ leads to a situation where the expansions on the left and right sides of Eq. 4.51 do not match in terms of $1/\epsilon$. Also, for $n < 1$, all matched terms lead to trivial solutions except where $1/\epsilon$ is raised to an integer power. It follows, therefore, that $n = 1$ in Eq. 4.51.

Matching terms in like-powers of $1/\epsilon$ in Eq. 4.51,

$$\left(\frac{1}{\epsilon}\right)^{o} : \frac{d^2 c_o}{dx^2} + \frac{2}{x}\frac{dc_o}{dx} = 0 \tag{4.52}$$

$$\left(\frac{1}{\epsilon}\right)^{1} : \frac{d^2 c_1}{dx^2} + \frac{2}{x}\frac{dc_1}{dx} = \lambda_o \tag{4.53}$$

$$\left(\frac{1}{\epsilon}\right)^{2} : \frac{d^2 c_2}{dx^2} + \frac{2}{x}\frac{dc_2}{dx} = \lambda_1 c_1 \tag{4.54}$$

Equations 4.52, 4.53, and 4.54 are terms the zero-order, first-order, and second-order equations, respectively.

The general procedure for finding the perturbation solution requires the integration of the zero-order, first-order and second-order equations, (e.g., Eqs. 4.52, 4.53, and 4.54) for c_o, c_1, and c_2, respectively. These expressions are then inserted into the expansion equation (e.g., Eq. 4.44), to give the general solution. Higher order solutions may be sought if desired but, generally speaking, these terms should add little to the applicability of the final solution.

When Eq. 4.45 is substituted into the boundary conditions, Eqs. 4.7a and 4.7b, those relationships become:

$$\underline{\text{BC 1}} \quad x = 0 : \quad \frac{dc_i}{dx} = 0 \text{ and } 0 < c_i < c_{so}, \quad i = 0, 1, 2, \ldots . \tag{4.55}$$

$$\underline{\text{BC 2}} \quad x = 1 : \quad \frac{d}{dx}\left[c_o + \left(\frac{1}{\epsilon}\right) c_1 + \left(\frac{1}{\epsilon}\right)^2 c_2 + \ldots . \right]$$

$$= \alpha \left[\frac{1}{h_e} - h_i \left(c_o' + \frac{1}{\epsilon} c_1' + \ldots . \right) \right] \tag{4.56}$$

or, matching terms in $\frac{1}{\epsilon}$ in Eq. 4.56,

$$\left(\frac{1}{\epsilon}\right)^o : \quad \frac{dc_o}{dx} = \alpha \left(\frac{1}{h_e} - h_i c_o' \right)$$

$$\left(\frac{1}{\epsilon}\right)^j : \quad \frac{dc_j}{dx} = \alpha h_i c_j' , \quad j > 1 \tag{4.57}$$

BC 2 can also be expressed as BC 2a by defining $\gamma = \alpha\epsilon$ such that Eq. 4.56 becomes:

$$\underline{\text{BC 2a}} \quad x = 1 : \quad \epsilon \frac{d}{dx} \left(c_o + \frac{1}{\epsilon} c_1 + \ldots . \right)$$

$$= \gamma \left[\frac{1}{h_e} - h_i \left(c_o' + \frac{1}{\epsilon} c_1' + \ldots . \right) \right] \tag{4.58}$$

Matching terms in $1/\epsilon$ in Eq. 4.58 gives

$$\epsilon^1 : \quad \frac{dc_o}{dx} = 0$$

$$\left(\frac{1}{\epsilon}\right)^o : \quad \frac{dc_1}{dx} = \gamma \left(\frac{1}{h_e} - h_i c_o' \right) \tag{4.59}$$

$$\epsilon^{-j} : \quad \frac{dc_{j+i}}{dx} = - \gamma h_i c_j' , \quad j = 1, 2, 3, \ldots$$

The definitions for α, ϵ, and γ are:

$$\alpha = \frac{Pr_o}{D_{is}} \quad ; \quad \epsilon = \frac{D_{is} c_{so}}{k_2 E_t r_o^2} \quad ; \quad \gamma = \frac{Pc_{so}}{k_2 E_t r_o} \quad .$$

In the limit of $k_2 E_t \rightarrow 0$ (slow reaction), $\epsilon \rightarrow \infty$ and $\gamma \rightarrow \infty$ but α remains constant. On the other hand, in the limit of $D_{is} \rightarrow \infty$ (rapid diffusion), $\epsilon \rightarrow \infty$ and $\alpha \rightarrow 0$, but γ remains constant. The use of a boundary condition in which two parameters are reaching limiting values simultaneously suggests that expansions should be carried out for both parameters. For example, if $k_2 E_t \rightarrow 0$, then a power series expansion of $c = c(\gamma)$ in Eq. 4.58 is also appropriate. To circumvent the need for further expansions, we suggest that the boundary condition containing one constant parameter be employed.

Therefore, the system under consideration indicates the use of BC 2 or BC 2a. If the rapid internal substrate transport, $\epsilon \rightarrow \infty$, is reached by small reaction rates, $k_2 E_t \rightarrow 0$, BC 2 should be applied. Conversely, if $\epsilon \rightarrow \infty$ because $D_{is} \rightarrow \infty$, as might be found in systems where facilitated transport of substrate is possible, then the use of BC 2a is advisable. Solutions for both cases are derived below for comparative purposes, without expanding the second limiting parameter.

The regular perturbation solutions of Eq. 4.44 are given in detail in Appendix C of this report where BC 1 (Eq. 4.55) is used in combination with BC 2 (Eq. 4.56) or BC 2a (Eq. 4.58). In summary, these solutions are:

Large ϵ, Finite α (BC 2)

$$\rho = \frac{1}{1 + H\kappa} \left[1 - \frac{H^2 \kappa}{(1 + H\kappa)^2} \Lambda \right] \tag{4.60}$$

Large ϵ, Finite γ (BC 2a)

$$\rho = \frac{c'_o}{c'_o + \kappa} \left\{ 1 - \frac{1}{15\epsilon \left[\frac{(1+H\kappa)^2}{H^2 \kappa} + \frac{1}{3h_i \gamma} \right]} \right\} \tag{4.61}$$

where

$$c'_o = \frac{1}{2} \left\{ \left(\frac{1}{H} - \kappa - \frac{1}{3h_i \gamma} \right) + \left[\left(\frac{1}{H} - \kappa - \frac{1}{3h_i \gamma} \right)^2 + \frac{4\kappa}{H} \right]^{1/2} \right\} \tag{4.62}$$

IV-4-B. Singular Perturbation Solution for Small ϵ

Murray [108] has given the singular perturbation solution to Eq. 4.43 for the case of zero membrane resistance and has compared the resulting concentration profiles to the numerical solutions of Keller [84] with good agreement. We will briefly discuss his solution and apply boundary conditions which include the effect of the membrane resistance.

When ϵ is very small, the concentration gradient is very high in a small region near the cell membrane. It becomes necessary to expand this region of high concentration change by means of the "stretched" radial coordinate defined by Murray as

$$\xi = \epsilon^{-1/2} (1 - x) \tag{4.63}$$

The correspondingly transformed concentration variable is $f(\xi) = c(x)$. The reasons for using $\epsilon^{-1/2}$ in Eq. 4.63 are explained in detail by Murray. Using these new variables, Eq. 4.43 is transformed to

$$\frac{d^2f}{d\xi^2} - \frac{3\epsilon^{1/2}}{1-\epsilon^{1/2}\xi}\frac{df}{d} = \frac{f}{f+\xi} = \lambda(f) \qquad (4.64)$$

This expression differs from the equivalent equation presented by Murray as his Eq. 36 by the negative sign in front of the second term on the left-hand side. Murray's error in presenting this equation does not affect his solution since this term does not contribute to the analysis.

Equation 4.64 suggests expanding f in a power series in $\epsilon^{1/2}$ as

$$f = f_o + \epsilon^{1/2} f_1 + \epsilon f_2 + \ldots \qquad (4.65)$$

Expanding $\lambda(f)$ in a Taylor Series, following Eq. 4.46 through 4.50,

$$\lambda(f) = \lambda_o + \epsilon^{1/2}\lambda_1 f_1 + \epsilon(\lambda_1 f_2 + \lambda_2 f_1^2) + \ldots \qquad (4.66)$$

Expanding $2\epsilon^{1/2}/(1-\epsilon^{1/2})$ using the Binomial Expansion,

$$\frac{2\epsilon^{1/2}}{1-\epsilon^{1/2}} = 2\epsilon^{1/2}(1+\epsilon^{1/2} + \epsilon^2 + \ldots)$$

$$= 2(\epsilon^{1/2} + \epsilon + \epsilon^{3/2} 2 + \ldots) \qquad (4.67)$$

Substituting Eqs. 4.65 - 4.67 into 4.64 and equating terms in like-powers of ϵ gives

$$\epsilon^{0} : \frac{d^2 f_o}{d\xi^2} = \lambda_o$$

$$\epsilon^{1/2} : \frac{d^2 f_1}{d\xi^2} - 2\frac{df_o}{d\xi} = \lambda_1 f_1 \qquad (4.68)$$

$$\epsilon^{1} : \frac{d^2 f_2}{d\xi^2} - 2\left(\xi \frac{df_o}{d\xi} + \frac{df_1}{d\xi}\right) = \lambda_1 f_2 + \lambda_2 f_1^2$$

The transformed boundary conditions are found by inserting Eq. 4.65 into Eqs. 4.7a and 4.7b:

BC 1

$$\xi = \infty : \frac{df_j}{d\xi} = 0 \text{ and } f_j = 0 \text{ for } j = 1, 2, 3, \ldots \qquad (4.69)$$

BC 2

$$\xi = 0 : -\epsilon^{-1/2}\left(\frac{df_o}{d\xi} + \epsilon^{1/2}\frac{df_1}{d\xi} + \ldots\right)$$

$$= \alpha\left[\frac{1}{h_e} - h_i(f_o' + \epsilon^{1/2} f_1' + \ldots)\right] \qquad (4.70)$$

or, matching terms in like-powers of ϵ,

$$\epsilon^{-1/2} : \frac{df_o}{d\xi} = 0 \text{ for all } \xi \; ; \; \therefore f_o = \text{constant} = 0$$

$$\epsilon^{0} : \frac{df_1}{d\xi} = -\alpha\left(\frac{1}{h_e} - h_i f_o'\right) = -\frac{\alpha}{h_e} \qquad (4.71)$$

$$\epsilon^{j/2} : \frac{df_j}{d\xi} = \alpha h_i f_{j-1}' \text{ for } j = 2, 3, 4, \ldots$$

If $\gamma = \alpha\epsilon$ is finite, following the logic developed in Section IV-4-A, then BC 2 is rewritten as BC 2a:

BC 2a

$$\xi = 0 : \quad -\epsilon^{1/2}\left(\frac{df_o}{d\xi} + \epsilon^{1/2}\frac{df_1}{d\xi} + \ldots\right)$$

$$= \gamma\left[\frac{1}{h_e} - h_i\left(f_o' + \epsilon^{1/2} f_1' + \ldots\right)\right] \qquad (4.72)$$

or, matching terms in like-powers of ϵ,

$$\epsilon^{o} : \quad \gamma\left(\frac{1}{h_e} - h_i f_o'\right) = 0 \; ; \quad \therefore \text{ for finite } \gamma, \; f_o' = 1$$

$$\epsilon^{j/2} : \quad \frac{df_{j-1}}{d\xi} = \gamma h_i f_j' \; , \quad j = 1, 2, 3, \ldots \qquad (4.73)$$

The singular perturbation solutions are given in detail in Appendix D. In summary, these solutions are:

Small ϵ, Finite γ (B 2)

$$\rho = 3\gamma\left\{\frac{1}{h_e} - h_i + \frac{\sqrt{2}\epsilon^{1/2}}{\gamma}\left[1 + \kappa \log_e\left(\frac{\kappa}{1+\kappa}\right)\right]^{1/2}\right\} \qquad (4.74)$$

Small ϵ, Finite α (BC 2a)

$$\rho = \frac{3\gamma}{h_e}\left[1 - \alpha\epsilon^{1/2}\kappa^{1/2}h_i - \alpha\epsilon\kappa h_i + \alpha^2\epsilon\left(\frac{h_i}{h_e} + h_i^2\kappa\right)\right] \qquad (4.75)$$

IV-5. Discussion Of The Steady-state Models

IV-5-A. Comparison of the Models

The substrate conversion models developed in Sections 3 and 4 of this chapter are summarized in Table 10. We will discuss briefly some of the interesting aspects of each model and attempt to indicate in which regime each is applicable. Where comparison to numerical computations is indicated, calculations were made by the procedure described in Section IV-2. The nature of the approximations used in Models 1 thru 4 are shown schematically in Figure 5.

Model 1: First-Order Kinetics

It can be easily seen from Figure 5 that the first-order approximation to the Michaelis-Menten kinetics will always predict a higher reaction rate than the enzyme kinetics, possibly even higher than $v_s = k_2 E_t$. The error in using this approximation can be expressed for a given local c_s as

$$\% \text{ Error} = \frac{\frac{k_2 E_t}{K} - \frac{k_2 E_t c_s}{K + c_s}}{\frac{k_2 E_t c_s}{K + c_s}} \times 100$$

$$= \frac{K}{c_s} \times 100 \qquad (4.76)$$

Use of the approximate first-order solution when local concentrations inside the enzyme phase are of O(K) can therefore result in an overprediction of the cell reaction rate of up to

Table 10

Summary of Substrate Conversion Models for Encapsulated Enzymes

$$\alpha = \frac{Pr_o}{D_{is}} \qquad \beta = \frac{k_2 E_t r_o^2}{D_{is} K} \qquad \kappa = \frac{K}{c_{so}} \qquad \epsilon = \frac{1}{\beta\kappa} = \frac{D_{is} c_{so}}{k_2 E_t r_o^2} \qquad \gamma = \alpha\epsilon = \frac{Pc_{so}}{k_2 E_t r_o}$$

Model #	Conditions of Derivation	Model Expression For Dimensionless Conversion Rate, ρ, (Eq. #)
1	$v_s = \frac{k_2 E_t}{K} c_{is}$, $(c_{is} \ll K)$	$\rho_1 = \frac{3\gamma}{h_e \beta\kappa} \left(\frac{\sqrt{\beta}\coth\sqrt{\beta} - 1}{\sqrt{\beta}\coth\sqrt{\beta} - 1 + \alpha h_i} \right)$ (4.21)
2	$v_s = k_2 E_t$, $(c_{is} \gg K)$	if $\beta\kappa \leq \frac{6h_i\alpha}{h_e(2h_i+\alpha)}$, $\rho_2 = 1$ (4.28a)
		if $\beta\kappa > \frac{6h_i\alpha}{h_e(2h_i+\alpha)}$, $\rho_2 = 1 - x_o^3$ (4.28b)
		and $\beta\kappa = \frac{6/h_e}{(2/\alpha)(1-x_o^3) + (1/h_i)(1-3x_o^2+2x_o^3)}$
3	$v_s = \frac{k_2 E_t \overline{c_{is}}}{K + \overline{c_{is}}}$ = constant	$\rho_3 = \frac{1}{2}\left(1 + \frac{1}{\Lambda}\left(\frac{1}{H} + \kappa\right)\right)\left\{1 - \left[1 - \frac{4}{\Lambda H\left(1 + \frac{1}{\Lambda}\left(\frac{1}{H}+\kappa\right)\right)^2}\right]^{1/2}\right.$ (4.39)
4	Binomial Approximation of # 3	$\rho_4 = \frac{1}{1 + H(\kappa + \Lambda)}$ (4.42)

Table 10

(continued)

Model #	Conditions of Derivation	Model Expression For Dimensionless Conversion Rate, ρ, (Eq. #)
5	Regular Perturbation Solution, Large ϵ, Finite α	$\rho_5 = \frac{1}{1+H\kappa}\left[1 - \frac{H^2\kappa}{(1+H\kappa)^2}\Lambda\right]$ (4.60)
6	Regular Perturbation Solution, Large ϵ, Finite γ	$\rho_6 = \frac{c_o'}{c_o'+\kappa}\left\{1 - \frac{1}{15\epsilon\left[\frac{(1+H\kappa)^2}{H^2\kappa} + \frac{1}{3\gamma h_i}\right]}\right\}$ (4.61)
		where c_o' is defined in Eq. 4.62
7	Singular Perturbation Solution, Small ϵ, Finite γ	$\rho_7 = 3\gamma\left\{\frac{1}{h_e} - h_i + \frac{\sqrt{2}\,\epsilon^{1/2}}{\gamma}\left[1+\kappa\log_e\left(\frac{\kappa}{1+\kappa}\right)\right]^{1/2}\right\}$ (4.74)
8	Singular Perturbation Solution, Small ϵ, Finite α	$\rho_8 = \frac{3\gamma}{h_e}\left[1 - \alpha\epsilon^{1/2}\kappa^{1/2}h_i - \alpha\epsilon\kappa h_i + \alpha^2\epsilon\left(\frac{h_i}{h_e} + h_i\kappa\right)\right]$ (4.75)

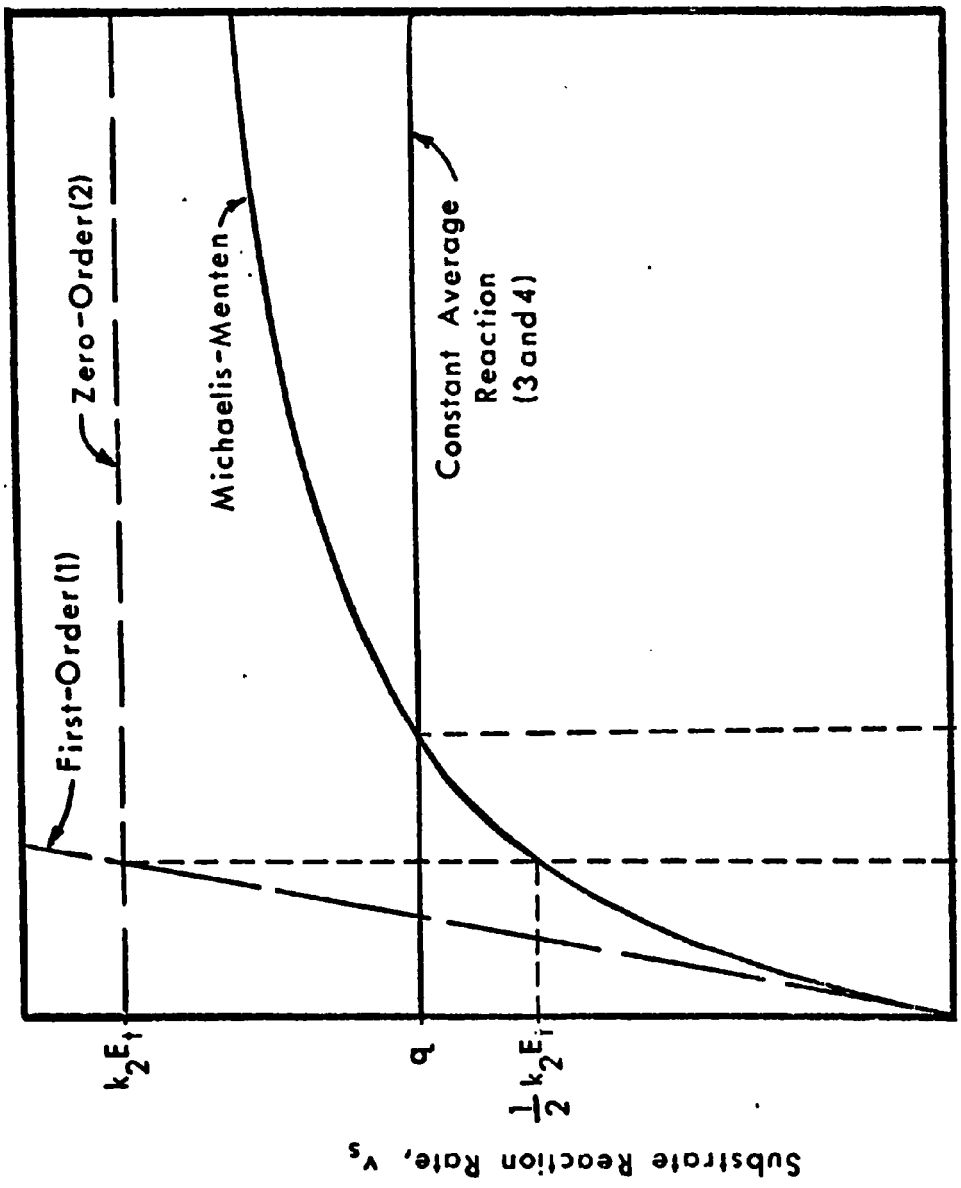

Figure 5. Schematic Interpretation of Reaction Rate Approximations For Models 1, 2, 3, and 4

100%. This argument emphasizes the necessity of using this approximation only when one is certain that $c_{is} \ll K$.

The curves in Figure 6 give the locus of points for which the use of Model 1 will result in an error of approximately 5% above the prediction using Michaelis-Menten kinetics. For example, if $\alpha = 1$ and $\beta = 100$, then for values of $\kappa = K/c_{so}$ greater than about 0.1, the error will be less than 5%.

Model 2: Zero-Order Kinetics

This model would seem to be difficult to solve when β is greater than the critical value, since an iterative solution is required for x_o in Eq. 4.28b. The use of the zero-order kinetics is useful, however, in placing a reliable upper limit on the expected substrate conversion rate when $c_{so} > K$. We can see no utility in using this model to estimate parameter values except when $\eta_o \approx 1$.

Model 3: Constant "Average" Reaction Rate

Rashevsky [116], Best [14], and Hearon [68] have discussed this model in detail. We feel that this development describes the system over the widest range of parameter combinations and as such is the one that probably should be considered first in selecting a model.

A schematic interpretation of this analysis is presented in Figure 7. The "average" reaction rate is given by the point of intersection of the "diffusion" rate line, written by rearranging Eq. 4.34 when H = 1 as

$$q = \frac{1}{\Lambda_s}(c_{so} - \bar{c}_{is}) \qquad (4.77)$$

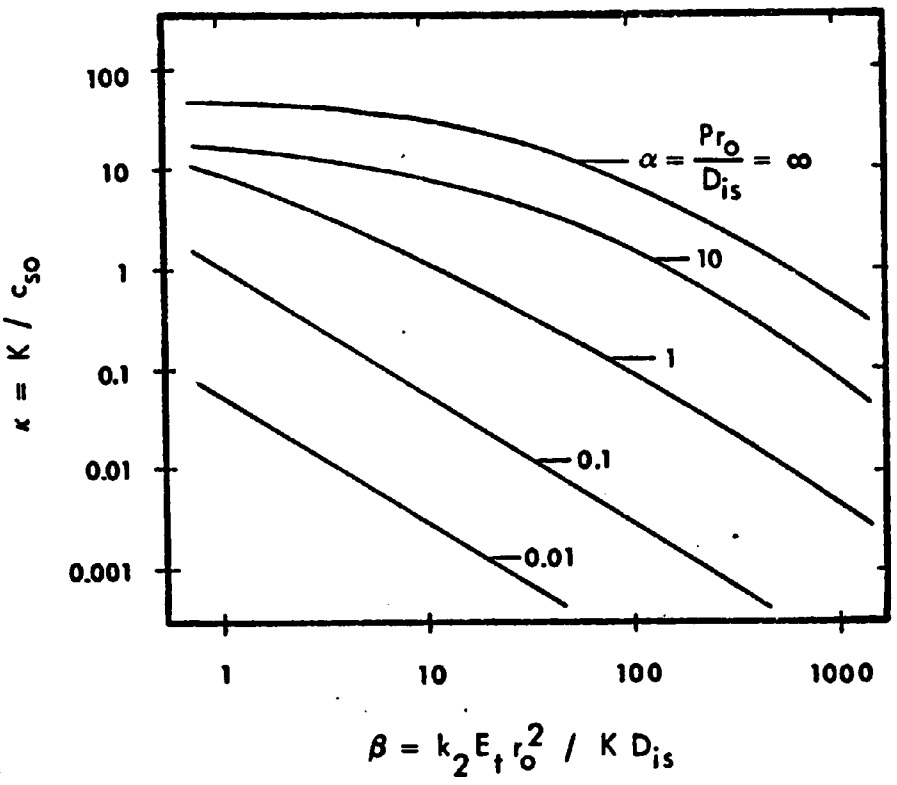

Figure 6. Locus of points for which model 1 is within 5% of the Michaelis-Menten kinetics reaction rate. The region of validity is above the appropriate line

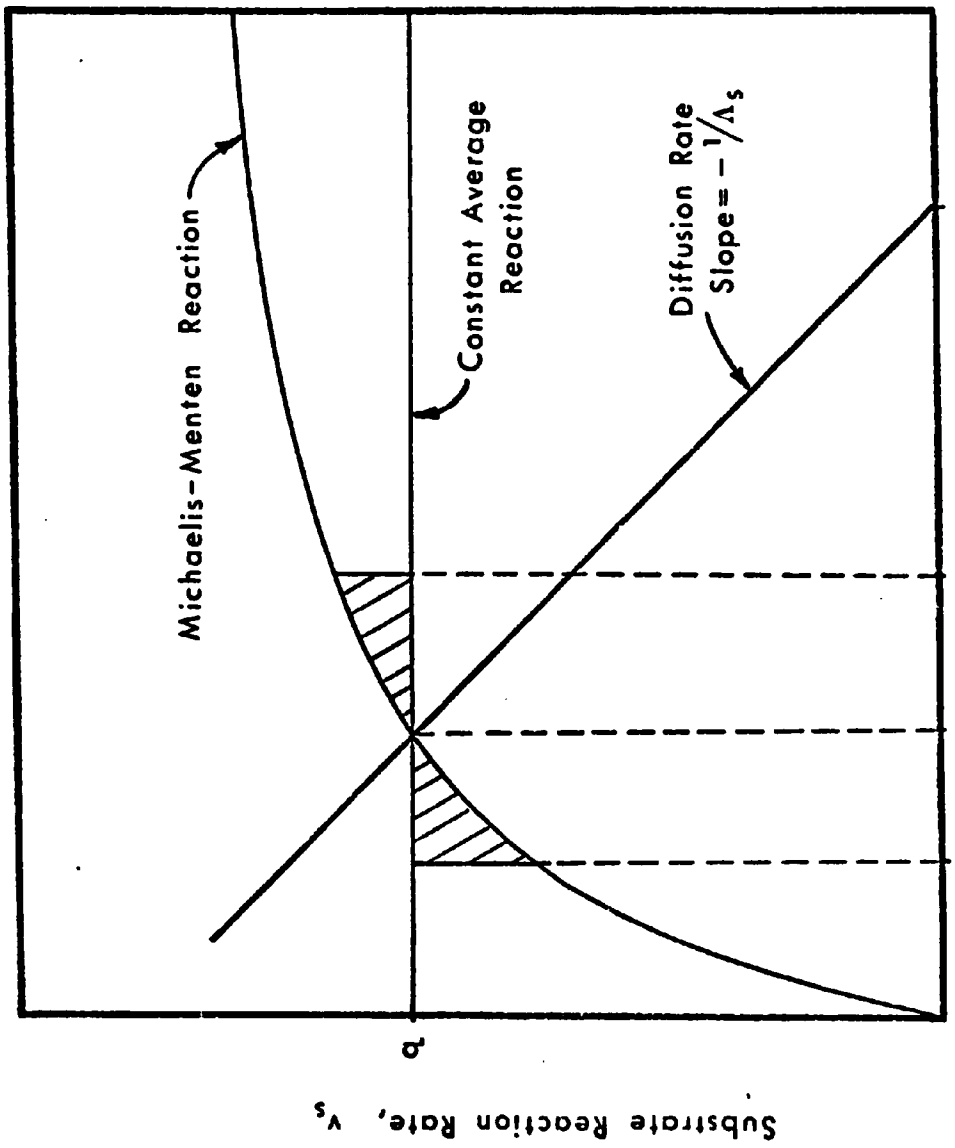

Figure 7. Average Reaction Rate Interpretation For Model 3

and the "reaction" rate curve

$$q = \frac{k_2 E_t \bar{c}_{is}}{K + \bar{c}_{is}} \tag{4.78}$$

The value of $\bar{c}_{is}$ arises from averaging the concentration over the interior of the capsule from c_{is} (x=0) to c_{is} (x-1) according to Eq. 4.33. Therefore, it should be expected that model 3 will be more realistic when the concentration change inside the cell is relatively small. This situation can occur when the external substrate concentration is small, the reaction rate, q, is low or diffusion rates, $1/\Lambda_s$, are high.

The parameter Λ_s is useful as a measure of the overall resistance to mass transfer in the system (cf. Best [14], p. 153, for further discussion of this point).

Following a different logic, Blum and Jenden [18] develop an expression which can be rearranged to exactly the same form as model 3. The reaction term on the right-hand side of Eq. 4.4 is linearized around an arbitrary internal concentration by Taylor series expansion. Later in the derivation, this concentration is taken to be the one in the Michaelis-Menten expression, Eq. 4.1, which will give the externally observed reaction rate. These authors also present a graphical method for estimating the system parameters when cells of varying diameters are available.

From Eq. 4.31 it follows that for

$$\frac{c_{so}}{Hq\left(\frac{r_o}{3h_i P} + \frac{r_o^2}{6D_{is}}\right)} < 1 \tag{4.79}$$

the predicted substrate concentration in the central region of the enzyme phase will be less than zero. Eq. 4.79 therefore is a useful criterion for the limit of the physical interpretation of model 3. Generally speaking, we have found from comparisons with numerical computations that this model should only be employed when $\Lambda < 1$.

Model 4: Binomial Approximation for Model 3

The binomial approximation used in Eq. 4.41 will be reasonable (<3% error) for $y < 0.4$. For $H = 1$ and $\chi \ll 1$,

$$y \doteq \frac{4}{(1+\frac{1}{\Lambda})^2} = \frac{4}{\Lambda + 2 + \frac{1}{\Lambda}} \qquad (4.80)$$

and y in Eq. 4.80 will be less than about 0.4 for $\Lambda > 10$ and $\Lambda < 0.1$. Since model 3 is not applicable for $\Lambda > 10$, then we do not expect model 4 to be either. In general, our computations have shown that model 4 is reasonably accurate for $\Lambda < 0.1$.

The interesting characteristic of Eq. 4.42 is that, for low reaction-to-diffusion rate ratios, the diffusive resistance enters into the kinetics as an additive term to the Michaelis-Menten constant. Experimental estimation of K for immobilized enzyme particles can therefore lead to prediction of mass transfer parameters P or D_{is} if the conversion rates are sufficiently low.

Models 5 and 6: Regular Perturbation Solutions

We find that models 5 and 6 are in acceptable agreement (error < 5%) with numerical computations up to values of somewhat higher than model 4 but lower than model 3. We see no advantage in using model 6 due to the complexity of the expression.

For approximate calculations, however, model 5 seems to be better suited for predicting diffusion resistances (Λ) than model 4 when estimates of ρ, H, and κ are available. Note in Eq. 4.60 that the effect of the mass transfer resistance is not to directly increase κ as in model 4. A "diffusion-correction" term is instead subtracted from the maximum possible reaction rate

$$\rho_{max} = \frac{c_{so}/h_e h_i}{\frac{c_{so}}{h_e h_i} + K} = \frac{1}{1 + H\kappa} \tag{4.81}$$

Since, for sufficiently small y,

$$1 - y \doteq \frac{1}{1 + y} \tag{4.82}$$

then, for small values of the "diffusion-correction" term,

$$\rho_5 = \frac{1}{1+H\kappa} \left[1 - \frac{H^2\kappa}{(1+H\kappa)^2} \Lambda\right] \tag{4.60}$$

$$\doteq \frac{1}{1+H\kappa} \left[\frac{1}{1 + \frac{H^2\kappa}{(1+H\kappa)^2}\Lambda}\right] \tag{4.83}$$

or

$$\rho_5 \doteq \frac{1}{1 + H\left(\kappa + \frac{H\kappa}{1 + H\kappa}\Lambda\right)} \tag{4.84}$$

Eq. 4.84 is very similar to model 4, except that the diffusive effect on the Michaelis-Menten constant is more complex then a simple additive term.

Models 7 and 8: Singular Perturbation Solutions

Many authors [58,101,125,131] have shown that for enzymes bound into planar membranes, an expression very similar to model 7, Eq. 4.7-4, rigorously relates the substrate concentrations and fluxes into the membrane at the surface. For example, the equation given by Selegny, Brown and Thomas [125] as their Eq. 5 can be rewritten in our notation as

$$(N_1)^2-(N_2)^2 = 2k_2E_tD_{is}\left[(c'_{s1}-c'_{s2})-K\log_e\left(\frac{c'_{s1}+K}{c'_{s2}+K}\right)\right] \qquad (4.85)$$

N_1 and N_2 refer to substrate fluxes into the membrane from sides 1 and 2 while c'_{s1} and c'_{s2} are the corresponding surface concentrations. The situation which directly corresponds to our system is for penetration of only one surface by substrate, i.e., $N_2 = 0$ and $c'_{s2} = 0$, so that

$$N_1^2 = 2k_2E_tD_{is}\left[c'_{s1} - K\log_e\left(\frac{c'_{s1}+K}{K}\right)\right] \qquad (4.86)$$

or, in terms of dimensionless quantities,

$$\rho = \sqrt{2}\,\epsilon^{1/2}\left[c'_1 - \kappa\log_e\left(\frac{c'_1+K}{K}\right)\right] \qquad (4.87)$$

Eq. 4.87 becomes equivalent to Eq. 4.74, except for the geometric factor of 3, when $h_e = h_i = 1$ and $c'_1 = 1$, i.e., no external resistance to mass transfer.

This discussion emphasizes the need for caution in using model 7 to describe the kinetics of substrate conversion in the spherical case. Although a similar expression analytically

solves the equation for planar geometry in the absence of external and membrane resistance, our development indicates that Eq. 4.74 is valid only asymptotically for the spherical case. In other words, model 7 applies only for the limiting conditions of zero substrate concentration at the center of the cell and "high" reaction-to-diffusion rate ratios. This model predicts the highest possible conversion rate in the absence of external mass transfer limitation. It should be noted here also that only the complexity of the algebra has kept the membrane resistance from appearing in the kinetic expression since only the "zero-order" term could be evaluated.

The expression presented as model 8 predicts, in the limit of small ϵ, very nearly the same value of ρ as model 1, the first-order solution. In fact, the range of parameter values for which it applies is somewhat smaller than for model 1. We can see no utility in the application of this model except in the simplicity of the terms. Use of only the zero- and first-order terms in Eq. 4.75, i.e., terms in ϵ^{0} and $\epsilon^{1/2}$, does not greatly effect the validity of the solution.

General Discussion of Models

Predicted values of ρ for the eight models presented in Table 10 as well as for numerical computations are presented in Figure 8 for the arbitrarily selected values of $\varkappa = 1$, $\alpha = 10$, and a range of ϵ. Since $\varkappa$ is fixed, an increase in ϵ in Figure 8 represents an increase in the quantity $D_{is}/r_o^2 k_2 E_t$. It can be seen from this figure that, although several of the models predict the expected reaction rate for a limited range of ϵ, none apply over the entire range.

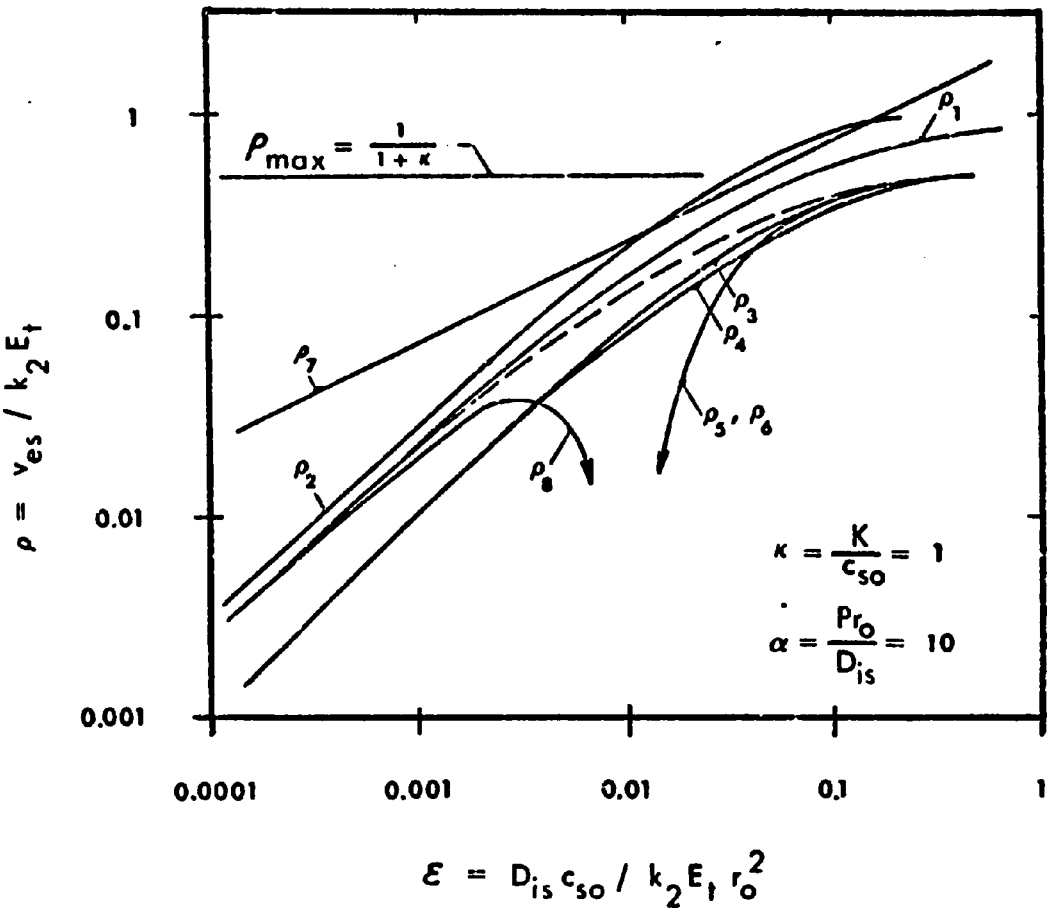

Figure 8. Illustration of the Regions of Validity for the Substrate Conversion Models Given in Table 10. The Dashed Line Is The Numerically Generated Solution.

In general, we have found that increasing α tends to enlarge the spread of the model predictions around the exact value while for very small α, nearly all the models predict the expected value well.

IV-5-B. Generalization to Other Geometries

Rony [120] has shown how the first-order model can be generalized for immobilized enzyme systems in planar, cylindrical, or spherical configurations. It can be easily shown that models 3 and 4 can be made to apply in general by defining

$$\Lambda_p = \beta \varkappa \left(\frac{1}{(p+2)h_i \alpha} + \frac{1}{(p+2)(p+4)} \right) \qquad (4.88)$$

where p is a geometric factor equal to -1, 0, and +1 for the planar, cylindrical, and spherical cases, respectively. For the planar case, r as we have defined it is measured from the point in the membrane at which Eq. 4.4b is valid. If substrate is entering from only one side of the membrane and cannot penetrate the other side, r_o is the thickness of the membrane. If substrate is entering both sides from solutions of equal concentrations, r_o is then one half the membrane thickness.

When p is defined as in Eq. 4.88, Eqs. 4.39 and 4.42 are correct for any of the three geometries.

IV-5-C. Effect of Electrostatic Membrane Charges on the Kinetics of Substrate Conversion

Several authors [59,66,73,128] have considered the effect of the electrostatic field produced by fixed charges on a nonporous surface on the rate of reactions catalyzed by enzymes bound to

the surface. Shuler et al. [128] have shown, for example, that the flux of substrate to the surface arising from combined diffusive and electrostatic forces will be of the form

$$N_s = D_{es} \frac{dc_{es}}{dy} + c_{es} \frac{zD_{es}F}{RT} \frac{d\psi}{dy} \qquad (4.89)$$

where c_{es} is the external substrate concentration, y is the distance measured from the surface, z is the substrate valence, D_{es} is the external substrate diffusivity, F and R are the Faraday's and gas constants, respectively, T is the absolute temperature, and $\psi(y)$ is the electrostatic potential at y.

Defining

$$\lambda^* = \frac{zF\psi(o)}{RT} \quad \text{and} \quad \delta = \frac{D_{es}}{k_e}$$

where δ is the external diffusion film thickness, Shuler et al. arrived at

$$N_s = M k_e [c_{so} - c'_{es} e^{\lambda^*}] \qquad (4.90)$$

where

$$M^{-1} = \frac{1}{\delta} \int_o \exp \left(\frac{\lambda^* \psi(y)}{\psi(o)} \right) dy \qquad (4.91)$$

Shuler et al. solved Eq. 4.91 using the Gouy diffuse double-layer expression

$$\psi(y) = \psi(o)\, e^{-\kappa^* y} \qquad (4.92)$$

where $1/\kappa^*$ is the thickness of the diffuse double-layer. Hamilton et al. [66] have more recently solved Eq. 4.91 for the more general Gouy-Chapman expression

$$\psi(y) = \frac{2RT}{zF} \log_e \left[\frac{C_1 + C_2 \exp(-\kappa^* y)}{C_1 - C_2 \exp(-\kappa^* y)} \right] \qquad (4.93)$$

where

$$C_1 = e^{\lambda^*/2} + 1 \quad \text{and} \quad C_2 = e^{\lambda^*/2} - 1 \ .$$

It is possible to incorporate these developments into our derivations for the case of fixed charges on the outside of the membrane. The boundary equation at $r = r_o$, Eq. 4.4a, becomes

$$\begin{aligned} r = r_o: \quad N_s &= P_s(c'_{es} - h_i c'_{is}) \\ &= Mk_e \frac{A_{R_o}}{A_{r_o}} (c_{so} - h_e e^{\lambda^*} c'_{es}) \\ &= P^* \left(\frac{c_{so}}{h_e^*} - h_i c'_{is} \right) \end{aligned} \tag{4.94}$$

where

$$\frac{1}{P^*} = \frac{1}{P_s} + \frac{1}{Mh_e^* k_e (A_{R_o}/A_{r_o})} \tag{4.95}$$

and

$$h_e^* = h_e e^{\lambda^*} \tag{4.96}$$

The use of P^* instead of P in the models derived above will therefore permit the inclusion of the electrostatic effects on the rate of substrate transport up to the enzyme phase. We note then, that although previous authors have shown how to correct the Michaelis-Menten constant for electrostatic effects, in the more general sense it is the external mass transfer coefficient which should be modified.

It seems reasonable to assume that if the fixed charge on the membrane affects the rate at which substrate approaches the surface from the outside, then an electrostatic effect may also

be manifested as the substrate leaves the surface on the inside of the cell. For a short distance just inside the membrane, the substrate diffusivity will also be a function of combined diffusive and electrostatic terms, as the external mass transfer rate is in Eq. 4.95. Unfortunately, no solutions to Eq. 4.3 are available when $D_{is} = D_{is}(r)$.

IV-6. Unsteady-state Kinetics

In the preceding section, the steady-state kinetics for the model MEC-enzyme system were discussed. When batch assays are used to measure reaction rates in particulate catalyst systems, however, the assumption of the achievement of the steady state is invalid in the initial stage of the reaction. If the reaction proceeds more slowly than the diffusion into the particle, then during this initial period a significant portion of the substrate which enters the cell may simply be accumulated inside the cell as indicated in the general diffusion-reaction equation, Eq. 4.3. In this section, an attempt is made to predict the duration of the unsteady-state phase, i.e. the time until the "pseudo-steady state" is achieved. Many attempts have been made to simplify Eq. 4.3 so that realistic solutions are possible.

In the limit of zero chemical reaction, Eq. 4.3 becomes for spherical coordinates

$$\frac{\partial c_s}{\partial t} = D_{is}\left(\frac{\partial^2 c_s}{\partial r^2} + \frac{2}{r}\frac{\partial c}{\partial r}\right) \qquad (4.97)$$

with the boundary conditions as given in Eqs. 4.4a and 4.4b. In addition, an initial condition must be given which, for the

case of diffusion of substrate into an initially "empty" capsule, is

$$t = 0: \qquad c_{is} = 0 \qquad \text{for } r < r_o \tag{4.98}$$

Crank [38a] has given the solution to Eq. 4.97 for the case of a capsule surrounded by an infinite solute medium such that c_{so} is a constant in time also. Morgensen [103] has recently solved the case of diffusion of solute into spheres from a limited solution. Flinn and Cherry [44] derived an expression for diffusion from a well-mixed capsule into an infinite solution which for their permeability studies (not reported) predicted the rate of efflux of solute from capsules as well as Crank's model. They concluded therefore that diffusion inside the capsule was not a significant factor in the mass transfer resistance. Shigeri and Kondo [127] used a similar expression for diffusion from well-mixed capsules into a limited volume.

Morgensen has also treated the limit of diffusion from a limited supply with first-order chemical reaction in which case for $c_s << K$, Eq. 4.1 reduces to

$$v_s = \frac{k_2 E_t}{K} c_s \tag{4.99}$$

and Eq. 4.3 becomes

$$\frac{\partial c_s}{\partial t} = D_{is} \left(\frac{\partial^2 c_s}{\partial r} + \frac{2}{r} \frac{\partial c_s}{\partial r} \right) - \frac{k_2 E_t}{K} c_s \tag{4.100}$$

The boundary and initial conditions are as given above. Best [14] has also considered this case but has used an approximate "constant average" reaction expression, as proposed by

Rashevsky [116], but for first-order reactions. Thus, the two equations for the inside of the capsule and the external solution are

$$r < r_o: \quad \frac{d\overline{c_{is}}}{dt} = -q + \frac{1}{\Lambda_s}(c_{so} - \overline{c_{is}}) \tag{4.101}$$

$$r > r_o: \quad \frac{dc_{so}}{dt} = -\frac{V_c}{V\Lambda_s}(c_{so} - \overline{c_{is}}) \tag{4.102}$$

where, for $\overline{c_{is}} << K$, Eq. 4.32 gives

$$q = \frac{k_2 E_t}{K}\,\overline{c_{is}} \tag{4.103}$$

No solution is available for the case of Michaelis-Menten reaction in capsules located in infinite or limited supplies of substrate. If, however, q is approximated as by Rashevsky in model 3 above, then Eq. 4.101 can be written as

$$\frac{d\overline{c_{is}}}{dt} = -\frac{k_2 E_t \overline{c_{is}}}{K + \overline{c_{is}}} + \frac{1}{\Lambda_s}(c_{so} - \overline{c_{is}}) \tag{4.104}$$

The solution to this equation for the case of an infinite external substrate solution (c_{so} = a constant) is possible. Thus, separating variables, making the following substitutions:

$$\begin{aligned} a_1 &= \frac{1}{\Lambda_s} \\ a_2 &= \frac{1}{\Lambda_s}(K - c_{so}) + k_2 E_t \\ a_3 &= -\frac{c_{so} K}{\Lambda_s} \\ a_4 &= \sqrt{a_2^2 - 4a_1 a_3} \end{aligned} \tag{4.105}$$

and integrating

$$-\int_0^t dt = \int_{\overline{c_{is}}(0)}^{\overline{c_{is}}(t)} \frac{K + \overline{c_{is}}}{a_1 \overline{c_{is}}^2 + a_2 \overline{c_{is}} + a_3} \, d\overline{c_{is}} \qquad (4.106)$$

For $c_{is} = 0$ at $t = 0$, Eq. 4.106 becomes

$$t = \frac{1}{2a_1} \log_e \left(\frac{a_3}{a_1 \overline{c_{is}}^2 + a_2 \overline{c_{is}} + a_3} \right) + \left(K - \frac{a_2}{2a_1}\right)\left(\frac{2}{a_4}\right)\left[\tanh^{-1}\left(\frac{2a_1 \overline{c_{is}} + a_2}{a_4}\right) - \tanh^{-1}\left(\frac{a_2}{a_4}\right)\right] \qquad (4.107)$$

In order to estimate the time required to reach the "pseudo-steady state" in a batch reactor, therefore, one can calculate the time for $\overline{c_{is}}$ to reach, say, 99% of the steady-state value as predicted by model 3 above. Calculations for two levels of external mass transfer resistance and a set of typical parameter values are included in Table 11.

Table 11

Estimated Time to Reach 99% of the Steady-State $\overline{c_{is}}$ *

P (cm/sec)	Λ_s (sec)	$k_2 E_t$ (μmoles/cm^3/sec)	q (μmoles/cm^3/sec)	$\overline{c_{is}}(t=\infty)$ (mM)	$t_{99\%}$ (sec)
10^{-4}	25.8	0.167	0.0383	0.0149	2.2
10^{-3}	3.25	0.167	0.152	0.501	13.4
10^{-3}	3.25	0.167	0.0159	0.948	14.9

* for K = 0.05mM; c_{so} = 1mM; $k_2 E_t$ = 10 (μmoles/cm^3/min);

$r_o = 75\mu$; $D_{is} = 5 \times 10^{-6}$ cm/sec

V. EXPERIMENTAL METHODS

The procedures used in this study for the preparation and characterization of nylon-MEC-trypsin are discussed in this chapter. The performance of the batch assay is also considered and the properties of the individual batches of microcapsules are summarized.

V-1. Preparation of Microcapsules

The method described by Chang, MacIntosh, and Mason [34] was used to prepare nylon microcapsules containing trypsin-hemoglobin solutions. A summary of this method follows.

A 10% by weight aqueous solution of Worthington Substrate Powder Hemoglobin is stirred for 5 minutes with a magnetic stirrer and filtered through Number 40 filter paper. Chang originally suggested using red blood cell hemolysate but has since discovered that the powdered hemoglobin solution has much more reproducible properties. To the hemoglobin solution is added Mann Research Laboratories trypsin (2X Crystallized, Salt Free, Lyophilized) to twice the concentration desired in the final capsules. This solution is prepared just prior to use and is mixed by magnetic stirrer at low speed for 5 minutes.

2.5 ml of the hemoglobin-trypsin solution is placed in a 100 ml beaker and 2.5 ml of buffered 1,6-hexamethlenediamine solution (0.4M in 0.45M $NaHCO_3$-Na_2CO_3 buffer, pH of buffer 9.8) is added. This solution is surrounded by ice and stirred by magnetic stirrer for 1 minute. The buffered hemoglobin-trypsin-diamine is then emulsified in 25 ml of "mixed solvent" (chloroform-cyclohexane, 1:4, containing 1% by volume Span 85 emulsifying agent) for 1 minute.

Without stopping the stirring, 25 ml of sebacyl chloride solution (0.018M sebacyl chloride, in mixed solvent) is added. Stirring is continued for 3 minutes. At the end of the reaction period, stirring is stopped and capsules are permitted to settle out of solution (for capsules less than 70-80μ, centrifugation is required here to remove capsules quickly). This takes about 1 minute. The cloudy supernatant is siphoned off and the capsules are suspended in 20 ml Tween 20 solution (1:1, Tween 20: water). The capsules are stirred in the Tween 20 solution for ~30 seconds and then the suspension is added to 200 ml of distilled water and stirring is continued for ~30 seconds. The capsules can then be washed repeatedly with distilled water followed by centrifugation, or can simply be permitted to settle out of the Tween 20 solution which has been diluted 10 times with distilled water. The capsules are stored in and washed with distilled water several times before use.

Glassware must be very clean and the hemoglobin and buffered diamine solutions should be filtered before use for best results. It is best to prepare the hexamethylenediamine solution just prior to use. If any precipitate is present in the bottom of the sebacyl chloride reagent bottle, the reagent should be discarded.

V-2. Assay of Tryptic Esterase Activity

The assay procedures suggested by Schwert and Takenaka [124] and Hummel [76] was used to assay both trypsin in solution and microencapsulated trypsin. These assays utilize the absorbance difference between N-benzoyl-L-arginine (BA) and its ethyl ester (BAEE) at 255mμ and p-toluenesulfonyl-L-arginine (TA) and its methyl ester (TAME), at 247mμ, respectively.

A Bausch and Lomb Spectronic 600 double beam, recording spectrophotometer and Sargent Model SRLG recorder were used to continuously monitor the increase in absorbance of 0.001M TAME and 0.001M BAEE solutions. The solutions are buffered with 0.04M Tris containing 0.01M $CaCl_2$ at pH 8.0.

V-2-A. Continuous (Steady-State) Assay Procedure

Initial attempts were made to assay microcapsule activity in a flow system so that steady-state conditions could be achieved (See Figure 9). The water-jacketed flow system was constructed from Lucite and had a sample chamber of approximately 30 cm^3.

Buffered substrate solution was metered by a Harvard Compact Infusion Pump, Model No. 975, fitted with two plastic 50cc syringes into the sample chamber. A piece of plastic filter cloth was placed across the outlet holes in the top of the sample chamber to prevent loss of microcapsules during the assay. The sample compartment was stirred continuously with a Cole-Parmer Magnetic "6 x 6" stirrer and a micro-stirring bar made from a section of 20 gauge syringe needle inbedded in a piece of polyethylene tubing. The jacket of the cell was continuously circulated by water from a MGW-Lauda Lauda-Thermostat, Type K2. The stream from the outlet of the cell was sent directly to a continuous-flow cell in the sample side of the Spectronic 600 Spectrophotometer.

All efforts to assay capsules using the flow system yielded unacceptable results primarily because of breakage of capsules. This finding confirms the experience of Morgensen [103] that a "gentle" assay for MEC-enzymes must be employed since the capsule walls will rupture if the reaction suspension is vigorously agitated. In order to overcome this breakage problem the batch assay described in the next section was employed for all succeeding assays.

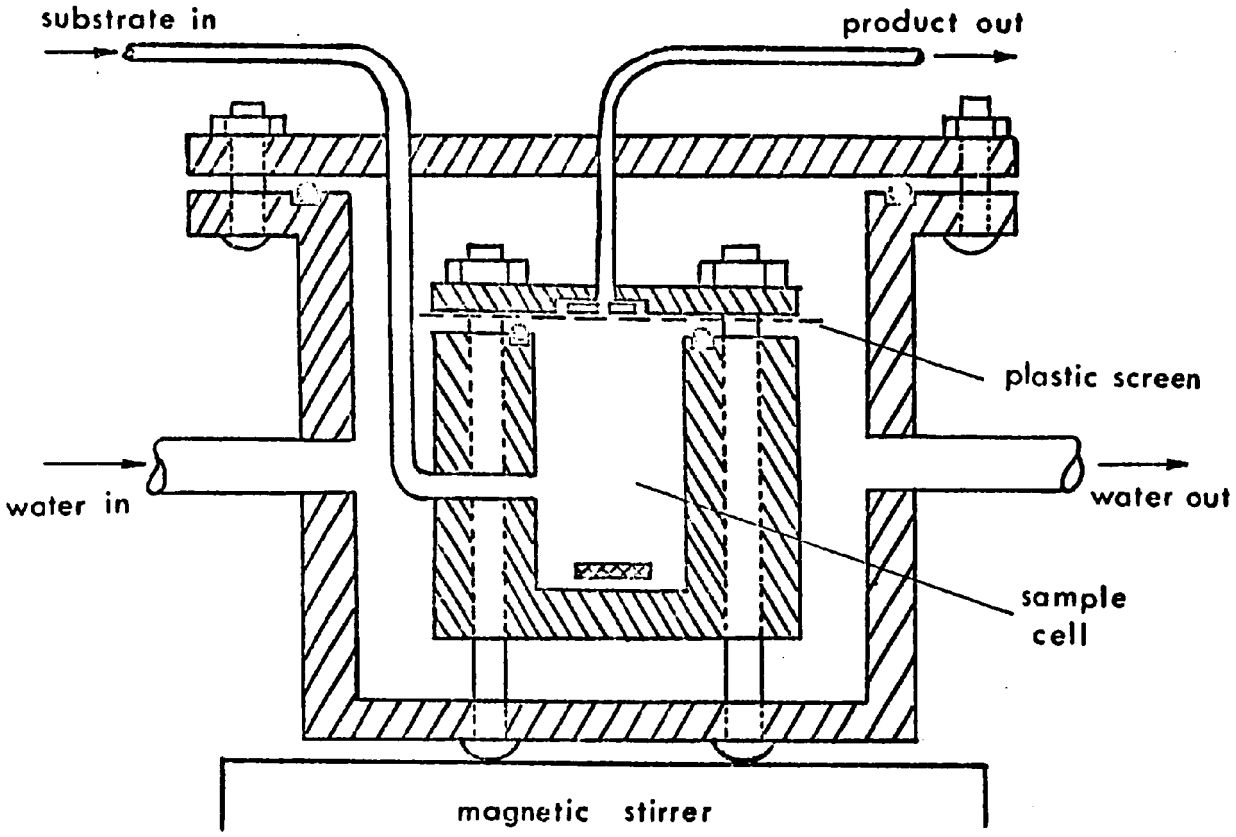

Figure 9. Continuous Assay System

V-2-B. Batch Assay Procedure

A description of the batch assay technique used throughout this study is given below.

The spectrophotometer is zeroed with two 1 cm u. v. -quartz cells each containing 0. 1 ml distilled water, 0. 3 ml 0. 01M BAEE or TAME substrate solution, and 2. 6 ml Tris buffer solution

(0.46M Tris, 0.0115M $CaCl_2$, pH 8.0). The cell in the sample side of the spectrophotometer is removed and cleaned, then filled with 0.3 ml 0.01M TAME solution and 2.6 ml Tris buffer solution. At time zero, 0.1 ml of enzyme solution or 0.1 ml of microcapsule suspension is pipeted into the cell, the cell is quickly mixed and inserted into the sample holder. When microcapsules are assayed, it is necessary to open the sample compartment every 2-4 minutes to resuspend the capsules using a small wire stirrer. The conditions of the assay are such that the capsules, for most of the reaction period, are settling in a stagnant liquid at their terminal velocity.

At these concentrations of TAME and BAEE, the enzyme is saturated and so the rate of increase of the absorbance is a direct measure of k_2E_t for the enzyme. The absorbance increases linearly until the reaction is $\sim$ 90% complete for both substrates. Using the Spectronic 600, the total $\Delta\epsilon$ observed following complete conversion of substrate to product was 470 A.U./M for TAME and 760 for BAEE, somewhat lower than the values reported by Barman (see Table 1).

In the early studies (when TAME was used as substrate) the spectrophotometer was located in an air-conditioned room. Temperatures in the sample compartment were observed to vary less than $\pm$ 1°C without the use of other temperature control devices with the average temperature in the cell $\sim$ 26°C. In later experiments (when BAEE was the substrate) the Lauda circulator was used to control the temperature of a Bausch and Lomb Spectronic 600 constant temperature cell to 25° $\pm$ 0.1°C.

The determination of the volume of microcapsules placed in the sample cuvette during the batch assay is of critical importance in the analysis of kinetic data. Two methods were

used to determine this value. It was observed that when microcapsules were stored at elevated temperatures for extended periods, the capsules tended to aggregate and to adhere to glass surfaces. Furthermore, older capsules tended to become less dense due to the loss of internal hemoglobin which was slowly digested by the trypsin. Both of these processes make capsule volume determination by centrifugation difficult since the capsules generally fail to settle out completely.

A 3 cm^3 cell with a 3 cm path length was constructed for a Klett-Summerson Photoelectric Colorimeter, Model 900-3. Following a batch assay, the contents of the sample cuvette were transferred to this 3 cm^3 cell and the Klett reading (a measure of turbidity) was obtained. The sample was then transferred to a Van Allen thrombocytocrit tube (A. H. Thomas Company) and the tube was centrifuged in an International Clinical Centrifuge, Model CL for at least 10 minutes at high speed. The volume of capsules which settled out was then read from the calibrated stem of the thrombocytocrit tube. Only readings in which very few microcapsules were left suspended were recorded. In this way, the Klett reading was calibrated using thrombocytocrit readings on freshly prepared capsules. The Klett reading was then used to find the volume of capsules, V_c, in the sample cell when "older" capsules failed to centrifuge out completely. For fresh capsules, the thrombocytrocrit reading was used to determine V_c.

Autohydrolysis of the substrate solution in the absence of trypsin was observed to proceed at a much slower rate than the reaction in the presence of the enzyme. This problem is also offset by the fact that the substrate is present in both sample and

reference cells in nearly the same concentration; autohydrolysis occurs in both cells and the net effect is for one to cancel the other. Thus no correction for this factor was required in this study.

V-2-C. Determination of Microcapsule Size Distributions

A sample of the microcapsule suspension was placed on the mirrored surface of a Hauser HY-LITE Counting Chamber with Improved Neubauer Double Rulings. Sufficient sample was used to cover the entire mirrored surface and the sample was allowed to stand for 2-3 minutes to permit settling of the microcapsules to the surface of the chamber. No coverslide was used. The counting chamber was then photographed using a Bausch and Lomb Type H Photomicrographic camera and Bausch and Lomb binocular microscope. The negative was enlarged 10X and the diameters of the capsules present were measured to the nearest 10μ. Alternatively, in several of the later batches, the capsule diameters were measured directly through the microscope.

Three statistics were employed to characterize the diameter of the capsule populations:

Mean Diameter:
$$\bar{d} = \frac{\Sigma n_i d_i}{N} \qquad (5.1)$$

Sauter Mean Diameter:
$$d_{32} = \frac{\Sigma n_i d_i^3}{\Sigma n_i d_i^2} \qquad (5.2)$$

Standard Deviation:
$$\sigma = \sqrt{\frac{\Sigma n_i d_i^2 - (\Sigma n_i d_i)^2/N}{N-1}} \qquad (5.3)$$

with $i = 1, 2, 3, \ldots m.$

where n_i is the number of capsules of diameter d_i and N and m are the total number of capsules and size classes observed, respectively. The Sauter mean diameter gives the size of the capsule in the population having the same average volume to average area ratio as the rest of the population. It was found that the capsule diameters were distributed from normally to log-normally in an apparently random pattern. It is likely that the different types of diameter distributions arose from variations in the production process, especially in separating the capsules from the reaction and wash solutions.

V-3. Properties of the Capsules

The properties of the capsules used in the studies reported in Chapter VI are summarized in Table 12. When batches have common first-numerals, e.g. 14-5 and 14-6, these batches were prepared on the same date and from the same reagent solutions but differ in capsule size or enzyme concentration. Photographs of two typical batches of nylon-MEC-trypsin are shown in Figure 10.

V-4. Performance of the Batch Assay Procedure

A sample chart tracing for a typical batch assay (BAEE, Batch 13-1 capsules) is shown in Figure 11. This portion of the recording covers about one third of the total conversion of the 1mM BAEE substrate solution. The initial slope is estimated by "bracketing" the output signal variation between lines drawn on the surface of and parallel to the straight edge of a transparent

Table 12

Properties of the Batches of Microcapsules

Batch #	Batch Diameters $\bar{d}(\mu)$	$d_{32}(\mu)$	$\sigma(\mu)$	N	Initial Trypsin Loading (mg/cm^3)*
10	129.4	142.0	29.9	1320	1.0
13-1	123.5	133.0	25.0	186	0.5
14-5	77.4	86.0	18.3	349	2.0
14-6	72.3	79.7	16.4	394	1.2
14-7	69.5	76.3	16.1	501	0.4
14-8	64.8	70.7	13.2	222	0.08
14-9	103.9	119.6	28.8	167	2.0
14-10	82.3	94.4	22.9	315	1.2
14-11	82.9	90.4	19.8	226	0.4
14-12	85.7	97.4	22.8	304	0.08
14-13	138.5	153.4	33.3	147	2.0
14-14	138.9	158.0	34.7	206	1.2
14-15	158.9	176.6	37.5	204	0.4
14-16	153.6	175.6	40.0	289	0.08
15-1	139.7	182.6	55.1	264	1.0
16-1	91.1	117.5	33.8	179	1.0
17-1	170.1	216.6	64.4	231	—
17-2	79.7	94.3	31.3	308	—
17-3	118.7	144.8	42.6	424	—
18-1	196.9	220.1	48.3	240	—
18-2	104.1	113.7	23.0	225	—

* 1 mg/cm^3 is approximately equal to 38.3 μmoles BAEE converted/min/cm^3 of the active enzyme in free solution



Batch 14-7

$d_{32} = 76.3\,\mu$

$\sigma = 16.1\,\mu$

100 μ

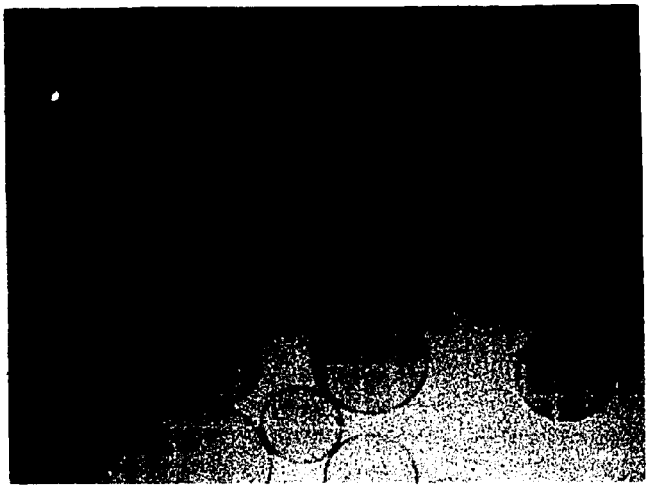

Batch 14-15

$d_{32} = 176.6\,\mu$

$\sigma = 37.5\,\mu$

Figure 10. Photographs of typical batches of nylon-MEC-trypsin.

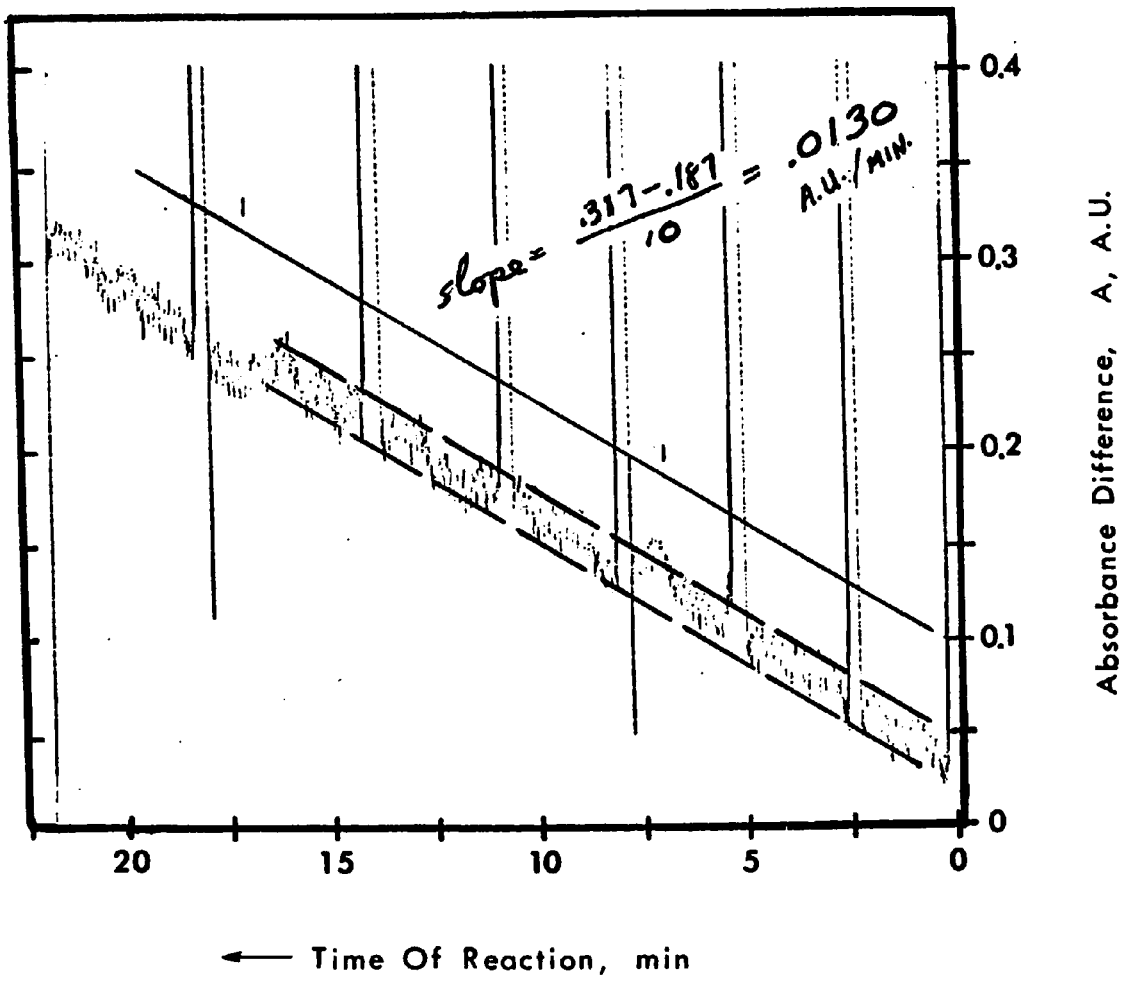

Figure 11. Typical batch reaction assay. Batch 13-1 capsules, 1.0mM BAEE, 25°C, V_c = 0.016 as read from thrombocytocrit tube.

ruler (shown in Figure 11 by dashed lines). A line is then drawn along the straight edge (solid line) and the slope of this line is determined directly from the scale of the chart paper. The lines extending vertically from the output tracing at 2-3 minute intervals indicate the opening and closing of the sample compartment to stir the reaction cell.

The conversion from the measured slope in Absorbance Units/min to Enzyme Units (μmoles substrate converted/min) is made according to Eq. 5.4.

$$\text{E. U.} = \frac{\text{A. U.}}{\text{min.}} \cdot \frac{1}{\Delta\epsilon} \quad \frac{\text{moles/liter}}{\text{A. U.}} \cdot V\text{cm}^3 \cdot \frac{1}{1000} \frac{\text{liter}}{\text{cm}^3} \qquad (5.4)$$

where $\Delta\epsilon$ is the total difference in the absorbance of 1M product and 1M substrate solutions and V is the total volume of the reaction liquid. For a typical BAEE assay then, $\Delta\epsilon = 760$ and $V = 3\ \text{cm}^3$, and

$$\text{E. U. (BAEE)} = 3.95 \frac{\text{A. U.}}{\text{min.}} \qquad (5.5)$$

For a typical TAME reaction, $\Delta\epsilon = 470$ and

$$\text{E. U. (TAME)} = 6.40 \frac{\text{A. U.}}{\text{min.}} \qquad (5.6)$$

A simple test was contrived to determine the relationship between the true volume of capsules used in a batch assay and the volume as measured by the thrombocytocrit tube. A suspension of microcapsules in distilled water was permitted to settle and the absorbance of the supernatant liquid (A_s) was measured. A hemoglobin solution was prepared so that the absorbance of the solution (A_H) was about 1.6. 2 ml of the hemoglobin solution and 3 ml of the capsule suspension were then mixed by spatula

in a 15 ml centrifuge tube for ~10 seconds and centrifuged for ~10 seconds at high speed. The absorbance of the mixture supernatant liquid (A_M) was then determined. The volume fraction of the capsules in the original suspension can be determined from Eq. 5.7, where f is the true volume of capsules per cm^3 of suspension.

$$2A_H + (3-3f)A_s = (5-3f)A_M \qquad (5.7)$$

Several 0.1 cm^3 samples of the original capsule suspension were also placed in the thrombocytocrit tubes and the resulting capsule fraction, f_T, was determined. All tests were run with Batch 18-2 capsules and all absorbance measurements were made at 280 mμ with distilled water in the reference cell of the spectrophotometer. The results are summarized in Table 13.

Table 13

Calibration of the Thrombocrytocrit Measurement of V_c

Test	A_S	A_H	A_M	f	f_T	$f_{T,avg}$	f/f_T
1	0.015	1.614	0.713	0.14	0.22, 0.22, 0.20, 0.17	0.20	0.70
2	0.008	1.614	0.684	0.083	0.16, 0.16, 0.14, 0.14	0.15	0.55
3	0.025	1.615	0.713	0.13	0.24, 0.20, 0.20	0.21	0.62
4	0.000	1.600	0.680	0.098	0.13, 0.15, 0.17, 0.20	0.16	0.61

The average value of f/f_T from Table 13 is 0.62 which indicates that the microcapsules do not tend to deform while packing in the stem of the thrombocytocrit tube. This finding

is generally in keeping with the observations of Jay and Edwards [80] in a study of the mechanical properties of nylon-MEC-erythrocyte hemolysate solutions. They found that the nylon membrane offered great resistance to stretching of the capsule wall as might be found when a capsule is forced through a capillary tube. They conclude that "the diameter of the smallest pipette through which a spherical microcapsule can pass without suffering irreversible change has been found to be no smaller than 90% of the microcapsule diameter...".

It should be pointed out, however, that the experiments by Jay and Edwards and the test reported herein were conducted with microcapsules containing hemoglobin only whereas the enzyme-loaded capsules used in the experiments discussed in Chapter VI contained hemoglobin-trypsin solutions. Since trypsin slowly hydrolyses hemoglobin into fragments small enough to escape from the capsule, the total internal pressure of the trypsin-containing capsules can be expected to be somewhat lower than for the hemoglobin-only capsules. This process is observable visually by a noticeable change in the MEC-trypsin solutions, from dark red when freshly prepared to nearly colorless after extended periods of time, depending on the original trypsin concentration encapsulated. Thus, trypsin-containing micro-capsules may be more susceptible to deformation upon centrifugation and therefore f/f_T will be somewhat higher than reported above. In fact, the author has observed on several occasions that, when viewed under the microscope, many of the trypsin-containing microcapsules had assumed non-spherical shapes upon centrifugation.

Another consideration is that the hemoglobin may tend to adsorb to the outside of the capsules in the dilution experiments presented above. If this were the case, then the value of A_M reported in Table 13 should be slightly higher, and the net effect is to raise the value of f/f_T. For example, in Test 1 in Table 13, if A_M in reality (i.e., in the absence of hemoglobin adsorption) were, say, 0.725, f/f_T would be 0.85. The attempt was made to minimize the possibility of adsorbing hemoglobin in this test by performing the mixing and centrifugation as quickly as possible.

In view of all of the factors discussed above, it was decided to assume for the sake of convention that f/f_T is 0.70, this being the packing factor one might expect for randomly packed rigid spheres. All values of V_c reported hereafter, therefore, refer to 0.7 times the volume determined by centrifugation of the reaction cell contents in a thrombocytocrit tube, unless V_c is otherwise specified. It should be understood that the somewhat arbitrary selection of the conversion to find V_c lends some uncertainty to the experiments wherein an "absolute" value of k_2E_t is assigned to a given batch of capsules. Since many of the tests described in Chapter IV depend on changes in the relative reaction rate within a given batch, however, this uncertainty should be cancelled out insofar as the interpretation of the experimantal results is concerned.

The results of multiple assays of two batches of capsules are presented in Figure 12. Batch 10 microcapsule assays using 1mM TAME in the standard procedure resulted in an average value of $(v_{es})_{10} = 14.8$ μmoles/cm^3/min with a standard deviation for 9 assays of $\sigma_{10} = 2.8$. Comparable

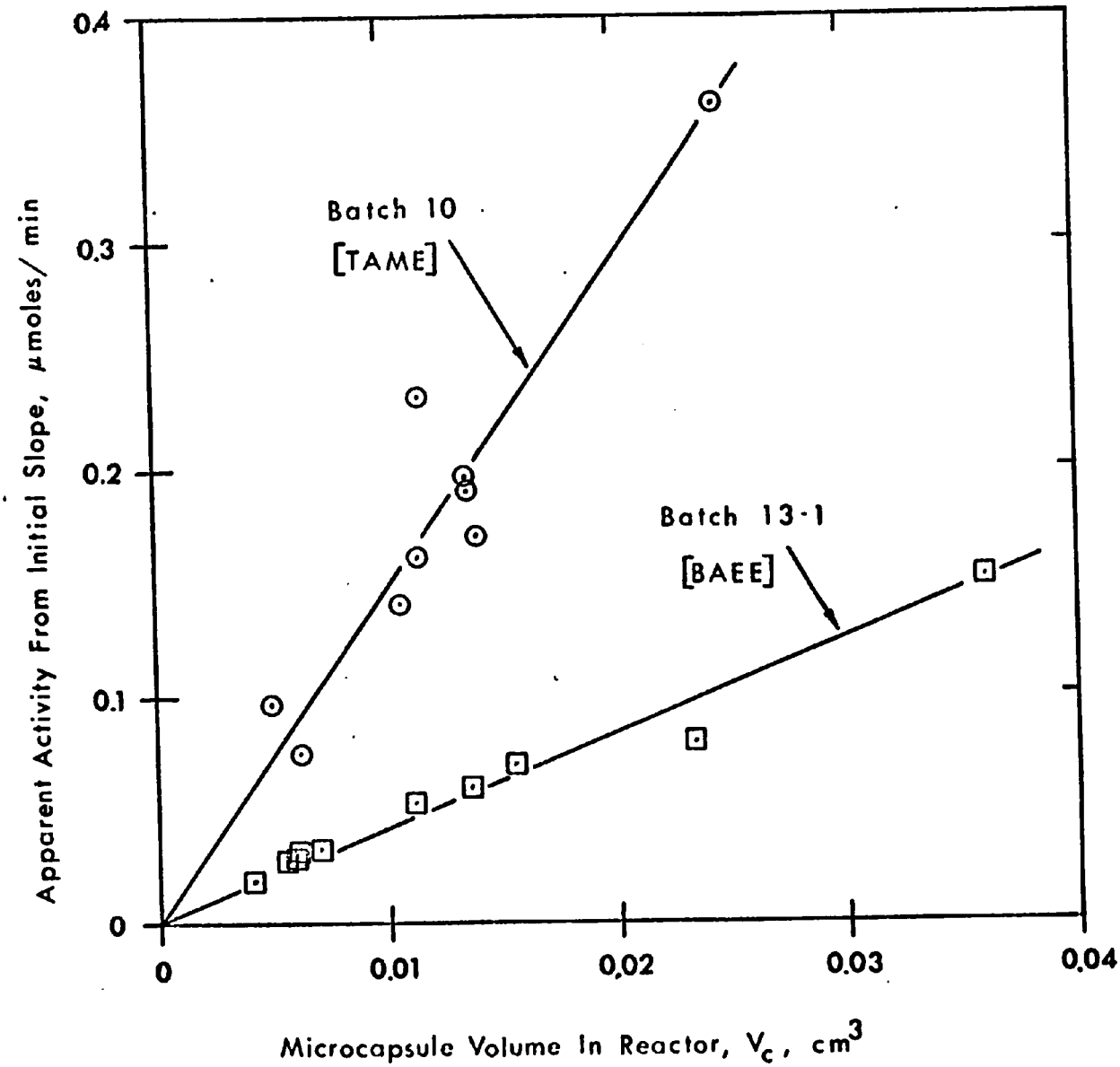

Figure 12. Capsule Volume-Activity Dependence For Batch Assay Technique

statistics for Batch 13-1 capsules in 1mM BAEE assays were $(v_{es})_{13-1} = 4.46$ and $\sigma_{13-1} = 0.49$ for 10 tests. The reduction in the variation of the measured activity for the Batch 13-1 capsules [$\sigma/(v_{es}/V_c) = 0.19$ for Batch 10 assays and 0.11 for Batch 13-1 assays] probably represents the improved temperature control of the reaction afforded by the acquisition of a controlled-temperature cell holder for the spectrophotometer just prior to these experiments.

Another possible deficiency in the batch assay of microcapsules was considered after the bulk of the experimental work had been completed. All of the assays discussed in Chapter VI were made by pipetting a suspension of microcapsules in distilled water into the buffered substrate solution. Thus the microcapsules were not initially equilibrated with the buffer solution, a process which conceivably could take some time to achieve. Comparisons of BAEE assay of two batches of water-equilibrated and buffer-equilibrated capsules are presented in Table 14. "Buffer-equilibrated" capsules were placed in a buffer solution equivalent to that used in the assay, but lacking the substrate, at least ten minutes prior to the assay. Inasmuch as the standard deviations of the batch assays described above were at least 10% of the mean value and the difference between the means of the buffer- and water-equilibrated activities is at most also about 10%, one cannot conclude that the initial suspension medium has a significant effect on the measured capsular activity.

Table 14

Comparison of BAEE Assays for Water-Equilibrated And Buffer-Equilibrated Microcapsules

Capsule Batch	Capsule Suspension	v_{es} (μmoles/cm^3/min)	v_{es} (μmoles/cm^3/min)
16-1	buffer	11.4, 12.0, 10.6, 11.2	11.3
16-1	water	12.2, 13.7, 12.1, 11.7	12.4
15-1	buffer	4.57, 3.89, 3.43	3.97
15-1	water	4.35, 4.23, 3.47	4.02

VI. EXPERIMENTAL RESULTS AND DISCUSSION

The results of experiments designed to investigate the behavior of nylon-MEC-trypsin solutions are presented in this chapter. Inquiries are made into the thermal stability, enzymatic activity response to changes in temperature and pH, mass transfer limitations, and the yield of active, encapsulated enzyme for this system. A brief discussion is provided after the description of each experiment to provide continuity to the presentation.

VI-1. Thermal Stability

Batch 10 microcapsules were prepared by the standard procedure, then washed repeatedly with and stored in distilled water at 4°C. A solution of trypsin in distilled water of concentration equivalent to the initial loading of the enzyme in the Batch 10 microcapsules (1 mg/ml) was prepared at the same time and stored at the same temperature. After one week of storage, the capsule suspension and enzyme solution were divided into 4 equal portions and placed in 15 cm^3 test tubes. One tube of the suspension and one tube of the solution were placed in each of three incubators set at 21°, 28°, and 37°C. The last tubes were returned to the 4°C refrigerator.

The tubes were periodically withdrawn from the incubators and assayed using the batch assay (1mM TAME). Trypsin solutions were diluted when necessary to permit accurate activity measurement. Supernatant liquid from the capsule tubes was drawn off and replaced with fresh distilled water before assaying. All tubes were allowed to stand at room temperature (22-23°C) for at least one hour before assaying.

The trypsin in solution denatured at an apparent first-order rate with a half-life of about 1 day at 37°C and about 3 days at 21°C as shown in Figure 13. The MEC-trypsin, however, experienced a rapid initial drop in activity, to a greater degree the higher the storage temperature, and then became relatively stable (Figure 14). A similar behavior, though less well documented, was also observed with another batch of MEC-trypsin.

Since no precautions were taken to retard microbial growth during these tests, the denaturation rate of free-solution trypsin was rechecked under more controlled conditions. A solution of trypsin in distilled water was sterile-filtered into 14 pre-sterilized, cotton-stoppered test tubes. 2 of the test tubes were assayed (1mM BAEE) upon filtering and 6 tubes each were placed in 37° and 21°C incubators. At various intervals the tubes were withdrawn from the incubators, a sample of the contents plated onto trypticase soy agar in Petri dishes, and BAEE assays of the tube contents were run. Petri dishes were incubated at 37°C for at least 48 hours and then checked for microbial growth. Assays of contaminated samples were rejected. Once assayed, the samples were discarded.

This test confirmed the half-life of about one day for trypsin in solution at 37°C. The denaturation rate at 21°C, however, was somewhat slower than previously indicated with the half-life being about 6-7 days. Thus it is likely that for the assays for the 21°C storage after about 10-15 days in Figure 13, microbial growth was serving to increase the apparent denaturation rate.

In Figure 15, the MEC-trypsin assays are replotted such that 100% activity represents the initially observed activity rather than the total initial activity. Figure 15 indicates that the rapid initial

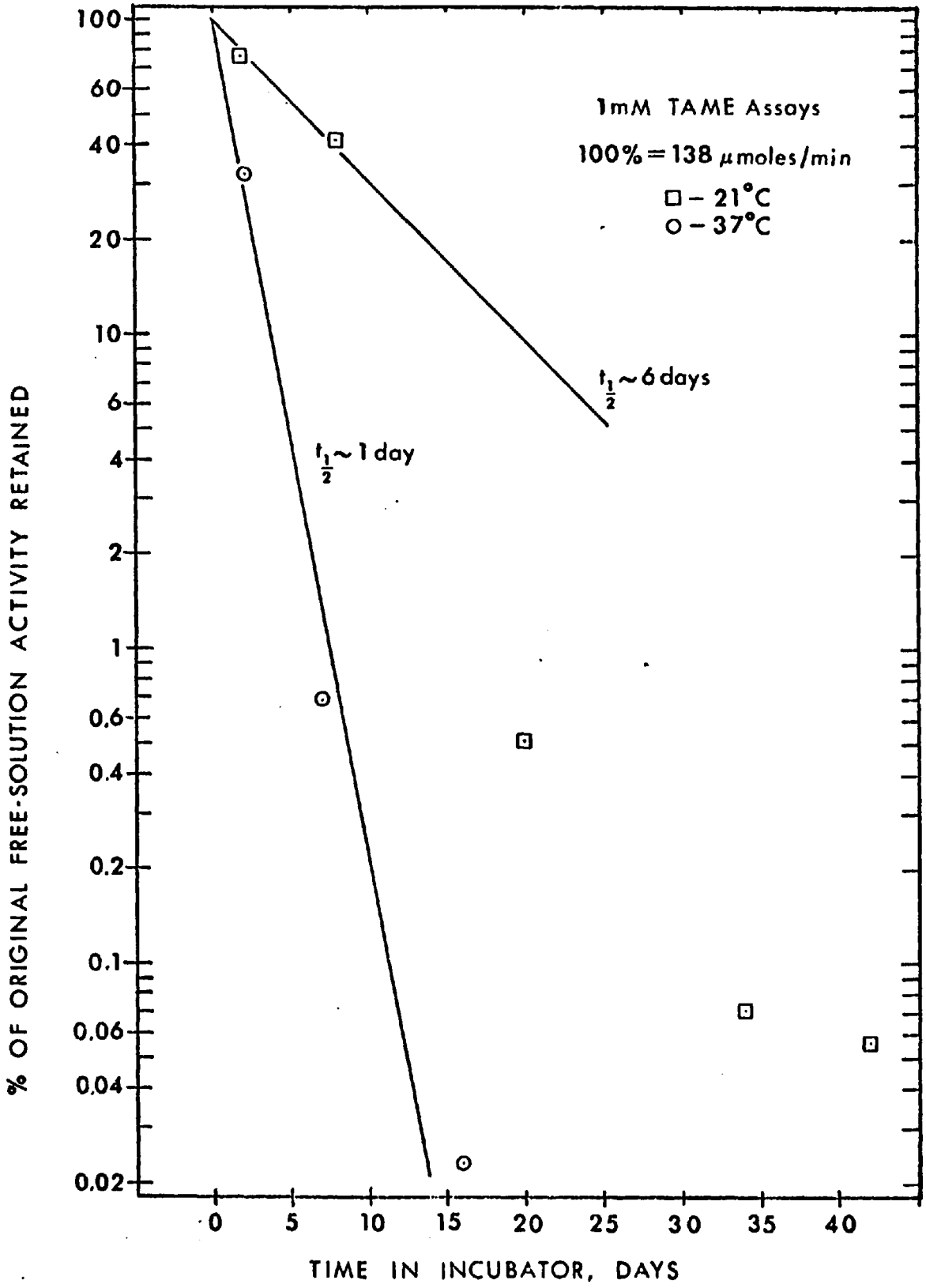

Figure 13. Storage Stability of Free-Solution Trypsin

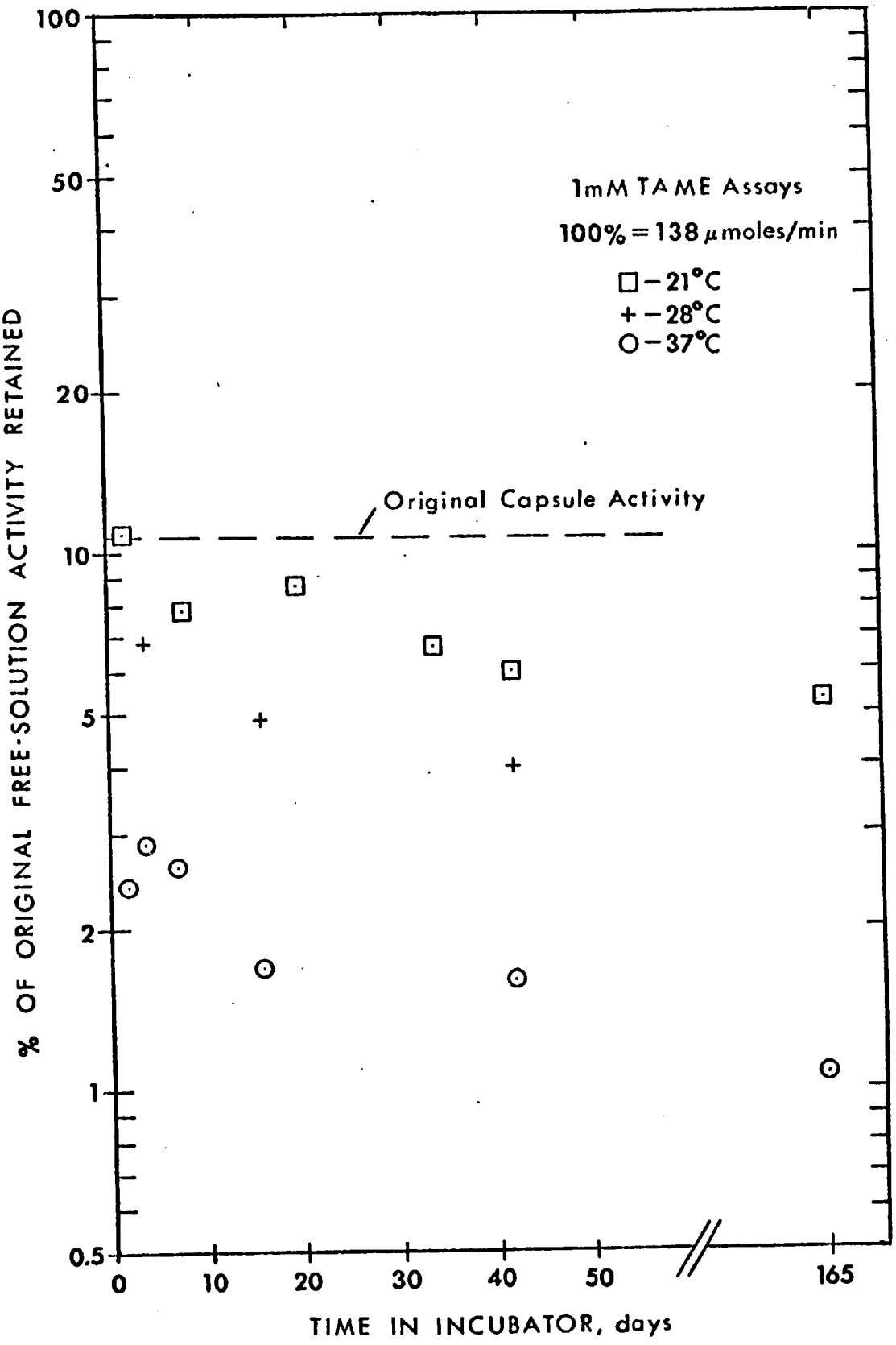

Figure 14. Storage Stability of Microencapsulated Trypsin, 100% = Initial Encapsulated Activity

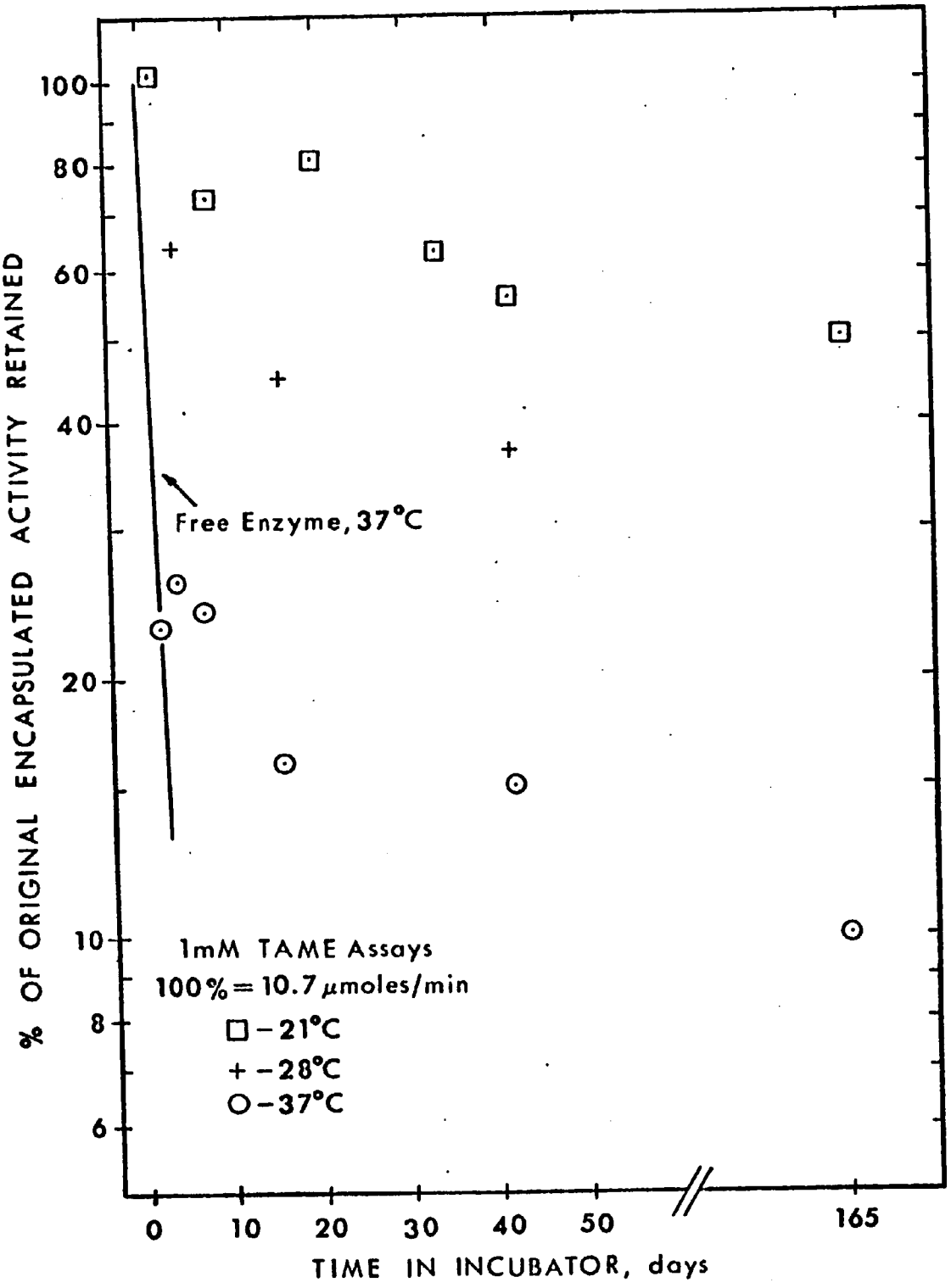

Figure 15. Storage Stability of Microencapsulated Trypsin, 100% = Initial Apparent Activity

activity loss at 37°C can be explained by the first-order denaturation rate of the free-solution enzyme. Inasmuch as the enzyme activity appears to stabilize after the initial activity loss, one might conclude that two "forms" of the active enzyme are present in the microcapsules, one form behaving like the free solution enzyme and the other exhibiting a more stable conformation.

It is unlikely that the hemoglobin originally encapsulated along with the trypsin could stabilize the MEC-trypsin as Chang [29] suggested since the capsules after ~ 1 month at 37°C were nearly colorless. Fragments of the hemoglobin as well as any other species which might serve to stablize the enzyme would surely have been dialyzed out of the capsule by the distilled water in which the capsules were suspended. A more likely possibility is that the presence of the nylon membrane served to reduce the MEC-trypsin denaturation rate; this possibility is also supported by evidence from assays of broken capsule membranes.

The membranes of the ultrasonically ruptured Batch 14 microcapsules described in Section VI-7 were collected by sedimentation and washed 4-5 times with distilled water over about a week of storage at 4°C. When observed through the microscope, nearly all cells were colorless, a good indication that the contents of the capsules had been released during the breaking process. Less than 1% of the capsules were estimated to be unbroken in most cases. After repeated washings, the membranes were placed in the 37°C incubator and the activity of the membranes was assayed periodically in the same manner as for whole capsules.

The results of the assays of Batch 14-9, 14-10, 14-11, and 14-12 membranes are shown in Figure 16. The initial membrane activity was based on the average of two assays of a given membrane suspension just prior to insertion of the sample into the incubator.

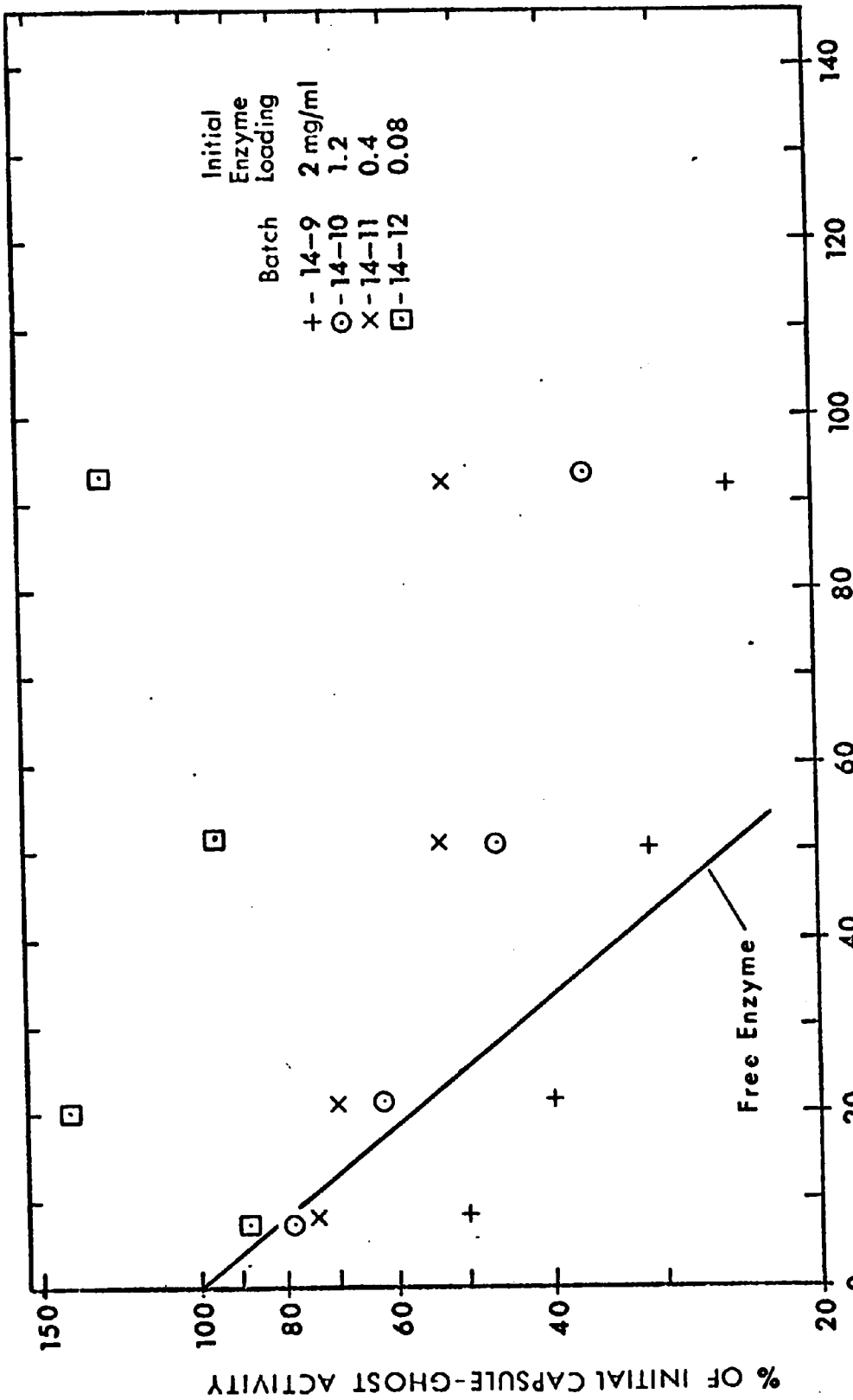

Figure 16. Storage Stability of Broken Capsule Membrane Enzyme Activity. (1mM BAEE Assays)

It will be observed that the denaturation process for the capsule membrane activity in Figure 16 is similar to the inactivation rate of the whole capsules in Figure 15; a rapid initial loss similar to the free-enzyme rate was followed by a lower denaturation rate after 4-5 days at 37°C.

It seems likely that only a negligible quantity of enzyme was present inside most of the broken membranes at the start of the incubation period since the capsules were repeatedly washed and the period of storage following breakage was so long. All of the activity initially measured was, therefore, probably adsorbed onto the nylon membranes.

If the enzyme-loading capacity of the membrane decreases with increasing temperature, then raising the temperature should cause the desorption of some of the enzyme from the membrane, resulting in a less stable conformation for some of the originally-bound enzyme. The greater the original enzyme activity associated with the membrane, the greater would be the loss of activity upon incubation at 37°C, in agreement with the data of Figure 16. It will be recalled that this interpretation is directly the opposite of the behavior observed by Kobamoto et al. [86] for trypsin adsorbing onto cellulose dialysis tubing. These authors found that the amount of enzyme adsorbed increased with increasing temperature. Furthermore, the enzyme was less stable in the presence of the membrane; all activity was lost by 1μM trypsin solutions after 48 hours and 3μM solutions after 72 hours when a piece of membrane was simply placed in the solution at 4°C. Obviously, the "...dynamic process of adsorption, unfolding, and desorption..." which was suggested by these authors to account

for the rapid denaturation rate is contrary to the observations in the present study. Indeed, the results presented herein indicate that the adsorbed enzyme is rather tightly bound to the surface in a very stable conformation since the long-term denaturation rate is quite low.

Unfortunately, no "absolute" measure was available for the volume of capsules originally surrounded by the membranes used in this test. The activities of the membrane suspensions were compared on a relative basis, however, from measurements of the suspension turbidity in the Klett instrument. The ratios of the membrane suspension activity to the corresponding suspension Klett reading were roughly equivalent after 90 hours for Batches 14-9, 14-10, and 14-11. The same ratio for Batch 14-12 was much lower. This suggests that on the basis of units of active enzyme adsorbed per unit of nylon membrane, the same enzyme loading was reached at the new temperature (37°C) by the more active capsule membranes.

VI-2. Adsorption of Trypsin Onto Microcapsule Membranes

Another experiment was conducted in order to verify the hypothesis that trypsin associates by adsorption with nylon microcapsule membranes. In this test, microcapsules which were prepared without trypsin inside were placed in trypsin solutions to determine whether the enzyme would adsorb to the outside of the capsules. If adsorption occurs on the outside, it seems likely that inside the cell the enzyme would also be found, at least to some degree, in higher concentrations at the membrane surface than in the solution in the interior of the capsule.

Seven ml of a 0.05 mg/ml trypsin-distilled water solution (2.5 BAEE enzyme units/ml, where one unit is the amount of enzyme which hydrolyzes 1μmole BAEE/min) and 1 ml of

concentrated Batch 18 capsule suspension were mixed in a 15 cm^3 test tube. The initial capsule suspension activity was found by BAEE assay and then the suspension was divided into two portions; one portion was kept at 4°C and the other was kept at room temperature (24°C). The samples were maintained at these temperatures for 3 days and were stirred once or twice per day with a spatula. After standing for 3 days the supernatant liquid in the test tubes was assayed (E_L), then the tubes were stirred and the suspension activity (E_S) was found. The enzymatic activity associated with the capsules (E_C) was then determined by "activity balance" from Eq. 6.1, where 0.1 ml is the volume of sample used in the batch assay.

$$V_c E_c + (0.1 - V_c) E_L = 0.1 E_S \qquad (6.1)$$

The possible decrease in capsular activity, E_c, caused by the diffusion across the unstirred liquid layer surrounding the capsules is not considered in Eq. 6.1.

The results of these experiments when Batch 18-1 and 18-2 microcapsules were used are summarized in Table 15. Activities of the supernatant liquid and suspensions reported are the average of three assays. In every experiment performed, the suspension of microcapsules was more active than the corresponding supernatant liquid.

Control samples of the 0.05 mg/ml trypsin solution which were stored along with the capsule suspensions in this three-day test indicated a small denaturation (< 5%) for the 4°C storage and 35-40% activity loss for the 24°C storage. If one assumes that the "equilibrium" between adsorbed and free solution enzyme is rapidly established so that the two forms tend to denature at

Table 15

Summary of Results for Adsorption of Trypsin
Onto the Outside of Nylon Microcapsules

Batch #	d_{32} (μ)	Storage Temperature (°C)	Enzymatic Activity (μmoles/cm^3/min) E_L*	E_S*	E_C**
18-1	220.1	4°	1.06	1.80	8.48
		24°	0.142	1.27	10.4
18-2	113.7	4°	1.25	1.66	6.87
		24°	0.138	1.29	10.1

* average of three assays
** as determined from Eq. 6.1

independent rates, then 85-90% of the initially present trypsin can be accounted for in the 4°C tests by attributing all denaturation to the enzyme in solution. For the 24°C tests, however, only about 50% of the original activity is accounted for when the same assumptions are made. This suggests that the enzyme is more rapidly denatured in the presence of nylon, as Kobamoto et al. [86] found to be the case for the trypsin-cellulose dialysis membrane system. A possible explanation for this phenomenon might be that, after the surface of the membrane becomes covered with, say, a monolayer of enzyme, further migration of enzyme into this "concentrated" enzyme phase results in an accelerated rate of autohydrolysis.

The somewhat lower activity associated with the capsules at 4°C than for the capsules at 24°C would appear to contradict the findings of the previous section. It may be true, however, that the lower activity is due to the fact that diffusion across the

"unstirred" hydrodynamic boundary layer surrounding the membrane is accompanied by chemical reaction. Since the bulk-liquid activity for the 4°C capsules is much higher than for the 24°C capsules, the substrate concentration in the unstirred film and at the membrane surface will be much lower, resulting in a decreased reaction rate in these regions. When the simple activity balance, Eq. 6.1, is employed to estimate E_c, the decrease in activity caused by increased diffusion limitations is thrown into E_c. If the "capsule" activity for the 4°C tests is set equal to 10 units/cm^3, then nearly 100% of the originally present enzyme activity is accounted for.

One should bear in mind that the capsule activity, E_C, in Table 15 is based on the volume of capsules present even though the enzyme is not inside the cells. Thus the concentration differences between the bulk liquid and capsule membrane will be much greater than between E_L and E_C if the latter concentration is based on the "surface concentration" on the membrane.

It is instructive to ask at this point whether the capsule activities, E_C, reported in Table 15 correspond to reasonable quantities of enzyme adsorbed in a monolayer to the surface of the capsules.

From the activity of the original enzyme solution used in this study, one finds that 1 mg of the enzyme is equivalent to about 50 BAEE enzyme units. Thus the enzyme activity associated with the membrane for Batch 18-1 capsules at 24°C represents about 0.208 mg enzyme or

$$0.208 \text{ mg} \times \frac{10^{-3}}{23,300} \frac{\text{mole}}{\text{mg}} \times 6.02 \times 10^{23} \frac{\text{molecules}}{\text{mole}}$$

$$= 5.4 \times 10^{15} \frac{\text{molecules}}{\text{cm}^3}$$

and the $\frac{\text{volume}}{\text{capsule}} = \frac{\pi}{6} d_{32}^3 = 5.6 \times 10^{-6} \frac{\text{cm}^3}{\text{capsule}}$

10.4 BAEE units/cm^3 therefore represent

$$5.4 \times 10^{15} \times 5.6 \times 10^{-6} = 3 \times 10^{10} \frac{\text{molecules}}{\text{capsule}}$$

The $\frac{\text{area}}{\text{capsule}} = \pi d_{32}^2 = 1.52 \times 10^{-3} \frac{\text{cm}^2}{\text{capsule}}$

and so 10.4 units/cm^3 is equivalent to

$$3 \times 10^{10} / 1.52 \times 10^{-3} = 1.98 \times 10^{13} \frac{\text{molecules}}{\text{cm}^2}$$

or about $5 \times 10^{-14} \frac{\text{cm}^2}{\text{molecule}}$

For monolayer coverage by square ($d_m \times d_m$) adsorption cells, where d_m is the molecular diameter, then 5×10^{-14} cm^2/molecule yields

$$d_m = 2.3 \times 10^{-7} \text{ cm}$$
$$= 23 \text{ Å}$$

This value for the molecular diameter of adsorbed trypsin seems to be much too small for a molecule of 23,300 molecular weight; a value of 40-50 Å would be more appropriate. One concludes, therefore, that a layer 3 or 4 molecules thick would be necessary to produce the activity indicated in Table 15. Multilayer coverage of the capsule membrane seems contradictory to the fact that the trypsin is more stable when adsorbed, unless the enzyme's proteolytic activity is greatly inhibited in this conformation.

VI-3. Temperature Effects

The esterase activities of an 0.025 mg/ml trypsin solution and Batch 14-8 and 14-13 MEC-trypsin were measured in tris-buffered BAEE solutions over the range of 20-35°C. The buffer solutions were adjusted to pH 8.0 at the appropriate temperature using HCl or NaOH. Microcapsule batches were equilibrated with the buffer in the absence of the substrate prior to the assays.

The results of this test are shown in Figure 17 with the "apparent" energy of activation for the hydrolysis reaction computed from the familiar Arrhenius relationship:

$$v = v_o \exp(-E_{act}/RT) \qquad (6.2)$$

E_{act} for the free trypsin solution is in good agreement with the value of 9.1-9.3 given by Ignagami and Sturtevant [77]. The higher values of the activation energy for the MEC-trypsin support the hypothesis of the preceeding section that the activity of the enzyme might be somewhat restricted if the enzyme is adsorbed to the inner membrane surface. The fact that E_{act} was higher for the Batch 14-8 capsules (initial loading 0.08 mg enzyme/ml) than for the 14-13 capsules (2.0 mg/ml) is contradictory, however, since one would expect more enzyme to be adsorbed to the membrane surface in the latter case. The difference may reflect the uncertainty in the estimation of the slope in Figure 17 or that a larger fraction of the enzyme is in the internal solution in the Batch 14-13 than in the 14-8 capsules. It is also true that if the "apparent" reaction rates used in this study were corrected for mass transfer limitation, the correction factor would be larger

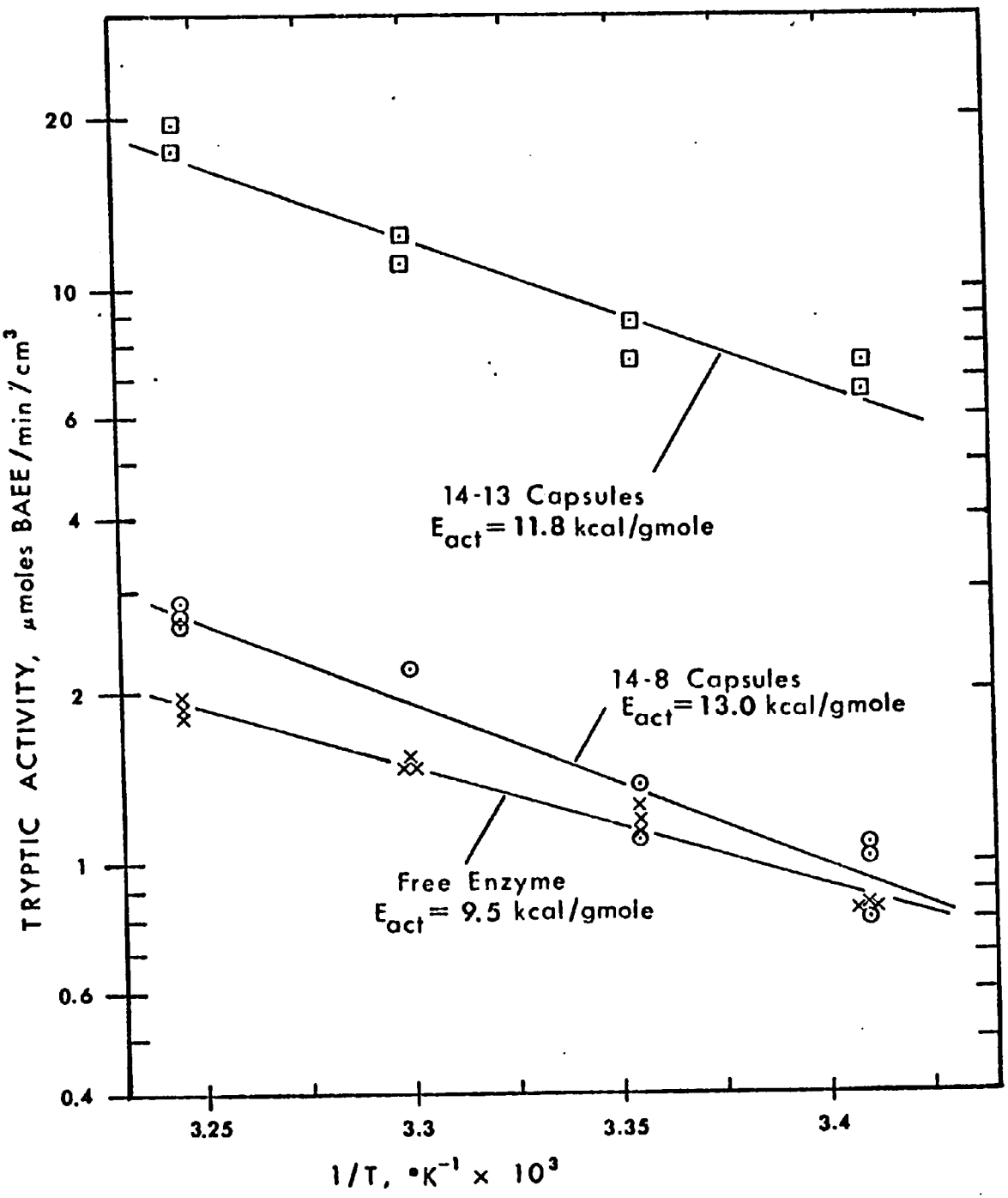

Figure 17. Effect of Temperature on Free-Trypsin and MEC-Trypsin Reaction Rates. (1mM BAEE Assays)

for higher values of the measured capsule activity. The net effect would be to increase the E_{act} for the Batch 14-13 to a greater extent than for the Batch 14-8 capsules, thus making the two activation energies closer than they appear above.

The higher value of E_{act} for MEC-trypsin than for free trypsin also suggests that the diffusion process is not contributing significantly to the overall MEC-trypsin kinetics. If diffusion were a significant factor, then one would expect a decrease in E_{act} since the E_{act} for diffusive transport is 3-4 kcal/gmole.

VI-4. pH Effects

Batch assays of a 0.04 mg/ml trypsin solution and Batch 14-9 and 14-12 microcapsules were made at 25°C and over the range of pH 7-9, the useful range of the tris buffer system. Buffer solutions were brought to the proper pH with HCl. The capsules were not equilibrated with the buffer prior to assaying.

As indicated in Figure 18, the behavior of MEC-trypsin deviated once again from that of the enzyme in free solution. Each point in Figure 18 represents the average of two assays; the reaction rate reported is the percent of the maximum observed rate for each enzyme form. The free-solution behavior agrees well over this limited pH range with the pH-profile presented by Goldman et al. [58]. The MEC-trypsin pH profile was displaced to higher pH's by $\sim$0.5 pH units which, using the logic developed in Section III-2-D, indicates a more polyanionic environment inside the capsule than outside.

Since the isoelectric point of trypsin is 10.8 [118], the enzyme would have a net positive charge (polycationic) in the pH range used in this test. Hemoglobin, however, has an isoelectric point

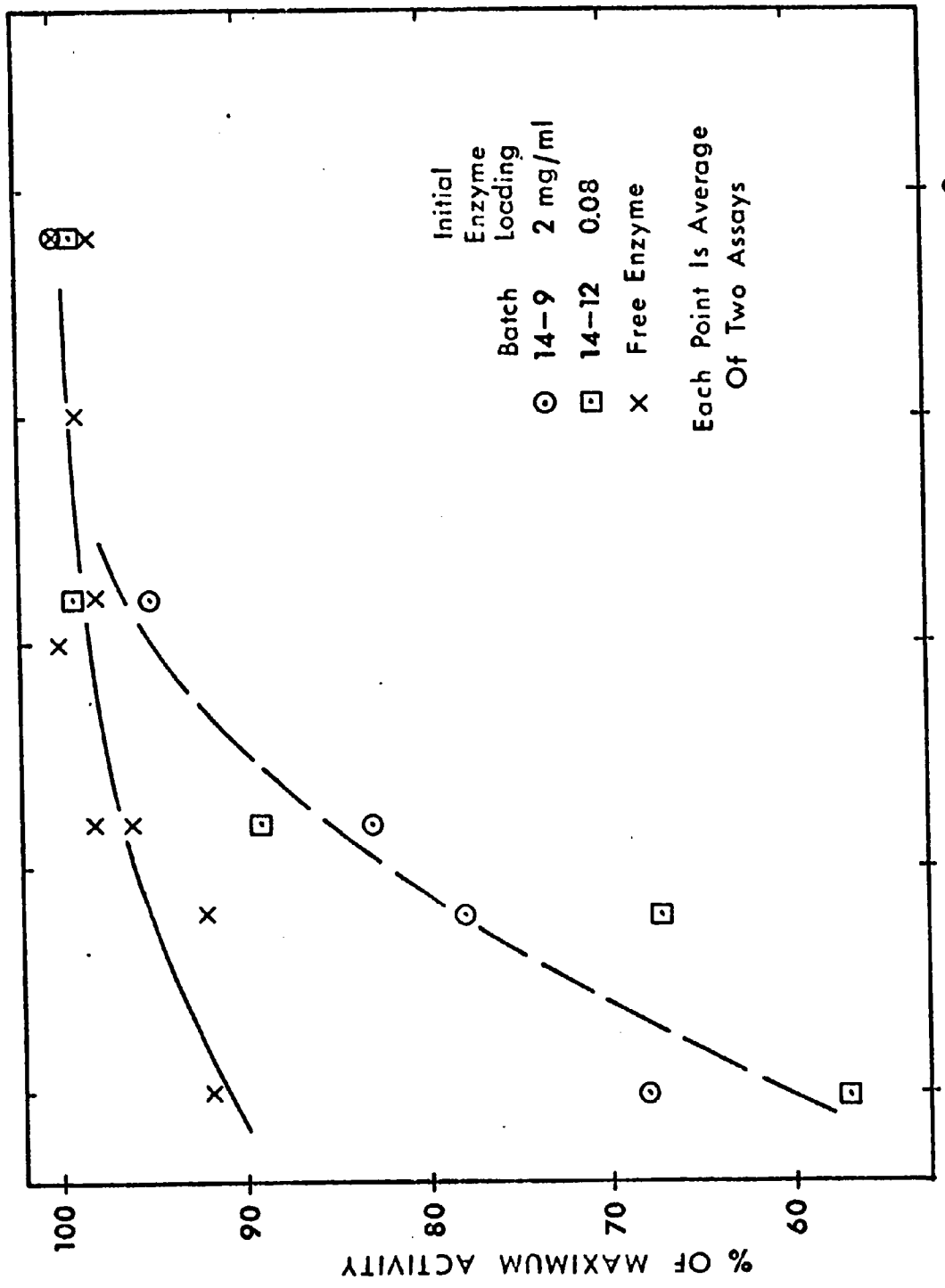

Figure 18. Effect of pH on Free-Trypsin and MEC-Trypsin Reaction Rates. (1mM BAEE Assays)

~pH 7 and so would be anionic under the test conditions. It is possible that unreacted amine groups on the inner surface of the nylon membrane are serving as "adsorption sites" for the enzyme. This process would serve to decrease the number of negatively charged groups on the enzyme, however, and thus serve to increase the isoelectric point even more. Hemoglobin bound or adsorbed to the membrane during encapsulation would provide the polyanionic microenvironment indicated by the results in Figure 18.

An alternative explanation of the altered pH behavior of trypsin inside capsules would be that the enzyme undergoes a change in conformation upon adsorption to the membrane. This behavior would be consistent with the observation of Section VI-3 that the activation energy for the reaction is also changed.

VI-5. Microcapsule Membrane Permeability Studies

The permeability coefficient for the microcapsule membrane and external unstirred film was estimated from measurement of the rate of efflux of solute from solute-loaded capsules as suggested by Flinn and Cherry [44] and Shigeri and Kondo [127].

Batch 17 capsules, which contained only hemoglobin, were employed in the following manner:

1) About 5 cc of capsules in a 15 cc centrifuge tube were equilibrated with 0.04 M tris buffer solution (standard assay concentration); capsules were allowed to settle and the supernatant drawn off;

2) About 10 cc of 10mM BAEE solution (in standard tris buffer) were pipeted into the centrifuge tube, the tube contents were stirred and permitted to stand at least 5 minutes, followed

by centrifugation, and removal of the supernatant liquid; this process was repeated 4 more times;

3) 2 cc of the final BAEE-loaded capsule suspension (~30-40% capsules) were pipeted into a 28 mm x 100mm round-bottom centrifuge tube which rested inside a 100 cc beaker on a magnetic stirrer;

4) A 9mm x 20mm teflon-coated stirring bar was placed in the tube and the suspension was stirred at the lowest possible speed to just keep the capsules suspended;

5) At t=0, 18 cc of 0.04M tris buffer solution were quickly poured into the tube (~1 second duration with the clock starting in middle of pouring);

6) Samples were periodically withdrawn from the tube and capsules simultaneously filtered out by using 2.5 cc syringes with 13mm diameter plastic filter holders (Millipore) and 13mm Gelman Type E glass fiber filters; the tip of the filter holders was placed at the center of the remaining suspension when the sample was withdrawn;

7) The test was repeated twice for each of the three sizes of Batch 17 capsules;

8) The solute (BAEE) concentration in the bulk liquid was measured at 255 mμ in the spectrophotometer with the absorbance of a 1mM BAEE solution equal to 1.90 Absorbance Units in the 1 cm cell.

The experimental results for this study are shown in Figure 19 with the curves computed from the "well-mixed" capsule model described below.

At any time, t, after dilution of the capsule suspension, the rate at which solute is leaving the capsules equals the rate of

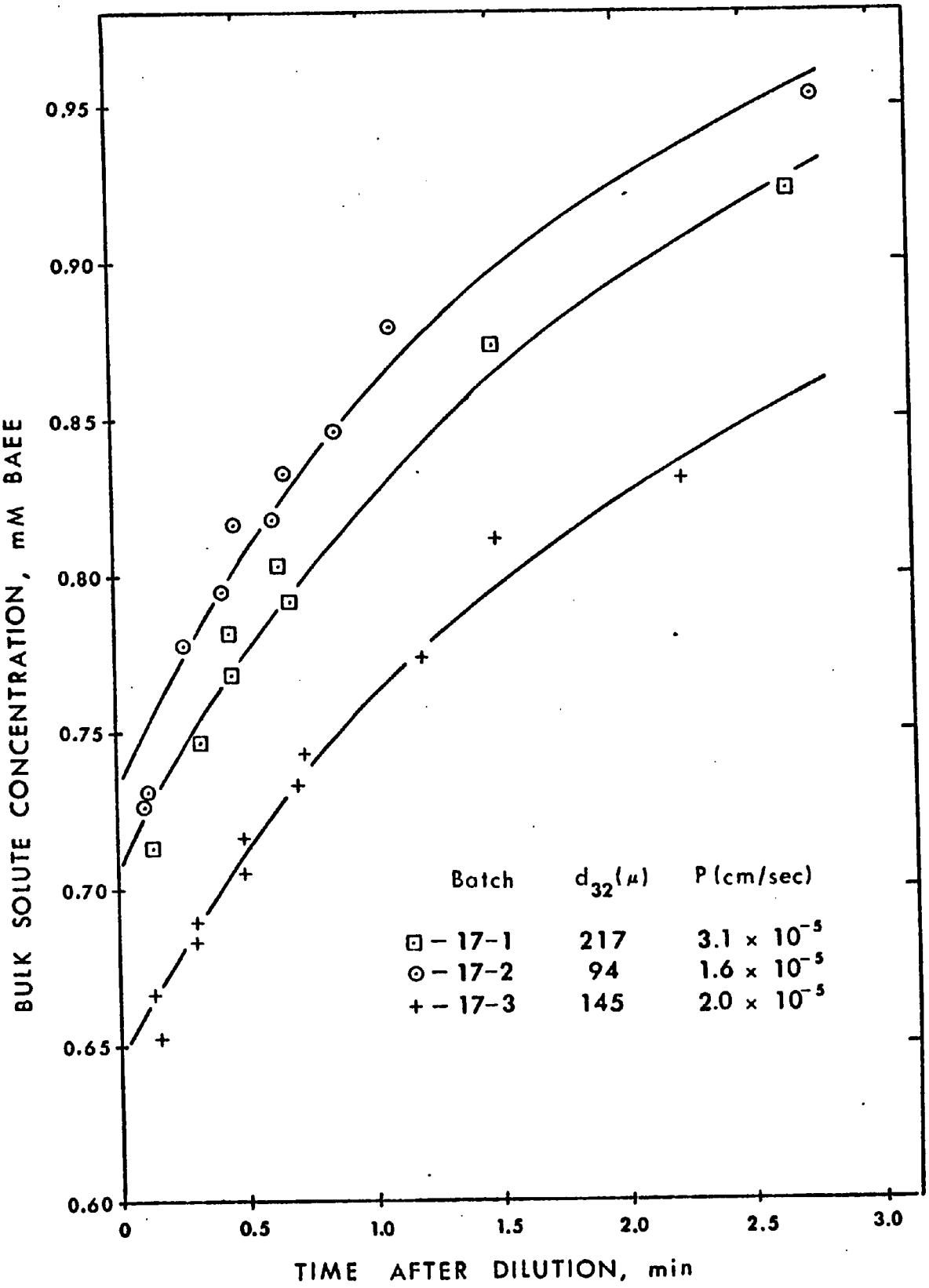

Figure 19. Efflux of BAEE From Trypsin-Free Microcapsules. Solid Lines Calculated From Eq. 6.5

accumulation in the bulk and, also, the total amount of solute transferred from the capsules equals the amount accumulated outside. Thus, for well-mixed capsules with c_c = constant for $r<r_o$ and for the conditions used in this experiment,

$$(20-V_c)\frac{dc_b}{dt} = PA_c(c_c-c_b) \tag{6.3}$$

and

$$(20-V_c)(c_b-c_b^o) = V_c(c_c^o-c_c) \tag{6.4}$$

where c_b and c_c are bulk and average capsular solute concentrations at any t and c_b^o and c_c^o are the same concentrations at t=0. V_c is the total volume of capsules initially in the centrifuge tube.

Solving for c_c in Eq. 6.4, then substituting this expression into Eq. 6.3 and integrating between t=0 and t=t, one arrives at Eq. 6.5.

$$\log_e \frac{c_c^o + (\frac{20-V_c}{V_c})c_b^o - \frac{20}{V_c}c_b}{c_c^o - c_b^o} = -PA_c\left[\frac{1}{V_c} + \frac{1}{20-V_c}\right]t \tag{6.5}$$

Eq. 6.5 was fitted to the data of Figure 19 by linear least-squares analysis. V_c was estimated from the initial and final (t> 30 minutes) bulk and capsule concentrations, since from Eq. 6.4

$$(20-V_c)(c_b^f - c_b^o) = V_c(c_c^o - c_b^f) \tag{6.6}$$

where the superscript f denotes the final bulk solute concentration (equal to the final capsular concentration). Since

$$20\,c_b^f = 2\,c_b^o \tag{6.7}$$

then Eqs. 6.6 and 6.7 can be combined to solve for V_c as

$$V_c = \frac{20\,(c_b^f - c_b^o)}{10\,c_b^f - c_b^o} \tag{6.8}$$

c_b^o was estimated by extrapolating the solute concentration data given in Figure 19 back to t=0 on semi-log paper. The estimates were in good agreement with the values computed from the least-squares lines in Figure 19.

The permeability coefficients for the combined membrane and external film range from 1.6×10^{-5} to 3.1×10^{-5} cm/sec as shown in Figure 19, and appear to increase slightly with increasing capsule diameter. These values are in the same range as those given by Chang and Poznansky [35], Table 7, for other solutes of similar molecular weight (the molecular weight of BAEE is 343).

One might argue that the well-mixed capsule model tends to underestimate the initial rate of efflux of BAEE from the capsules as shown in Figure 19. An alternate method for estimating P is based on the relationship given in Eq. 6.3 at t=0, at which time the intracapsular concentration should be constant throughout.

Lines were drawn by eye through the first few points ($t < 0.5$ min.) of the data in Figure 19 and used to estimate $\frac{dc_b}{dt}$ at t=0. Values of the permeability coefficient computed in this manner from Eq. 6.3 gave $P = 4.8 \times 10^{-5}$ cm/sec for 17-1 capsules and $P = 2.5 \times 10^{-5}$ cm/sec for both 17-2 and 17-3 capsules. These values, although somewhat higher than those

predicted by the integrated model used above, are still much lower than the values which might be expected from the discussions of Morgensen [103].

VI-6. Capsule Diameter and Enzyme Loading Effects

In this experiment, twelve batches of microcapsules were prepared in random order from the same reagents on the same day. The batches represented four initial enzyme loading levels with three sizes of capsules for each level. The enzyme loading was obtained just prior to forming the capsules by diluting a 4 mg/ml trypsin - 10% hemoglobin solution to the proper final concentration with trypsin-free hemoglobin solution. Capsules were washed several times and stored at 4°C in distilled water for one day, then assayed three times over a four day period. Between assays the capsules were stored at 4°C.

The averages of three assays for each of the batches are presented in Figure 20. The most striking aspect of these results is that, although the measured MEC-activity is generally lower than that expected if all of the enzyme were encapsulated and remained active, the observed activities are clearly higher than would be predicted based on the permeability constants computed in the preceding section. For example, for the Batch 14-14 capsules ($d_{32} = 158\mu$) $v_{es} = 8.8$ BAEE units/cm^3. If $P = 5 \times 10^{-5}$ cm/sec based on the findings of Section VI-5, and $k_2 E_t = 46$ BAEE units/cm^3 (100% of the encapsulated activity), $D_{is} = 5 \times 10^{-6}$ cm^2/sec, $c_{so} = 1$mM and $K = 0.05$mM, then

$$\alpha = Pr_o/D_{is} = 0.079$$

$$\beta = k_2 E_t r_o^2/D_{is} K = 192$$

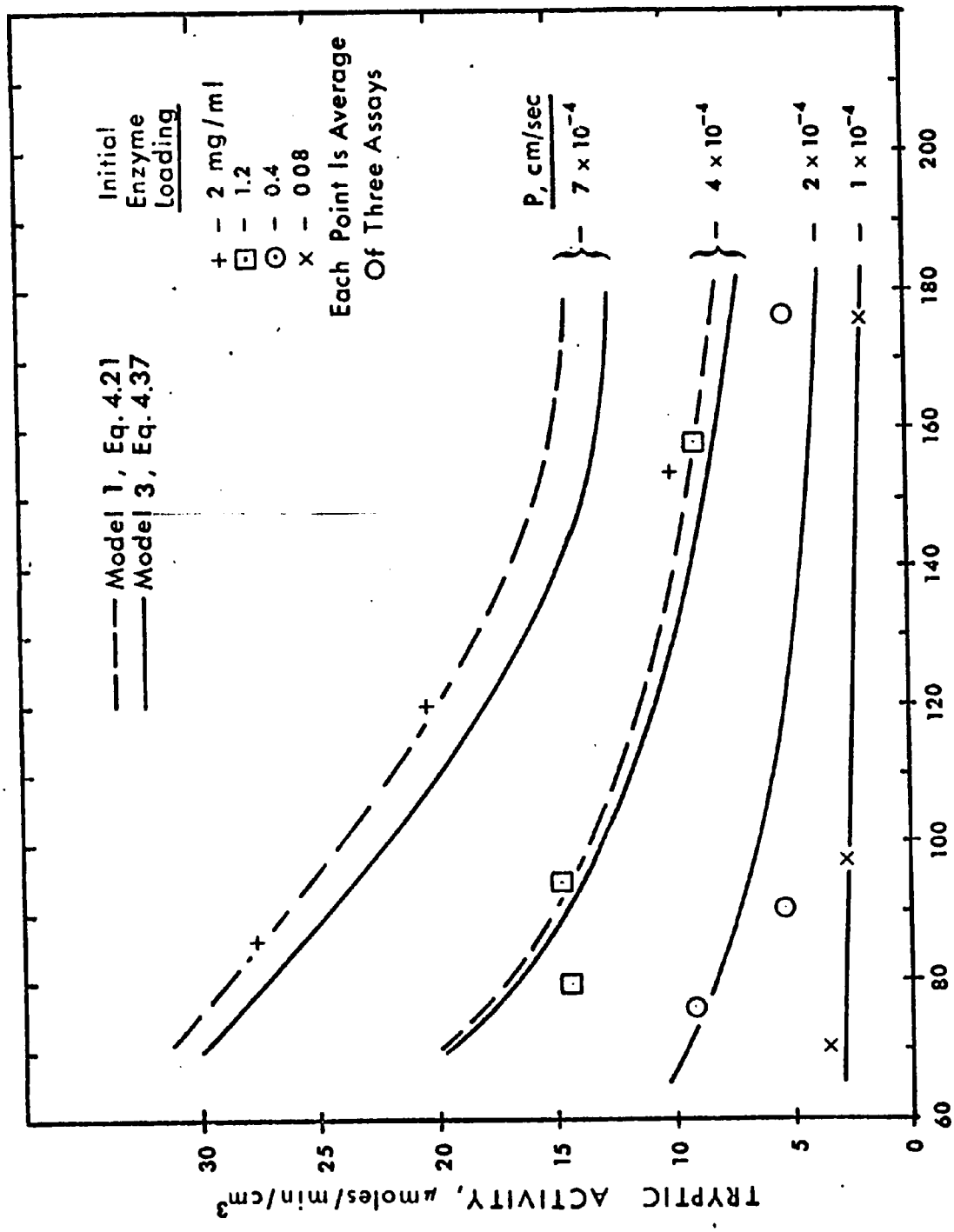

Figure 20. Effects Of Capsule Diameter and Enzyme Loading on "Apparent" Microencapsulated Activity

$$\kappa = K/c_{so} = 0.05$$

and $$\phi = [\beta\kappa/(1+\kappa)]^{1/2} = 3.0$$

From Figure 4, for these values of α and ϕ, one finds that the expected overall effectiveness factor is $\sim$0.02. Therefore, the maximum $v_{es} = \eta_o V_{max} c_{so}/(c_{so} + K) = 0.87$ units/cm^3, only about 10% of the measured reaction rate.

Similarly, for Batch 14-7 capsules ($d_{32} = 76.3\mu$, $v_{es} = 9.2$ BAEE units/cm^3), $k_2 E_t = 15$ units/cm^3, and the other parameter values used above, $\alpha = 0.0382$, $\beta = 44.8$, $\kappa = 0.05$, and $\phi = 1.46$. From Figure 4, η_o is expected to be about 0.04. The maximum predicted reaction rate is $v_{es} = 0.57$, or about 6% of the observed activity.

The lines in Figure 20 were calculated to approximately fit the data in an attempt to estimate the value of P, the combined external film-membrane permeability, consistent with the measured reaction rates and 100% yield of the initially-charged active enzyme. These values then represent the lower limits for P if some enzyme activity is lost upon encapsulation.

The solid lines in Figure 20 were computed using model 3, Eq. 4.39, the "constant-average" reaction rate approximation, as derived in Chapter IV. The dashed lines were calculated from model 1, Eq. 4.31, the first-order reaction rate approximation. The other parameter values used in the computations were $K = 0.05$mM, $c_{so} = 1$mM, and $D_{is} = 5 \times 10^{-6}$ cm^3/sec. Both the model 1 and model 3 lines are shown for the two highest initial enzyme loadings to indicate that there was not a great disparity between the two predictions. For the highest enzyme level (77 units/ml), the first-order (model 1) approximation is

the more appropriate of the two as can be verified from Figure 6. For the next lower loading (46 units/ml) both models predict nearly the same reaction rate.

An interesting aspect of these calculations is that larger permeability coefficients are required at the higher enzyme loadings in order to reasonably predict the observed reaction rates. This behavior suggests that the higher the initial enzyme loading, the greater is the fraction of the active enzyme which successfully survives the encapsulation process.

Two other factors must be considered in analyzing the observed capsule activities: how much, if any, of the enzyme was denatured during encapsulation and how is the enzyme distributed inside the capsule?

It seems likely that some of the active enzyme initially encapsulated would be rendered irreversibly denatured in some way, perhaps through interaction with the various reagents present or by binding directly into the capsule membrane. If some of the enzyme were denatured during encapsulation, however, the observed overall effectiveness factors are actually even higher than reported above. In order to lower the observed effectiveness factor one must hypothesize that the encapsulated activity is even higher than that originally charged.

Alternatively, if the originally encapsulated enzyme contained a significant portion of reversibly inactive enzyme, then the equilibrium between active and inactive enzyme might be shifted in favor of the active form in the MEC-environment. As mentioned in the Literature Review, lower pH's tend to favor the formation of reversibly denatured trypsin in free solution [92]. If the pH optimum for the MEC-enzyme was shifted to higher pH's because the microenvironmental pH inside the capsule is actually lower

than the bulk condition, then reversible denaturation would be favored in the capsule rather than the formation of more active enzyme.

"Active site" titrations, as suggested by Bender et al. [9], would appear to be the only techniques available for conclusively detecting the shift in the equilibrium between active and inactive enzyme. Breaking the capsules to assay the contents would generally serve to destroy the MEC-microenvironment. The active site analysis was not performed in this study.

Although active site titrations would reveal the number of active enzyme molecules, no information would be obtained regarding the location of the enzymes inside the capsules. In the first two sections of this chapter, evidence was presented which suggests that trypsin will be found in higher concentration at the membrane surface than in the interior of the cell. The net effect of adsorption of enzyme onto the membrane would be to make the "apparent" internal substrate diffusivity higher than in free solution. Furthermore, if all of the enzyme was adsorbed to the inner membrane surface, then the effect of internal diffusion on the system kinetics would be negligible, since the substrate would not have to diffuse into the capsule at all. Note also that the mathematical models developed in Chapter IV will not be strictly valid when the enzyme is not homogeneously distributed throughout the capsule.

In order to evaluate the importance of internal diffusion rates, one might assume that the "effective" internal diffusivity is, say, 100 times higher than the value assumed above, owing to localization of the enzyme on the membrane. For the Batch 14-14 capsules, the assumption of $P = 4 \times 10^{-4}$ cm/sec and the

same values of the other parameters chosen above yield $\alpha = 0.63$, $\beta = 192$, $\kappa = 0.05$, and $\phi = 3.0$ when $D_{is} = 5 \times 10^{-6}$ cm/sec and $\alpha = 0.0063$, $\beta = 1.92$, $\kappa = 0.05$, and $\phi = 0.3$ when $D_{is} = 5 \times 10^{-4}$ cm/sec. From Figure 4, therefore, $\eta_o \equiv 0.1$ for the homogeneously distributed case (low D_{is}) and $\eta_o \equiv 0.17$ (higher D_{is}). These calculations show that adsorption of the enzyme will tend to increase the observed whole-capsule activity. The increase is not likely to be great enough, however, to account for the greater than tenfold increase in P as estimated from the diffusion-only studies of the preceding section.

VI-7. Estimation of Effectiveness Factors by Breaking Capsules

Three methods were employed in this study to break capsules containing trypsin in order to determine the internal capsular activity in the absence of diffusion limitations.

A Corning Ten Broeck-type homogenizer (tissue grinder) was used to rupture the capsules mechanically. Homogenization of capsule suspensions for one minute was generally sufficient to break nearly all of the capsules used in this study. When trypsin solutions having activities similar to the resulting broken-capsule suspension activity were homogenzied in the same way, however, only 25% of the initial activity of the solution was retained after one minute. Cooling the grinder in an ice bath and adding 10% glycerin by volume helped to improve the retained activity slightly but still only $\sim$35% retention resulted. This level of denaturation was considered unacceptably high since it added uncertainty to the estimation oı the broken-capsule activity.

Attempts to rupture microcapsules by repeated freezing and thawing generally were ineffective. Typically, after three freeze-thaw cycles, nearly all of the capsules had assumed distorted configurations but only a small fraction were broken.

Ultrasonic breakage of the capsules was also carried out. 10cc of either a capsule suspension or free-enzyme solution were placed in a 25cc glass vial. The probe of a titanium-tipped transducer (Dukane Corporation) was inserted into the liquid so that the base of the probe was 1/8" below the surface. Power was supplied by a Type 500-1 Multisons broad band generator from Multisonics Corporation. Cavitation was observed at 19-20 kilocycles in all breakage tests.

The retained activity of ultrasonically irradiated free-trypsin solutions (initially 6 BAEE units/ml) are shown in Figure 21 as a function of the exposure time. Each point in Figure 21 represents the average of two assays. It should be noted that the very high local temperatures often associated with cavitation did not cause a drastic denaturation rate of the free solution trypsin.

30 second irradiation periods were found to be sufficient to break nearly all of the capsules in a given suspension (typically > 99%, based on estimates made through the microscope). A summary of several breakage tests on Batch 14 microcapsules is presented in Table 16. Based on the denaturation rate in Figure 21, the "free-enzyme" resulting from the rupturing of the cells, was assumed to undergo a 30% activity loss during the 30 second irradiation period. The effectiveness factor was therefore computed from the relationship

$$\eta_o = \frac{\text{whole capsule activity}}{(\text{broken capsule activity})/0.7} \qquad (6.7)$$

The effectiveness factors presented in Table 16 are generally of the same order as those observed for capsules of various sizes and enzyme loadings in Section VI-6. These data therefore tend to support the hypothesis that the membrane permeability

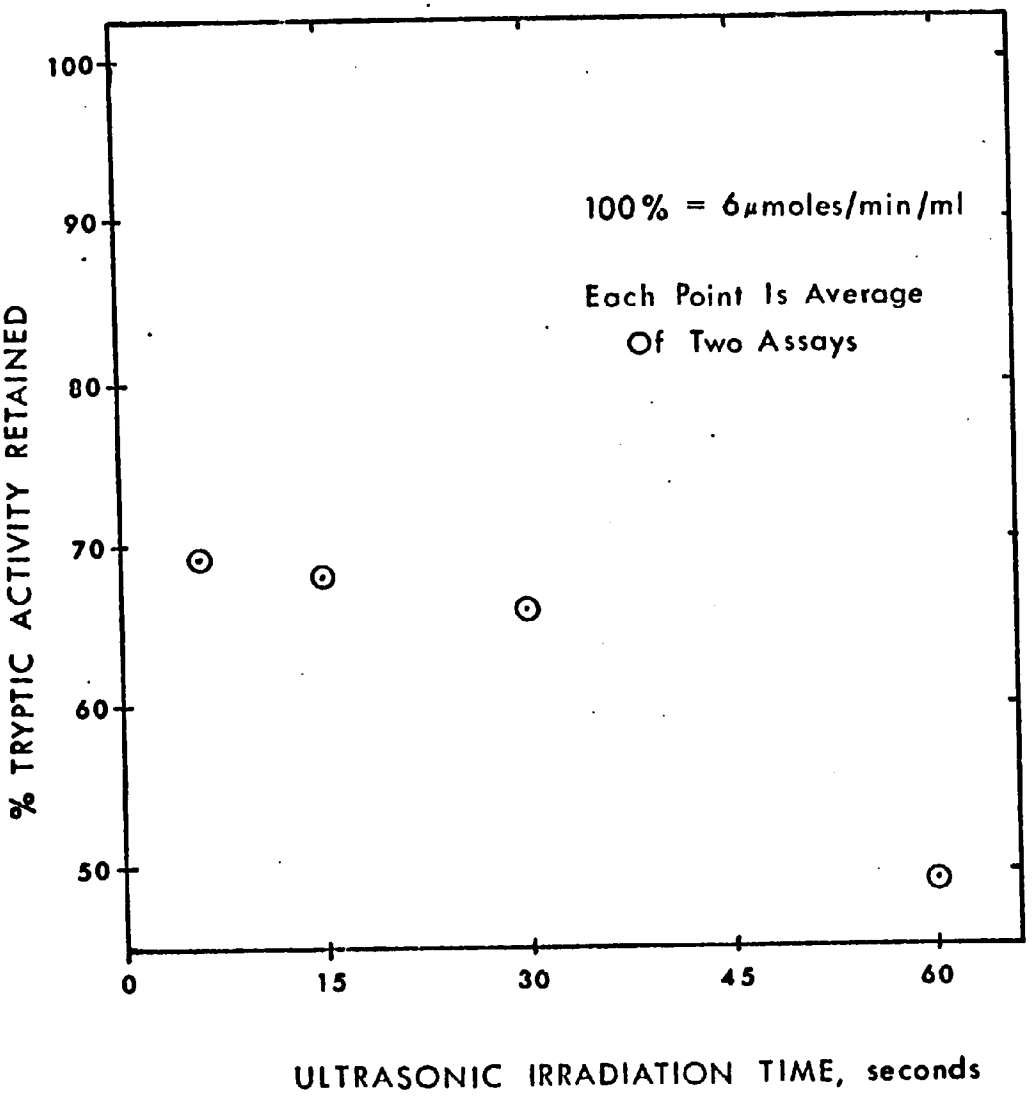

Figure 21. Retention of Activity of Ultrasonically Irradiated Trypsin Solution

Table 16

Effectiveness Factors From Assays Of Ultrasonically Broken and Whole Microcapsules

Sample #	d_{32} (μ)	Capsule Activity (BAEE units/cm^3) whole	broken	Observed Effectiveness Factor η_o^*
14- 9	120	16	26	0.43
14-10	94	13	15	0.63
14-11	90	4.8	8.5	0.39
14-12	97	2.4	2.0	0.85
14-15	177	4.9	6.2	0.55
14-16	176	1.4	0.99	1.02

* as calculated from Eq. 6.9

for MEC-trypsin is actually higher than the estimates made in Section VI-5 with enzyme-free microcapsules.

In the whole-capsule assays of Section VI-6, the yield of the initially encapsulated enzyme ranged from 25% to nearly 100% when based upon the apparent activity. Thus the actual yield, after correction for mass transfer limitation based on the effectiveness factor estimates reported in Table 16, should be 60-100% of the initially encapsulated activity.

VI-8. Prediction Of Kinetic Parameters From Batch Reaction Rates

As stated in Chapter II of this report, one of the primary objectives of this study was to statistically fit the kinetic models developed in Chapter IV to substrate concentration vs. substrate conversion rate data. In this way, characteristic parameter values for the system would be estimated and, subsequently, reaction rate data could be "corrected" for the effects of mass transfer limitation. Procedures are described in this section for the implementation of these computations and attempts at fitting the model conversion rate expressions to batch reaction data are discussed.

As mentioned in Chapter V, the somewhat fragile nature of the nylon microcapsules prepared in this study was discovered early in the experimental program. The use of the continuous flow (steady state) reactor system described in Section V-2-A was discontinued, therefore, in the hope that a more "gentle" assay could be developed which would eliminate capsule breakage but still be revealing with respect to the system kinetics.

The batch reaction assay was developed in order to produce conditions in which the capsules would be agitated just enough to be maintained in suspension. The data for the complete-conversion batch reactions were very similar to that given in Figure 11 with the exception that the reaction was permitted to proceed until the reaction had gone to completion. The data were interpreted by "bracketing" the signal noise as shown in Figure 11 by the dashed lines and then taking the absorbance midway between these lines as the absorbance at a given value of reaction time. These absorbance-time pairs were determined at various intervals during the reaction and converted to concentration-time data by the appropriate conversion. It should be recognized that this data reduction process tends to damp out the "noise" inherent in the reaction data as well as any high frequency information contained in the signal. The noise is caused by the presence of discrete catalyst particles (the microcapsules) which periodically interfere with the spectrophotometer light beam. Typical batch reaction data of the type described are shown in Figure 22 for reactions utilizing Batch 10 and 13-1 microcapsules.

The inherently transient nature of the batch reaction forces one to question the validity of the use of "steady-state" models to describe presumably "unsteady-state" kinetics. It seems reasonable,

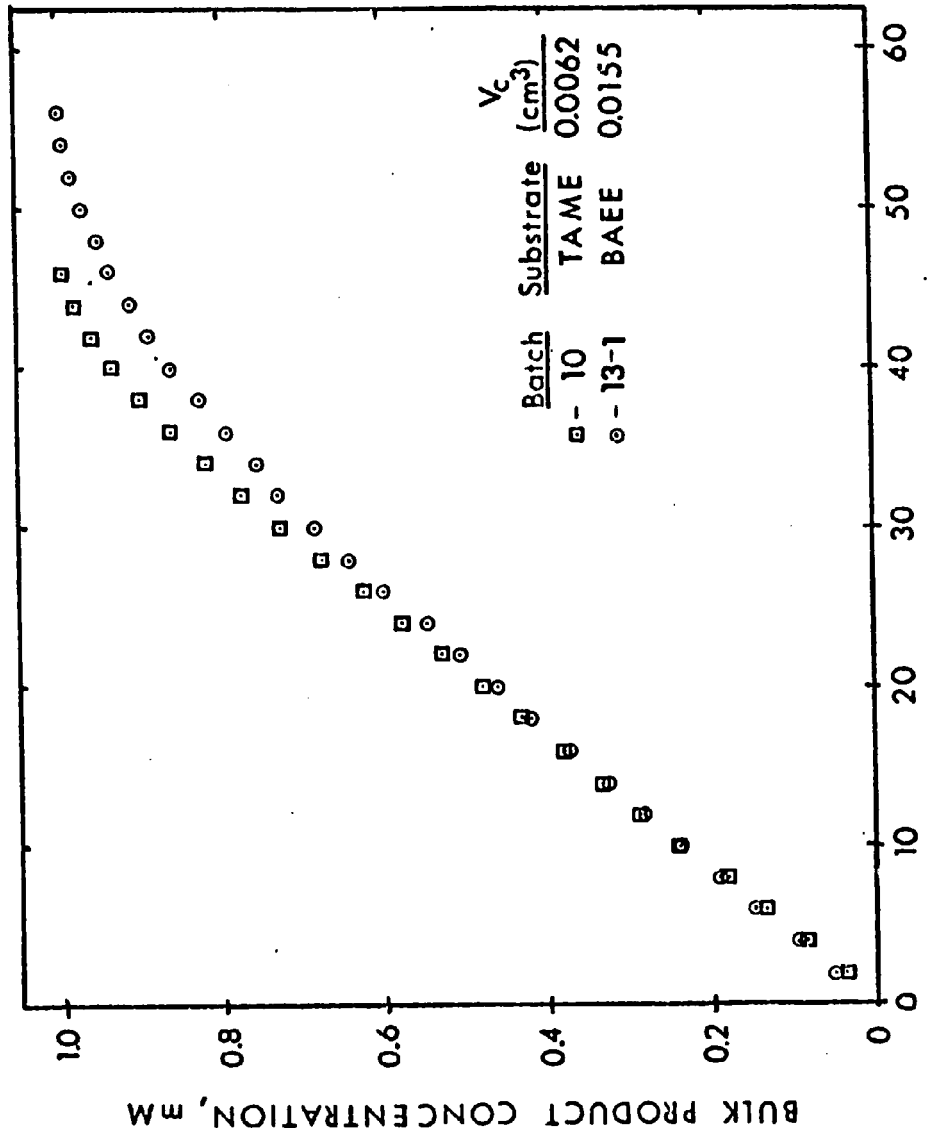

Figure 22. Typical Batch Reaction Data For Complete Conversion Of 1mM Substrate Solution In 3 ml Reactor

however, to treat the batch reaction as though the steady-state was attained at any instant during the reaction in view of the following evidence:

1) Equilibration of solute across the membrane in the absence of reaction was relatively rapid when compared to the time required for complete conversion of substrate in the batch reaction ($t_{1/2}$ for equilibration was about 2 minutes from Figure 19; complete conversion of 1mM substrate typically took from 30 to 60 minutes).

2) The unsteady-state reaction rate expression, Eq. 4.107, derived in Section IV-6 predicts the very rapid attainment of near-steady-state conditions. Even if this model underpredicted by an order of magnitude the time to reach 99% of the steady-state conditions, this would probably only invalidate the steady-state assumption during the first few minutes of the reaction.

The initial attempts in this study to fit the batch reaction data were made using the following algorithm:

1) The steady-state was assumed to obtain at every instant during the reaction. Thus, for given values of the system kinetic parameters (K_m, V_{max}, P, D_{is}), capsule diameter (d_{32}), volume of capsules in the reactor (V_c), and bulk substrate concentration (c_{so}), one of the models developed in Chapter IV could be used to compute the moles of substrate converted during a given increment of reaction time, Δt;

2) The bulk substrate concentration was corrected for the quantity of substrate converted, t was set equal to $t + \Delta t$ and the substrate conversion was computed under the new reactor conditions. In this way, the batch reaction was simulated until nearly complete conversion (99.99%) was obtained;

3) The substrate concentration-reaction time profile generated in this manner was compared to the corresponding experimental data and new estimates of the system parameters were generated by a nonlinear regression program utilizing Marquardt's optimization scheme [95]. The program used was IBM No. 309, 401 as distributed through the IBM Share Library.

Unfortunately, data analysis of this type never led to convergence to a physically-possible set of parameter values. If convergence was obtained at all, negative parameter values or impossibly high or low parameter values resulted.

Further insight into the problems involved with this type of analysis was gained by a more complete investigation of the batch reaction data. For example, Figures 23 and 24 indicate the results of numerically differentiating the data given in Figure 22. The derivatives were obtained using Eq. 6.10

$$\left.\frac{dc_{so}}{dt}\right|_t = \frac{c_{so}(t+\Delta t) - c_{so}(t-\Delta t)}{2\Delta t} \qquad (6.10)$$

While the reaction rate (dc_{so}/dt) vs. c_{so} plots are reminiscent of the type of behavior expected from Michaelis-Menten kinetics (first-order at low c_{so}, zero-order at high c_{so}), the double-reciprocal, Lineweaver-Burk-type plots indicate an obvious departure. Many of the numerically differentiated data sets showed a tendency for $1/[dc_{so}/dt)]$ to be constant or even decrease with increasing $1/c_{so}$ on the Lineweaver-Burk plots. In other words, for many of the runs the catalyst became more active as the substrate was depleted in the reactor. The apparent increase in activity is fairly pronounced in Figure 23 for the Batch 10 microcapsules and was even more noticeable in several other reactions. In Figure 23, the apparent reaction rate increases by

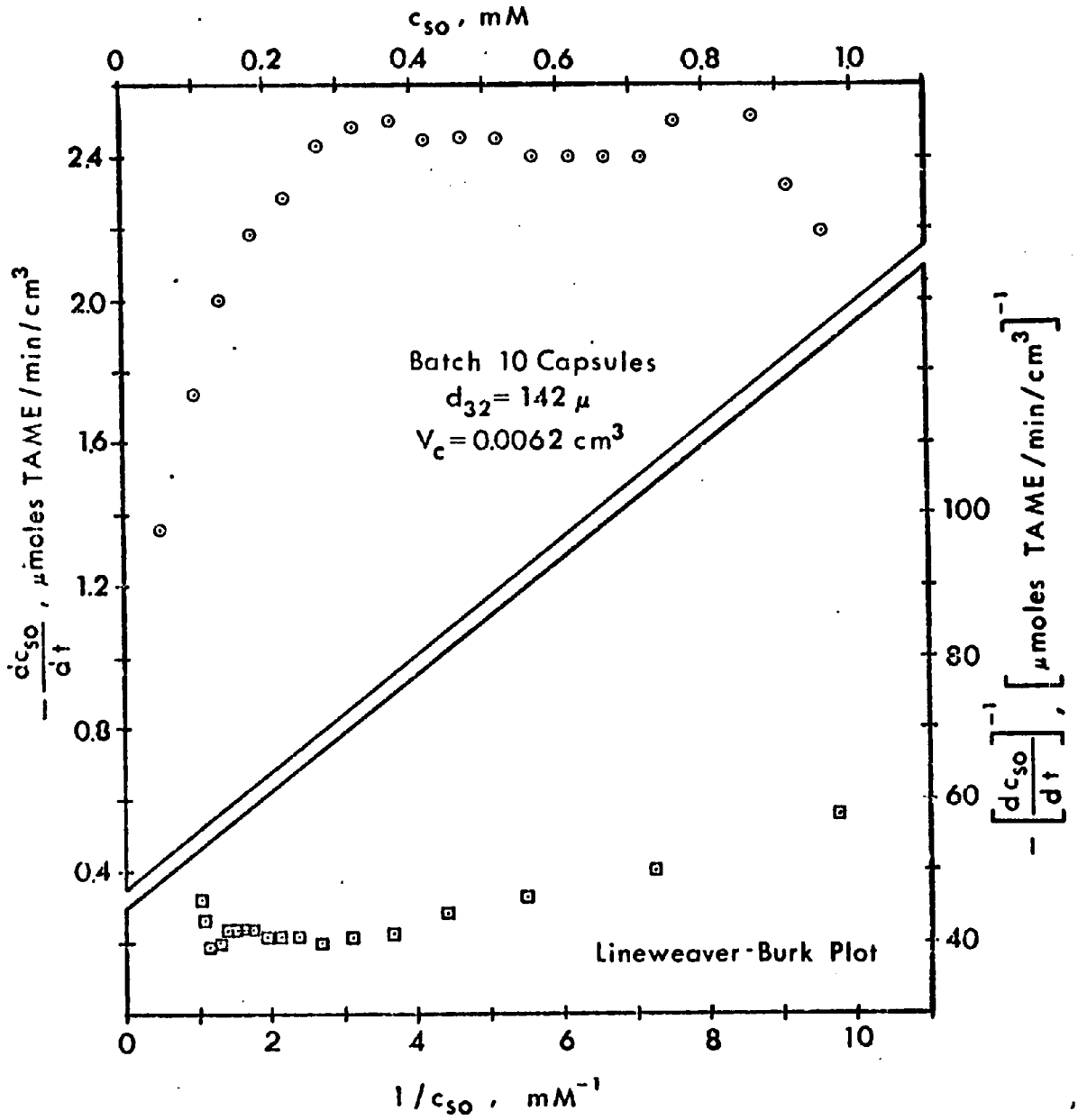

Figure 23. Concentration-Reaction Rate and Lineweaver-Burk Plots For Batch 10 MEC-Trypsin Reaction

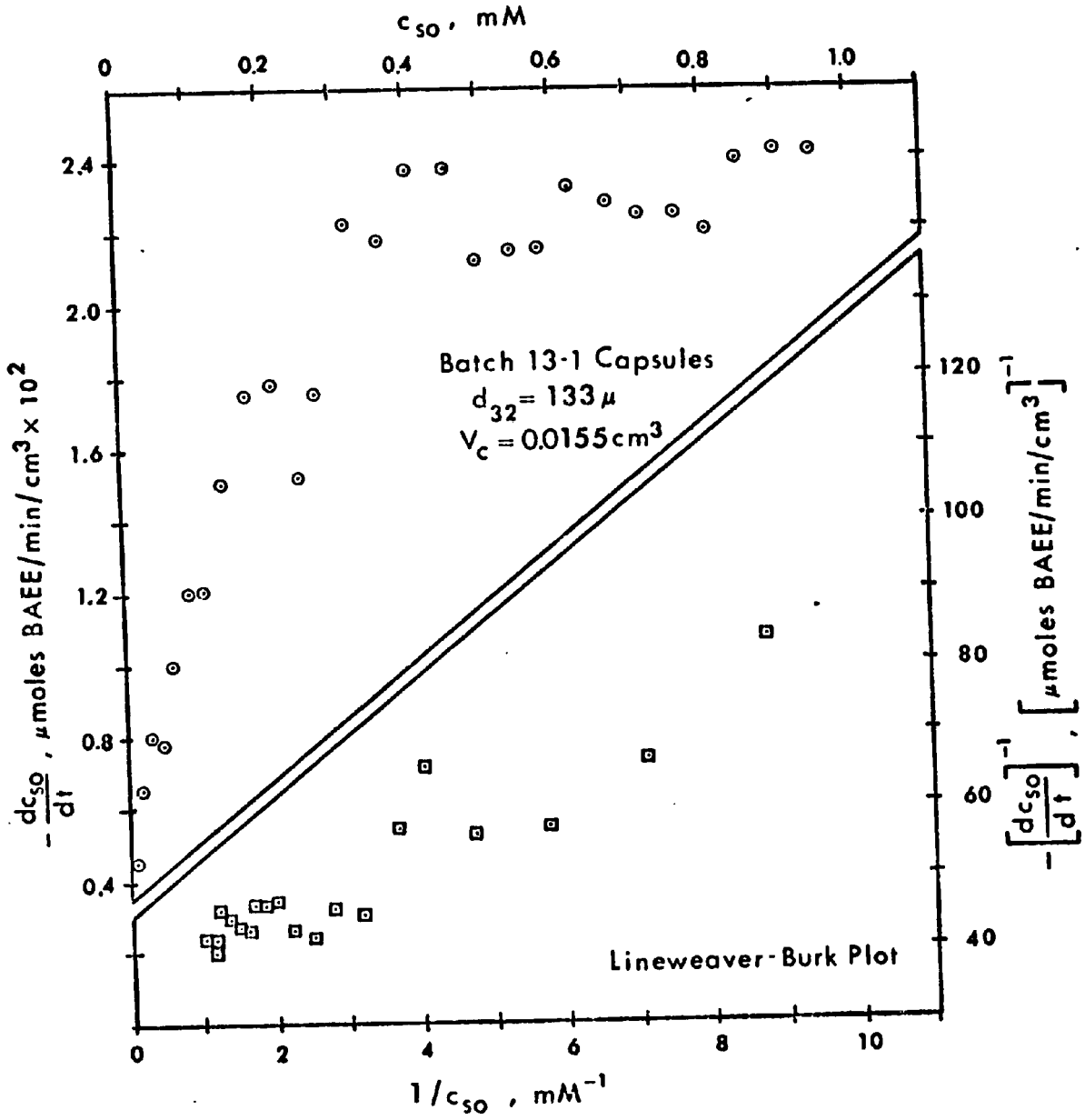

Figure 24. Concentration-Reaction Rate and Lineweaver-Burk Plots For Batch 13-1 MEC-Trypsin Reaction

about 20% in the range of c_{so} = 1 down to about 0.3 mM, i.e., until nearly 2/3 of the substrate is depleted.

An increase in activity during the reaction was generally observed with the Batch 10 microcapsules (d_{32} = 142μ, 1.0 mg enzyme/cm^3) and was not nearly as apparent when Batch 13-1 capsules (d_{32} = 133μ, 0.5 mg enzyme/cm^3) were used. Higher reaction rates per cm^3 of capsules, caused by the higher initial enzyme loading and the use of the more active TAME as substrate, may have acted to accentuate the activation process in the Batch 10 tests. It can be seen from Figure 22 that nearly the same activity was displayed by each batch of capsules, even though the volume of capsules in the reactor was nearly 2.5 times higher for the Batch 13-1 capsules.

It is important to observe that the increase in apparent capsular activity is not easily discernible from the reactor concentration-time plots in Figure 22. This behavior cannot be predicted by any of the steady-state models derived in Chapter IV. Furthermore, the "activation" was observed over a much longer time period than could be explained by the transient models discussed in Section IV-5. Note that the decrease in $1/[dc_{so}/dt]$ (or <u>increase</u> in dc_{so}/dt) continues in Figure 23 until $1/c_{so} \sim 3$, i.e., about 25 minutes into the reaction. Similar tests on the free-solution enzyme did not display this apparent increase in activity.

The increase in reaction rate as the external substrate concentration is decreasing cannot be explained by a lag in the rate at which product begins to appear in the external solution. The capacity of the capsule phase (less than 1% of the total reactor volume) is not great enough to accumulate the quantity of product required to explain this behavior, assuming the mass transport properties of product and substrate are about the same.

The author would speculate in this regard that the increasing activity during the reaction probably is due to an activation process which occurs as the reaction proceeds. For example, it may be that some of the enzyme tends to desorb from or adsorb to the membrane in the presence of the substrate, leading perhaps to an increased activity. Alternatively, the process might be one of activation of the enzyme created by the binding of Ca^{++} ions which were, it will be remembered, not introduced into the capsules until the reaction was initiated. In any event, it seems likely that the batch reaction should have reached pseudo-steady-state with respect to mass transfer, but remained unsteady-state in terms of some unknown kinetic process.

Inasmuch as the tendency for this apparent "activation" process was less noticeable in many reactions in which the Batch 13-1 capsules were employed with BAEE as substrate, further attempts to fit kinetic models to the data were attempted. For these capsules, the observed activity was rather low. It was hoped therefore, that an "apparent" K_m for the system could be defined from which P, the membrane-external film mass transfer coefficient, could be determined via Eq. 4.42. Parameters from the integrated Michaelis-Menten expression as given in Eq. 3.19 were determined from linear least-squares analysis using the variables $1/t \log_e(c_{so}^o/c_{so}^t)$ and $(c_{so}^o - c_{so}^t)/t$ as discussed in Section III-5-A.

The results of fitting nine sets of batch reaction data with 1mM BAEE as the initial substrate concentration are shown in Figure 25. The average values and standard deviation for these estimates are: $\bar{V}_{max} = k_2 E_t = 5.32$ μmoles/min/cm^3 with $\sigma_{V_m} = 0.75$ and $\bar{K}_m' = 0.159$ mM with $\sigma_{K_m'} = 0.053$. The value

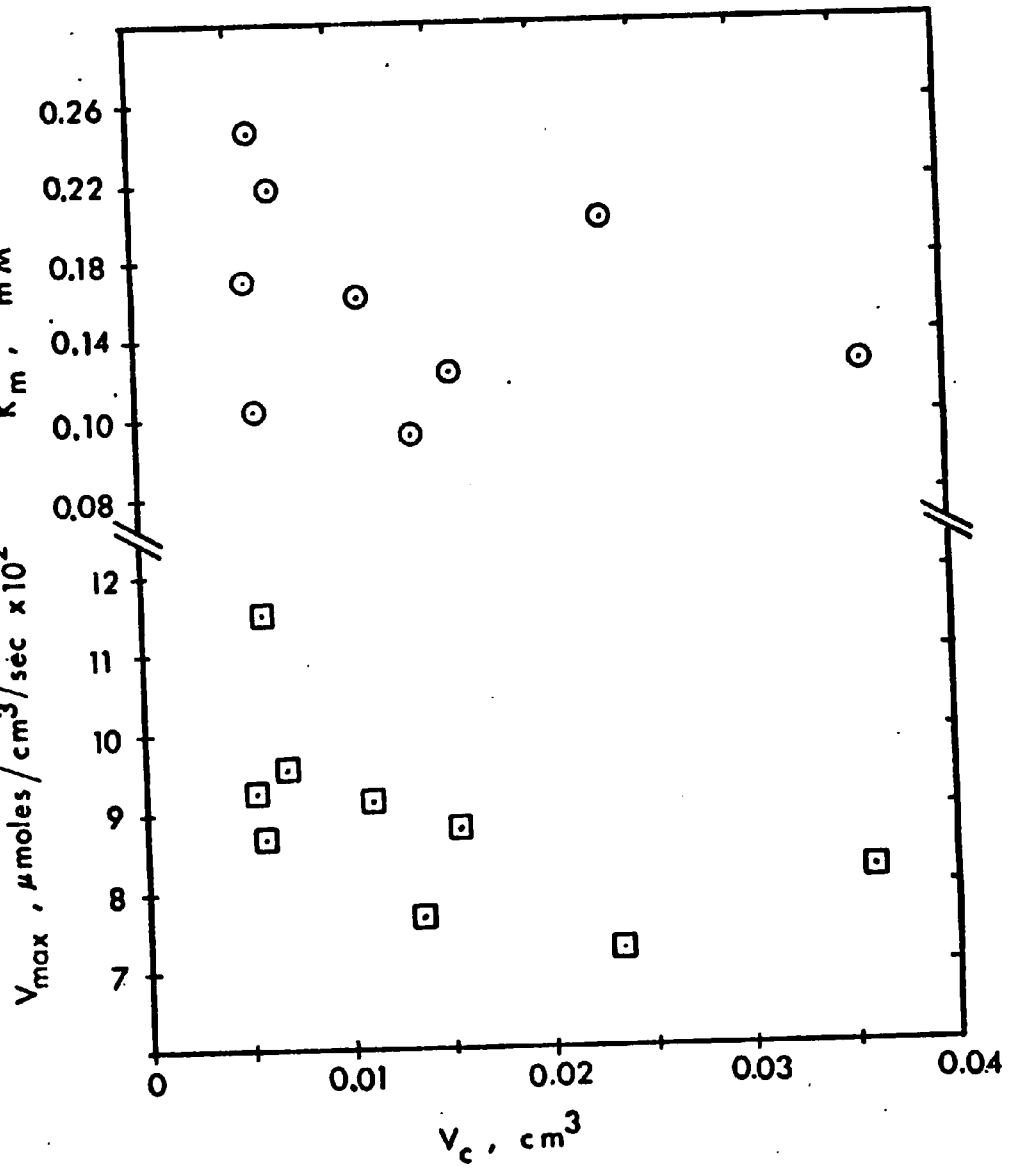

Figure 25. "Best Fit" Kinetic Parameters Computed From Batch Reactions Using Batch 13-1 Capsules

of $\bar{v}_{es}$ based on the initial slope method discussed in Chapter V was $\bar{v}_{es} = 4.46$ with $\sigma_{v_{es}} = 0.49$. $\bar{v}_{es}$ was significantly lower than $\bar{V}_{max}$ with a probability greater than 99% based on a Student's t test of the difference between the sample means. In computing the values of V_{max} from the integrated batch reactor data, several initial points were discarded from a few of the reactions because there appeared to be some "activation" proceeding during the experiment. Figure 25 suggests that the "best-fit" value for V_m decreased slightly when higher capsule volumes were used in the reactor while K'_m was more independent of V_c.

The value of K_m for the free-enzyme was determined from several batch reaction experiments to be in the range $K_m = 0.05$-0.06 mM. Another estimate of the overall effectiveness factor is therefore given by

$$\eta_o = v_{es}/(V_{max} c_{so}/(K_m + c_{so})) = 4.46/(5.32 \times 1/(1 + 0.05)) = 0.88 \quad (4.6e)$$

This value of η_o is slightly higher than the measured effectiveness factors given in Table 16, based on broken capsule assays, for capsules of similar size and activity as the Batch 13-1 capsules. For example, for Batch 14-11 and 14-15 the measured $\eta_o = 0.39$ and 0.55, respectively.

From model 4, Eq. 4.42,

$$\kappa' = \kappa + \Lambda \quad (6.11)$$

or

$$K'_m = K_m + V_{max} \Lambda_s \quad (6.12)$$

$$= K_m + V_{max} \left[\frac{r_o}{3P} + \frac{r_o^2}{15 D_{is}}\right] \quad (6.13)$$

For $K_m = 0.05$ mM, $r_o = 66.5\mu$, $D_{is} = 5 \times 10^{-6}$ cm^2/sec, and the values of K'_m and V_{max} determined above:

$$P = \frac{r_o}{3}\left[\frac{1}{(K'_m - K_m)/V_{max} - r_o^2/15D_{us}}\right] \qquad (6.14)$$

$$= 3.5 \times 10^{-3} \text{ cm/sec}$$

For the largest value of K'_m determined in this study, $K'_m = 0.249$, and assuming $K_m << K'_m$ then the value of P computed using the same parameter values as above is $P = 1.0 \times 10^{-3}$ cm/sec. These computations indicate that the overall mass transfer coefficient (combined external film and membrane) is about an order of magnitude greater than the lower-limit estimate made in Section VI-6 based on 100% yield of the encapsulated enzyme.

It is of interest at this point to estimate the value of Λ for these computations in order to ascertain the validity of the use of model 4. Thus, for the parameter values given above with $c_{so} = 1$ mM and $P = 10^{-3}$ cm/sec,

$$\Lambda = \frac{V_{max}}{c_{so}}\left[\frac{r_o}{3P} + \frac{r_o^2}{15D_{is}}\right]$$

$$= 0.22$$

The model 4 solution is therefore nearly valid under these conditions ($\Lambda < 0.1$ was the criterion of validity suggested in Chapter IV). Since Λ will i crease with decreasing c_{so}, i.e., as the batch reaction proceeds, then the validity of model 4 in this case is increasingly more questionable.

VI-9. General Discussion

Several interesting properties of microencapsulated trypsin have been demonstrated in the data presented in this report. Contrary to what one might initially expect, the MEC-enzyme displays behavior differing from the free enzyme in several respects.

The stability upon storage is increased for MEC-trypsin, probably due to adsorption onto or inclusion in the capsule membrane. The energy of activation based on the apparent activity is somewhat higher for the MEC-enzyme, an indication that diffusion is not significantly limiting the reaction. Furthermore, the pH-apparent activity curve for MEC-trypsin was displaced to higher values of pH, also indicating that the microenvironment inside the capsule may be slightly different from the bulk solution conditions. It should be noted here that "correction" of the latter two sets of data for diffusion resistance would serve to enhance the observed differences in behavior between free and encapsulated enzyme since the correction factor would be greater with higher values of the observed reaction rate. This computation was not attempted here owing to the uncertainty in the determination of the system parameters.

The permeability coefficient for the combined membrane-external film was estimated to be: $2\text{-}5 \times 10^{-5}$ cm/sec if carried out in the absence of reaction (Sec. VI-5); $1\text{-}7 \times 10^{-4}$ cm/sec when estimated based on 100% encapsulation of the initially active enzyme (Sec. VI-6); and $\sim 3 \times 10^{-3}$ cm/sec when estimated from batch reaction data and the use of model 4 of Chapter IV (Sec. VI-8). The wide range of estimates of P (over two orders

of magnitude) is probably due to a number of factors such as the adsorption of enzyme to the capsule membrane, loss of activity upon encapsulation, possible modification of the membrane formation in the presence of enzyme, and the transient nature of the batch assay technique. The high values of P given above are similar in magnitude to those obtained by Morgensen [103] while the low values are similar to those given by Chang and Poznansky [35].

The overall effectiveness factor for the MEC-trypsin system was generally greater than about 0.4, based on comparison of whole-capsule and broken-capsule catalysis rates. These factors are inconsistent with a membrane permeability which is lower than 10^{-4} cm/sec. It is possible that the adsorption of the enzyme on the membrane serves to increase the overall effectiveness factor for the MEC-trypsin to a certain extent.

It seems evident from these experiments that the type of microcapsule activity assay has limited the analysis of experimental data and the deduction of intrinsic MEC-enzyme kinetic parameters. More revealing methods for the determination of system properties should therefore include the following features: 1) an active site titration procedure as proposed by Bender et al. [9] to permit the estimation of the amount of active enzyme successfully encapsulated without having to break the capsules; 2) the use of a continuous-flow apparatus to permit steady-state assay conditions. The glass-wool supported column suggested by Morgensen [103], used in conjunction with the recirculation reactor described by Ford et al. [45], and operated at low total-column conversion would seem to be a good initial system for the

continuation of these studies; 3) the characterization of the transport properties of the microcapsules in the presence of enzyme but the absence of reaction by using a non-reactive tracer solute; and 4) the use of larger substrate molecules, e.g. polypeptides of 5-10 amino acid residues, in order to establish whether or not the proteolytic activity of the MEC-trypsin has been altered.

When compared to the properties of immobilized trypsin prepared by other techniques, nylon-MEC-trypsin appears to offer both favorable and unfavorable properties. First, the enzyme was as stable upon storage for 5 months at 37°C as most other types of insolubilized derivatives, after the rapid initial loss of activity had occurred. If the increased stability is caused by adsorption to the cell membrane, then the activity retention at elevated temperatures will be limited by the surface area of the capsules. At 4°C, the MEC-enzyme was nearly completely stable in distilled water. These findings contradict the results of Kobamoto et al. [86] who found that the free solution enzyme was more rapidly denatured in the presence of cellulose membranes.

The use of the membrane to contain the enzyme limits the possible reactions using MEC-trypsin to rather small substrates[23]. For the substrates used in this study, however, the apparent MEC-activity was generally as close to the free-solution activity ($\eta_o > 0.4$) as for other types of derivatives (Table 5). The high yield of active MEC-trypsin (>60%) also compares favorably with other types of immobilization techniques.

The major disadvantage in using MEC-enzymes seems to be the tendency for the capsules to break upon agitation. It is likely that thicker membranes can be obtained, especially by the

coacervation technique of Chang [34], but the added mechanical strength will be gained at the expense of the high-flux properties of the capsules used in this study.

The mathematical models presented in Chapter IV of this report are generally applicable to a wide variety of biological and engineering problems. The homogeneously-distributed enzyme solution inside a membrane diffusion resistance describes other immobilized enzyme systems and also serves as a simple model of many single-cellular reactions.

The tendency for MEC-enzyme to adsorb to the capsule membrane introduces some error when the model is used to describe this system. This error is not very great, however, when most of the diffusion resistance in the system is offered by the membrane.

Simple relationships between the free-enzyme Michaelis constant, K_m, and the corresponding apparent constant, K'_m, for the MEC-enzyme are given by models 4 (Eq. 4.42) and 5 (Eq. 4.60). These models should give a reliable method for estimating system kinetic parameters if the enzyme loading is sufficiently low ($\Lambda < 0.1$) that the models are valid. Since the above criterion was not satisfied under the conditions of the reactions carried out in this study, some error is to be expected in the estimated kinetic parameter values.

VII. SUMMARY AND CONCLUSIONS

Many procedures have been developed in recent years for successfully immobilizing enzymes. These enzyme-derivatives often are more suitable for catalyzing reactions than the corresponding enzyme in free solution for a number of reasons: 1) ease of recovery of the enzyme from the reaction mixture; 2) improved stability of the enzyme upon storage or at elevated temperatures; and 3) apparent alteration of the catalytic behavior, e. g. shifted pH optima. On the other hand, loss of catalytic activity upon immobilization and decreased activity due to the effects of mass transfer limitation may serve to limit the efficiency of immobilized enzyme reactions.

The preparation of microencapsulated enzymes, due mainly to the extensive work of Chang [30], involves the inclusion of active enzyme solutions inside semipermeable spherical membranes. The membranes are permeable to small substrate molecules which can enter from the external solution; large enzyme molecules are successfully trapped inside the capsules, however, and thus effectively immobilized. Microcapsule membranes are prepared in situ by means of polymerization reactions or coacervation (polymer deposition) at the interface of aqueous droplets suspended in an immiscible organic liquid.

The microencapsulated enzyme system has been mathematically modelled as a homogeneous enzyme phase surrounded by a semi-permeable membrane and located in an infinite substrate medium. Diffusion of substrate across the external hydrodynamic boundary layer and the capsule membrane, and combined diffusion-reaction inside the cell can influence the rate of substrate conversion.

The equations relating the reaction kinetic parameters, physical properties of the capsules, and bulk substrate concentration have been described for the microencapsulated enzyme model. Numerical solution of these equations has been carried out for wide ranges of the system parameters for the case of a Michaelis-Menten reaction rate expression and steady-state catalysis. The transformation procedure proposed by Na and Na [109] was employed. Generalized effectiveness factor charts have been prepared for enzymes encapsulated in planar, cylindrical, and spherical membranes. These correlations are useful in quickly establishing the approximate limitation of the overall reaction rate by diffusion inside the capsule and across the membrane and external "unstirred" film. These charts can also be used for other types of immobilized enzyme systems if properly defined parameters are employed. The uniqueness of these figures lies in the presentation of the joint effects of the mass transfer resistance outside the reaction zone in combination with internal diffusion resistance.

Analytical solutions for the general diffusion-reaction equations cannot be obtained. Semi-analytical solutions of the steady-state equations were found, however, which permit computation of the expected substrate conversion rate over limited ranges of system parameter values. The regimes of validity of these approximate solutions were established by comparison with numerically computed substrate conversion rates. The most generally valid solution, especially for low reaction rate/diffusion rate ratios ($\Lambda < 1$), was found to be that due to Rashevsky [116] in which a "constant-average" reaction rate was employed for the interior of the capsule (model 3). The solution for first-order reaction kinetics (model 1) was more valid at higher reaction/diffusion ratios.

Simple expressions, although valid over a somewhat smaller range of parameters, were also generated which relate the "apparent" Michaelis constant of the system, K'_m, to the actual enzyme Michaelis constant and the system mass transfer parameters. These models were obtained by binomial approximation of model 3 (model 4), and by regular perturbation solution of the general diffusion-reaction equations (model 5). The effects on the rate of conversion of charged substrates by fixed electrostatic charges on the carrier was also discussed. An original solution for the case of unsteady-state substrate conversion by encapsulated enzymes in an infinite substrate solution was described, based on the approximation of reaction kinetics following the method of Rashevsky. Very rapid attainment (< 20 seconds) of pseudo-steady-state conditions was predicted by this expression for parameter values in the range used in this study.

Nylon microcapsules formed by interfacial polymerization were found to be quite fragile when assayed in a continuous-flow, stirred tank reactor as also observed by Morgensen [103]. A simple batch assay was developed in which the capsule suspension was introduced into the sample cell of a u.v. spectrophotometer in the same manner as for the free-enzyme assay. The reaction solution was stirred periodically to maintain the capsules in suspension.

Microencapsulated trypsin was more stable upon storage than free trypsin. At 37°C, the free enzyme denatured completely with a half-life of about 1 day while the MEC-enzyme experienced a rapid initial activity loss, then stablized; 10% of the original capsular activity was retained after 165 days at 37°C. At 21°C, the free enzyme denatured with a half-life of about 6 days while

encapsulated trypsin retained 50% of the original activity after 165 days. Capsule membranes recovered after ultrasonic rupturing of several batches of microcapsules displayed much the same stability behavior as MEC-trypsin when stored at 37°C. Experiments in which trypsin was adsorbed to the outside of trypsin-free capsules offered further evidence that much of the MEC-enzyme is probably adsorbed to the inner surface. When adsorbed to the membrane, the enzyme is presumably more stable.

MEC-trypsin displayed a higher apparent energy of activation for the hydrolysis of BAEE (E_{act} = 11.8 - 13.0 kcal/gmole) than the free enzyme (E_{act} = 9.5 kcal/gmole). The pH optimum for this reaction was shifted by about 1/2 unit to higher pH's when compared to the free enzyme.

The combined external film-membrane permeability, P, for BAEE was estimated to be 2-5 x 10^{-5} cm/sec based on the measured rate of efflux from enzyme-free capsules. The assumption of zero internal mass transfer resistance was made in this computation.

When the substrate uptake rates for capsules having different diameters and different initial enzyme loadings were approximately fit by models 1 and 3, P for BAEE ranged from 1-7 x 10^{-4} cm/sec for 100% retention of the encapsulated activity. These values therefore represent minimum values of P. Since P increased with larger initial enzyme loadings, these results suggest that the encapsulation process is more efficient for higher enzyme concentrations.

Another estimate of P was made by fitting batch reaction data with an integrated Michaelis-Menten reaction rate expression. The permeability was estimated from the average value of K'_m, the

apparent Michaelis constant for the MEC-trypsin, to be approximately 3×10^{-3} cm/sec based on model 4. Some error was probably introduced into this calculation since the reaction was sufficiently high that model 4 was not strictly valid.

Direct measurement of the overall effectiveness factors for several batches of MEC-trypsin was made by ultrasonic breakage of the capsules. The effectiveness factors were generally greater than 0.4, an indication that P is greater than about 1×10^{-4} cm/sec.

In conclusion, trypsin inside nylon microcapsules exhibits behavior different from the free enzyme in several respects. The MEC-enzyme is more stable upon storage at 37°C in distilled water. The energy of activation for the hydrolysis of BAEE is higher and the pH optimum is shifted to higher pH in the capsular environment. These changes in enzyme behavior are probably caused by the tendency of the enzyme to adsorb to the nylon membrane.

The membrane was effective in trapping the enzyme inside while permitting rapid transfer of substrate from the external solution. The permeability of the membrane for BAEE was found to be higher when estimated from batch reaction experiments ($P > 10^{-4}$ cm/sec) than when computed from transport rates in the absence of reaction.

The high-flux properties of the membrane, the high yield of active encapsulated enzyme, and the increased enzymatic storage stability are distinct advantages in processes utilizing immobilized enzymes. Since the capsules were found to be rather easily broken, however, increased mechanical strength of the membranes must be attained in order to produce practical immobilized enzymes by microencapsulation.

Suggested improvements in the experimental methods used in this study include: 1) the use of an active site titration method [9] to estimate the amount of active enzyme successfully encapsulated; 2) the use of a continuous-flow apparatus to permit steady-state assay conditions; 3) the use of non-reactive tracer solutes in the mass transport studies to determine mass transfer rates in enzyme-containing microcapsules; and 4) the use of larger polypeptide substrates to determine any changes in the proteolytic activity of the MEC-enzyme.

APPENDIX A

GENERALIZED INTERNAL EFFECTIVENESS FACTOR CHARTS FOR PLANAR AND CYLINDRICALLY ENCAPSULATED ENZYMES

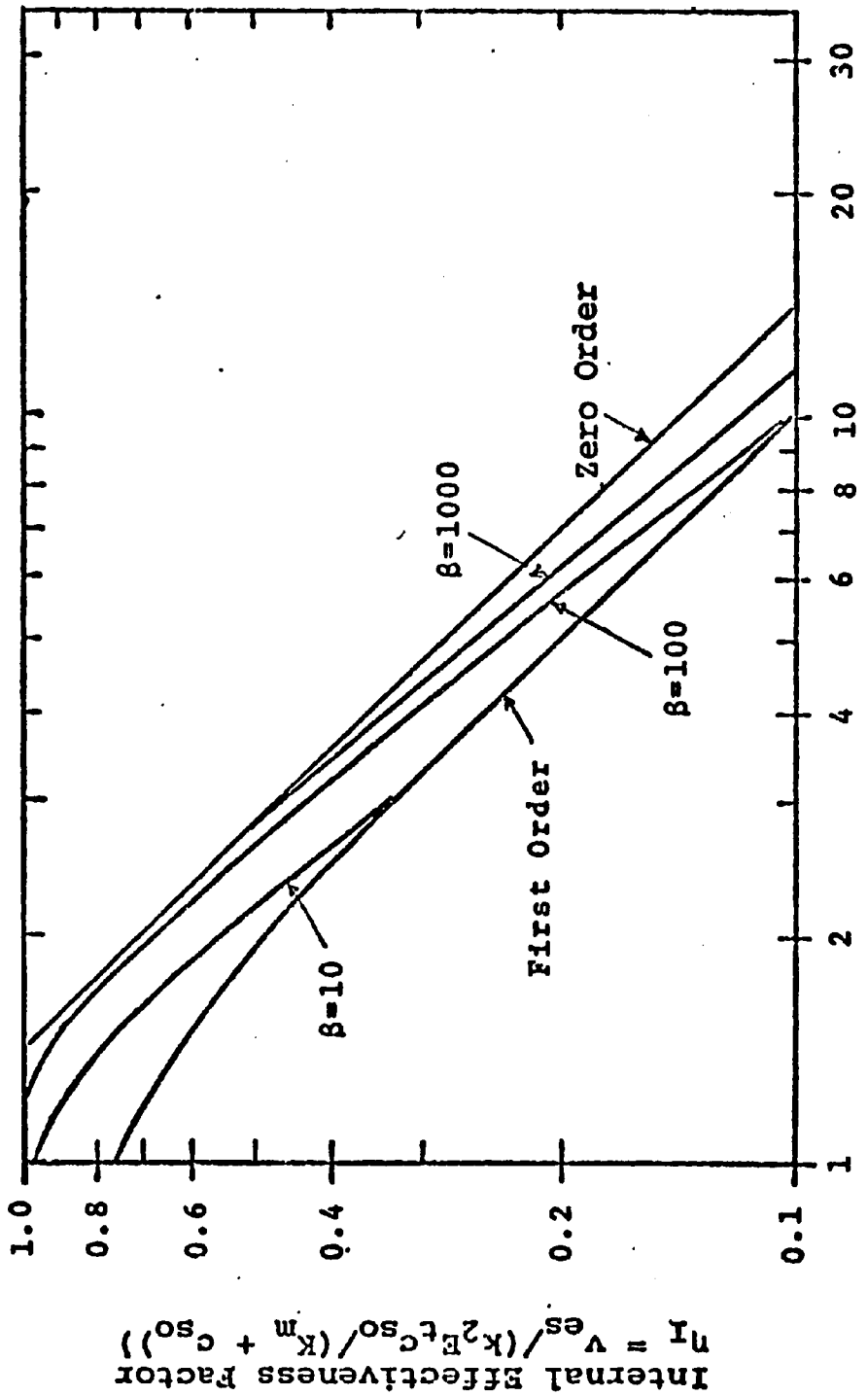

Figure A-1. Generalized Internal Effectiveness Factor Chart For Enzymes Encapsulated In Planar Membranes

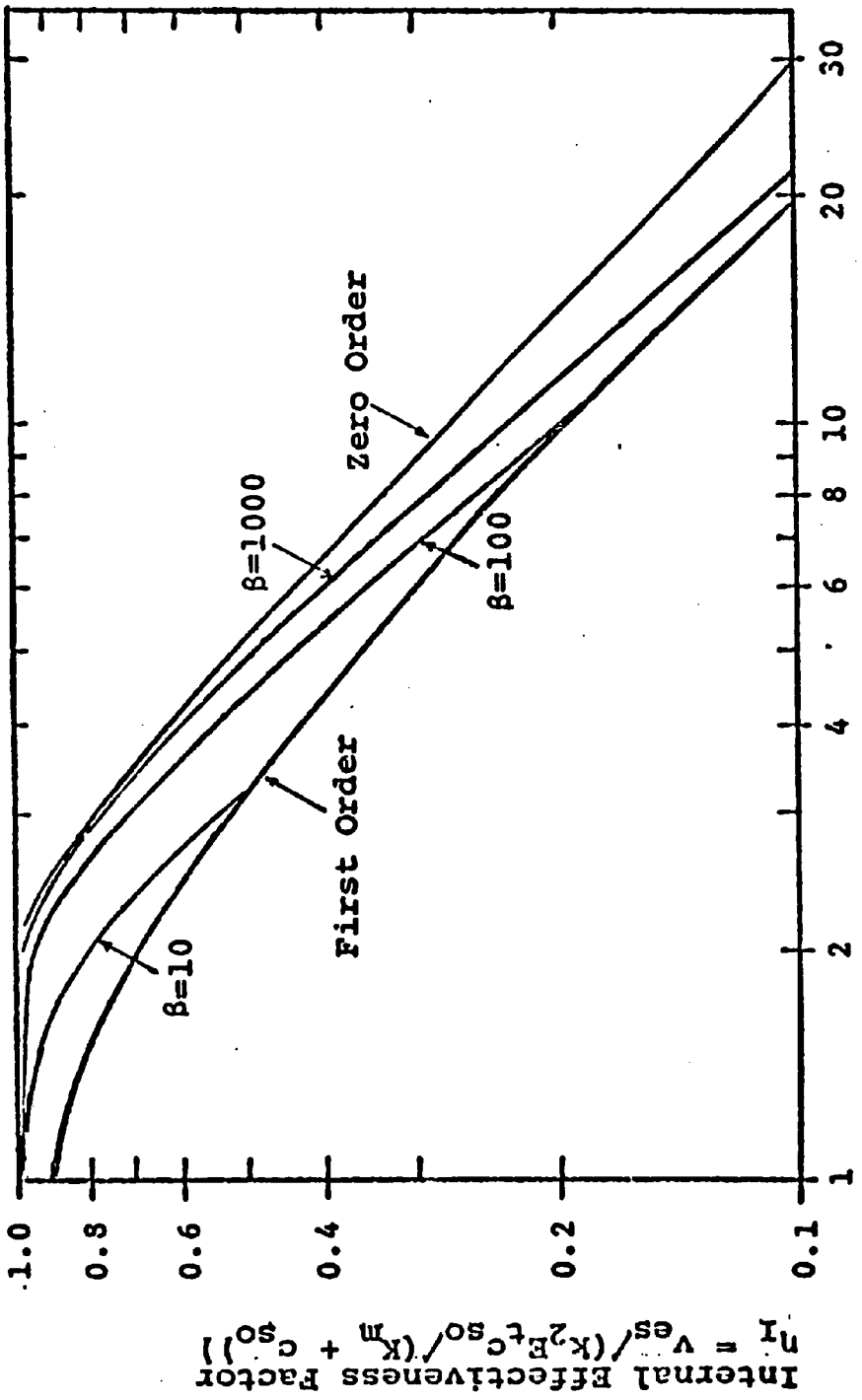

Figure A-2. Generalized Internal Effectiveness Factor Chart For Enzymes Encapsulated In Cylindrical Membranes

APPENDIX B

GENERALIZED OVERALL EFFECTIVENESS FACTOR CHARTS FOR PLANAR AND CYLINDRICALLY ENCAPSULATED ENZYMES

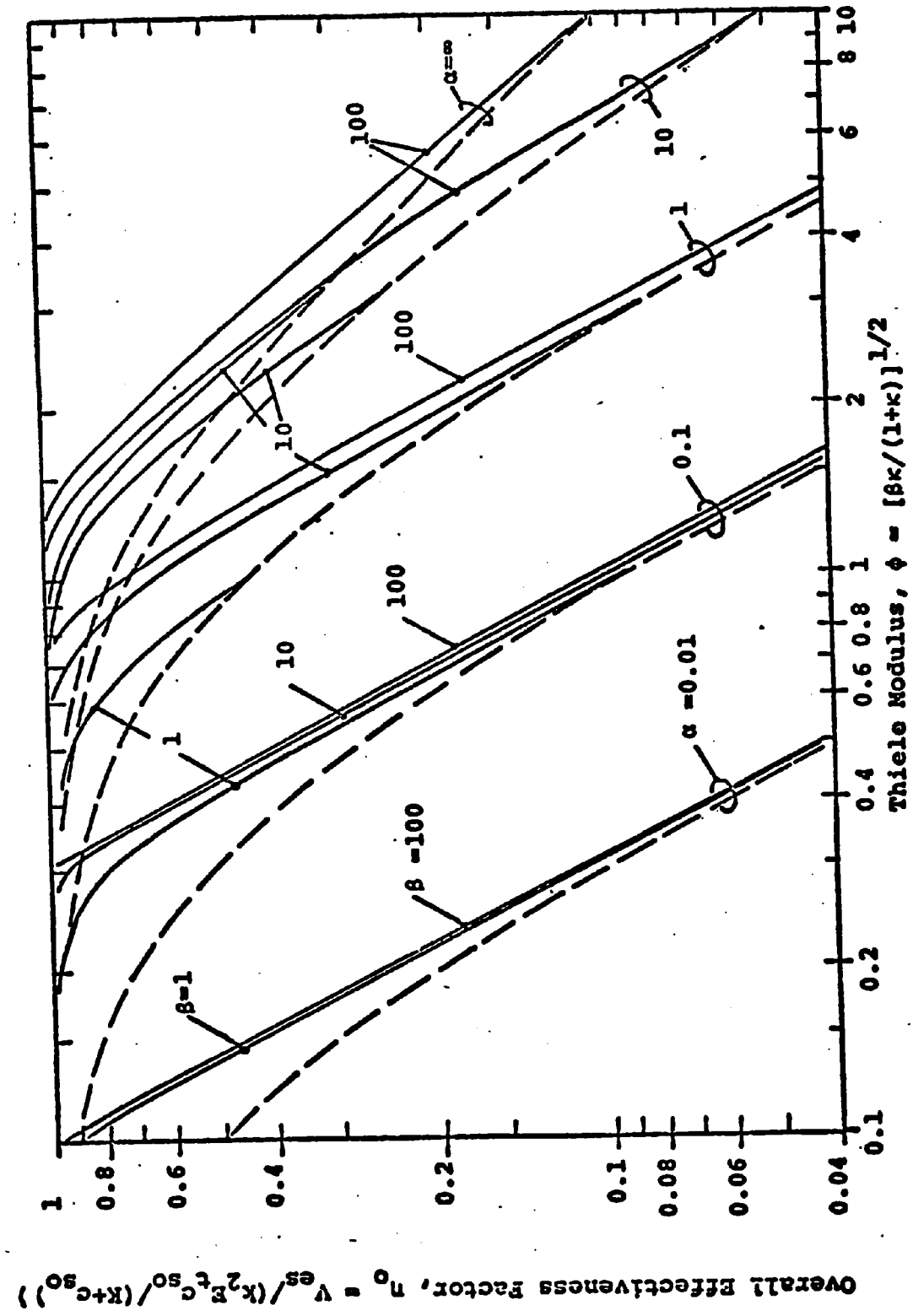

Figure B-1. Generalized Overall Effectiveness Factor Chart For Enzymes Encapsulated In Planar Membranes. Dashed Lines Are For Analytical Solution Of First-order Reaction Kinetics.

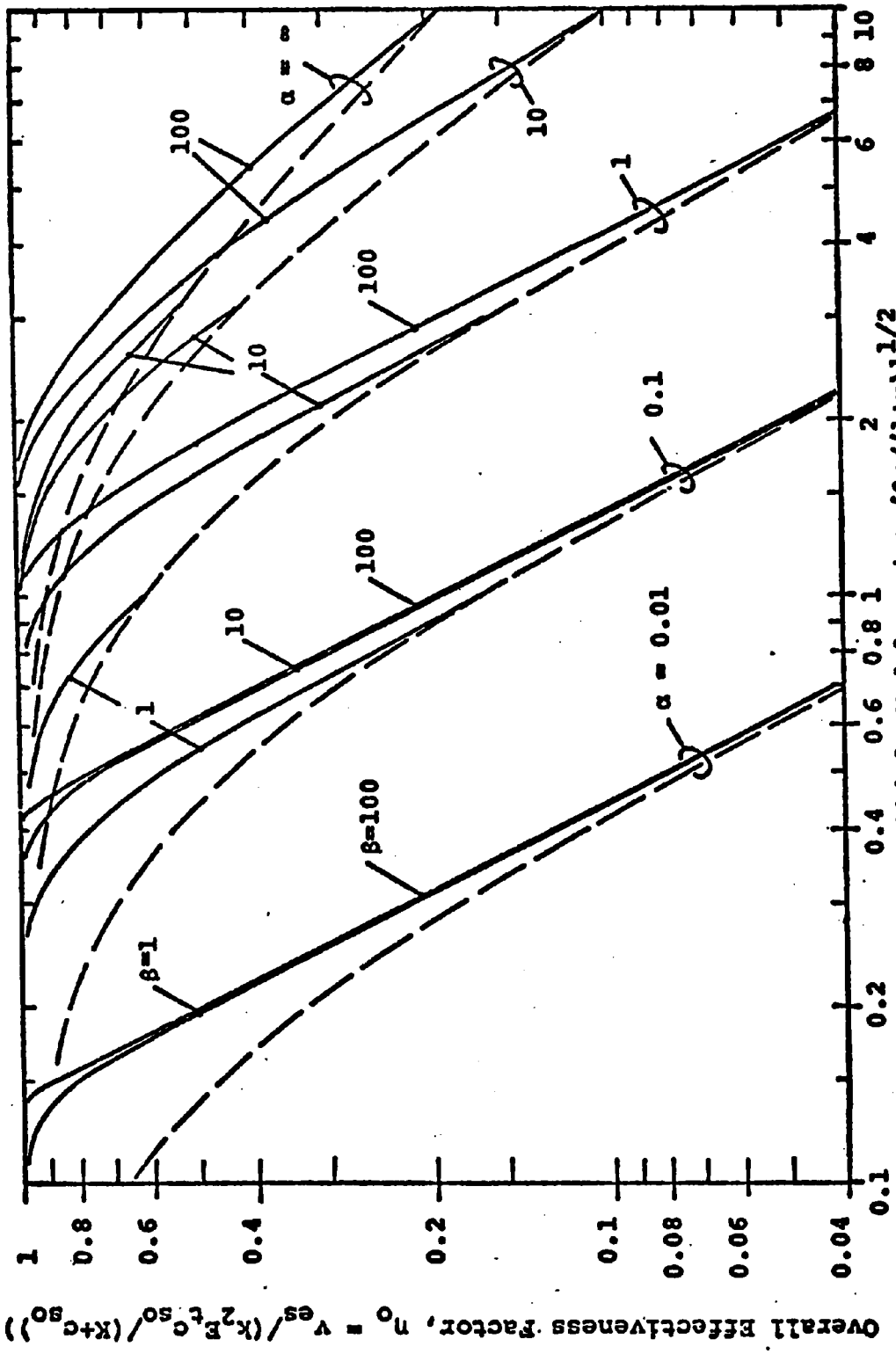

Figure B-2. Generalized Overall Effectiveness Factor Chart For Enzymes Encapsulated In Cylindrical Membranes. Dashed Lines Are For Analytical Solution Of First-order Reaction Kinetics.

APPENDIX C

Regular Perturbation Solutions For Steady-state Kinetics

C-1. Large ϵ, Finite α (BC2)

Zero-Order Solution

$$\frac{d^2c_0}{dx^2} + \frac{2}{x}\frac{dc_0}{dx} = 0 \qquad (4.52)$$

is satisfied only by $c_0 = c_0' =$ a constant.

Therefore, $\frac{dc_0}{dx} = 0$, and from Eq. 4.57,

$$\alpha\left(\frac{1}{h_e} - h_i c_0'\right) = 0 \qquad (C.1)$$

For finite α, $c_0' = \frac{1}{H}$.

First-Order Solution

$$\frac{d^2c_1}{dx^2} + \frac{2}{x}\frac{dc_1}{dx} = \lambda_0 \qquad (4.53)$$

Separating Eq. 4.53 and integrating twice,

$$c_1 = \frac{\lambda_0}{6}x^2 + \mu_1 + \mu_2\frac{1}{x} \qquad (C.2)$$

where μ_1 and μ_2 are constants of integration. $\mu_1 = 0$ to satisfy BC 1, Eq. 4.55. At x=1,

$$c_1' = \frac{\lambda_0}{6} + \mu_1 \qquad (C.3)$$

Therefore, $c_1 = \frac{\lambda_0}{6}(x^2-1) + c_1'$ (C.4)

Differentiating Eq. C-4 and applying BC2,

$$\left.\frac{dc_1}{dx}\right|_{x=1} = \frac{\lambda_0}{3} = -\alpha h_i c_1' \qquad (C.5)$$

$$\text{or } c_1' = -\lambda_0 / 3\alpha k_i \tag{C.6}$$

$$\text{and } c_1 = \frac{\lambda_0}{6}(x^2-1) - \frac{\lambda_0}{3\alpha k_i} \tag{C.7}$$

Second-Order Solution

$$\frac{d^2c_2}{dx^2} + \frac{2}{x}\frac{dc_2}{dx} = \lambda_1 c_1 \tag{4.54}$$

Substituting for c_1 from Eq. C-7, separating and integrating twice,

$$c_2 = \frac{\lambda_0\lambda_1}{6}\left(\frac{x^4}{20} - \frac{x^2}{6}\right) + \frac{\lambda_1 c_1'}{6}x^2 + \mu_3 + \mu_4\frac{1}{x} \tag{C.8}$$

where μ_3 and μ_4 are constants of integration. $\mu_4 = 0$ to satisfy BC1 and, at $x = 1$ in Eq. C-8,

$$c_2' = -\frac{7\lambda_0\lambda_1}{360} + \frac{\lambda_1 c_1'}{6} + \mu_3 \tag{C.9}$$

$$\text{and } c_2 = \frac{\lambda_0\lambda_1}{360}(3x^4 - 10x^2 + 7) + \frac{\lambda_1 c_1'}{6}(x^2-1) + c_2' \tag{C.10}$$

Differentiating Eq. C.10, applying BC2, and substituting Eq. C-6,

$$\left.\frac{dc_2}{dx}\right|_{x=1} = -\frac{\lambda_0\lambda_1}{45} - \frac{\lambda_0\lambda_1}{9\alpha k_i} = -\alpha k_i c_2' \tag{C.11}$$

$$\text{or } c_2' = \frac{\lambda_0\lambda_1}{3k_i\alpha}\left(\frac{1}{15} + \frac{1}{3k_i\alpha}\right) \tag{C.12}$$

General Solution

Combining Eqs. 4.7a and 4.8,

$$\rho = \frac{3\alpha}{\beta K}\left(\frac{1}{h_e} - h_i c'\right) = 3\alpha\epsilon\left(\frac{1}{h_e} - h_i c'\right) \qquad (C.13)$$

From Eq. 4.45, $c' = c'_0 + \left(\frac{1}{\epsilon}\right) c'_1 + \left(\frac{1}{\epsilon}\right) c'_2 + \cdots$ (C.14)

Substituting Eqs. C.1, C.6, and C.12, into C.14 and neglecting terms of order higher than $\left(\frac{1}{\epsilon}\right)^2$,

$$c' = \frac{1}{H} - \frac{\lambda_0}{3h_i\alpha}\left(\frac{1}{\epsilon}\right) + \frac{\lambda_0\lambda_1}{3h_i\alpha}\left(\frac{1}{15} + \frac{1}{3h_i\alpha}\right)\left(\frac{1}{\epsilon}\right)^2 \qquad (C.15)$$

and $$\rho = 3\alpha\epsilon\left[\frac{1}{h_e} - \frac{1}{h_e} + \frac{\lambda_0}{3\alpha\epsilon} - \frac{\lambda_0\lambda_1}{3\alpha\epsilon^2}\left(\frac{1}{15} + \frac{1}{3h_i\alpha}\right)\right] \qquad (C.16)$$

$$= \lambda_0 - \frac{\lambda_0\lambda_1}{\epsilon}\left(\frac{1}{15} + \frac{1}{3h_i\alpha}\right) \qquad (C.17)$$

From the definition of λ_p in Eq. 4.48, it follows that

$$\lambda_0 = \frac{c_0'}{c_0' + K} = \frac{1}{1 + HK} \qquad (C.18)$$

and

$$\lambda_1 = \frac{K}{(c_0' + K)^2} = \frac{H^2 K}{(1 + HK)^2} \qquad (C.19)$$

Therefore,

$$\rho = \frac{1}{1+HK}\left[1 - \frac{H^2 K}{(1+HK)^2\epsilon}\left(\frac{1}{15} + \frac{1}{3h_i\alpha}\right)\right]$$

$$= \frac{1}{1+HK}\left[1 - \frac{H^2 K}{(1+HK)^2}\Lambda\right] \qquad (C.20)$$

C-2. Large ϵ, Finite γ (BC2a)

Zero-Order Solution

As for the previous case, $c_o = c'_o$ = a constant.

First-Order Solution

The solution is the same as for the preceeding derivation up to Eq. C.4,

$$c_1 = \frac{\lambda_o}{6}(x^2-1) + c_1' \qquad \text{(C.4)}$$

Differentiating Eq. C.4 and applying BC2a, Eq. 4.59,

$$\frac{dc_1}{dx} = \frac{\lambda_o}{3} = \gamma\left(\frac{1}{h_e} - h_i c_o'\right) \qquad \text{(C.21)}$$

Solving for c'_o from Eqs. C.21 and C.18,

$$\frac{c_o'}{3(c_o'+k)} = \gamma\left(\frac{1}{h_e} - h_i c_o'\right) \qquad \text{(C.22)}$$

From the quadratic formula,

$$c_o' = c_o = \frac{1}{2}\left\{\left(\frac{1}{H} - \kappa - \frac{1}{3h_i\gamma}\right) + \left[\left(\frac{1}{H} - \kappa - \frac{1}{3h_i\gamma}\right)^2 + \frac{4\kappa}{H}\right]\right\} \qquad \text{(C.23)}$$

The positively signed term in the quadratic expression was taken since in Eq. C.22, $c'_o = \frac{1}{H} - \frac{1}{3\gamma h_i}$ when $\kappa = 0$.

Second-Order Solution

The solution is the same as for the previous derivation up to Eq. C.10, but with c_1' as yet unknown.

$$c_2 = \frac{\lambda_0\lambda_1}{360}(3x^4 - 10x^2 + 7) + \frac{\lambda_1 c_1'}{6}(x^2 - 1) + c_2' \qquad \text{(C.10)}$$

Differentiating Eq. C.10 and applying BC2a,

$$\left.\frac{dc_2}{dx}\right|_{x=1} = -\frac{\lambda_0\lambda_1}{45} + \frac{\lambda_1 c_1'}{3} = -\gamma h_i c_1' \qquad \text{(C.24)}$$

or

$$c_1' = \frac{\lambda_0\lambda_1}{15(3\gamma h_i + \lambda_1)} \qquad \text{(C.25)}$$

and

$$c_1 = \frac{\lambda_0}{6}(x^2 - 1) + \frac{\lambda_0\lambda_1}{15(3h_i\gamma + \lambda_1)} \qquad \text{(C.26)}$$

General Solution

Substituting Eq. C.26 into Eq. C.14 and neglecting terms of order greater than $(\frac{1}{\epsilon})^1$,

$$c' = c_0' + \frac{\lambda_0\lambda_1}{15\epsilon(3\gamma h_i + \lambda_1)} \qquad \text{(C.27)}$$

From Eq. C.13, then,

$$\rho = 3\gamma\left(\frac{1}{h_e} - h_i c_0' - \frac{\lambda_0\lambda_1 h_i}{15\epsilon(3h_i\gamma + \lambda_1)}\right) \qquad \text{(C.28)}$$

Combining Eqs. C.18, C.19, and C.28,

$$\rho = \frac{c_o'}{c_o' + K} \left\{ 1 - \frac{1}{15\epsilon \left[\frac{(1+HK)^2}{H^2 K} + \frac{1}{3 R_i \gamma} \right]} \right\} \quad \text{(C. 29)}$$

where c_o' is given by Eq. C.23.

APPENDIX D

Singular Perturbation Solutions For Stead-state Kinetics

D-1. Small ϵ, Finite γ (BC2a) following Murray [108]

Zero-Order Solution

$$\frac{d^2 f_o}{d\xi^2} = \lambda_o = \frac{f_o}{f_o + K} \tag{4.68}$$

and, therefore,

$$\int_0^\infty \frac{d^2 f_o}{d\xi^2} \frac{df_o}{d\xi} d\xi = \int_0^\infty \frac{f_o}{f_o + K} \frac{df_o}{d\xi} d\xi \tag{D.1}$$

Integrating Eq. D.1 and applying BC1, Eq. 4.69,

$$\left.\frac{df_o}{d\xi}\right|_{\xi=0} = -\sqrt{2}\left[1 + K \log_e\left(\frac{K}{1+K}\right)\right]^{\frac{1}{2}} \tag{D.2}$$

From BC2a, Eq. 4.73,

$$\left.\frac{df_o}{d\xi}\right|_{\xi=0} = \gamma h_i f_1' \tag{D.3}$$

and so,

$$f_1' = -\frac{\sqrt{2}}{h_i \gamma}\left[1 + K \log_e\left(\frac{K}{1+K}\right)\right]^{\frac{1}{2}} \tag{D.4}$$

General Solution

Substituting into Eq. 4.65 at $\xi = 0$ and neglecting terms of order greater than $\epsilon^{1/2}$,

$$f' = f_o' + \epsilon^{1/2} f_1'$$

$$= 1 - \frac{\sqrt{2}\,\epsilon^{\frac{1}{2}}}{h_i \gamma}\left[1 + K \log_e\left(\frac{K}{1+K}\right)\right]^{\frac{1}{2}} \qquad \text{(D. 5)}$$

From Eq. C.13,

$$\rho = 3\gamma\left(\frac{1}{h_e} - h_i f'\right) \qquad \text{(C. 13)}$$

$$= 3\gamma\left\{\frac{1}{h_e} - h_i + \frac{\sqrt{2}\,\epsilon^{1/2}}{\gamma}\left[1 + K \log_e\left(\frac{K}{1+K}\right)\right]^{\frac{1}{2}}\right\} \qquad \text{(D. 6)}$$

Attempts to analytically solve for f_o or to solve for higher order solutions are fruitless due to the complexity of the algebra.

D-2. Small ϵ, Finite α (BC2)

Zero-Order Solution

$$\frac{d^2 f_o}{d\xi^2} = \frac{f_o}{f_o + K} = 0 \qquad \text{since } f_o \equiv 0 \text{ for all } \xi, \text{ from BC 2, Eq. 4.71.}$$

First-Order Solution

$$\frac{d^2 f_1}{d\xi^2} - 2\frac{df_o}{d\xi} = \lambda_1 f_1 \qquad \text{(4.68)}$$

Since $\frac{df_0}{d\xi} = 0$, Eq. 4.68 becomes

$$\frac{d^2 f_1}{d\xi^2} - \lambda_1 f_1 = 0 \qquad \text{(D.7)}$$

The solution of Eq. D-7 has the form

$$f_1 = A_1 e^{\sqrt{\lambda_1}\,\xi} + B_1 e^{-\sqrt{\lambda_1}\,\xi} \qquad \text{(D.8)}$$

$A_1 = 0$ because f_1 remains finite at $\xi \to \infty$. At $\xi = 0$,

$f_1 = f_1' = B_1$ from Eq. D.8 and, therefore,

$$f_1 = f_1' e^{-\sqrt{\lambda_1}\,\xi} \qquad \text{(D.9)}$$

Differentiating Eq. D.9 and applying BC2,

$$\left.\frac{df_1}{d\xi}\right|_{\xi=0} = -\sqrt{\lambda_1}\, f_1' = -\frac{\alpha}{k_e} \qquad \text{(D.10)}$$

or $$f_1' = \frac{\alpha}{k_e \sqrt{\lambda_1}} \qquad \text{(D.11)}$$

and $$f_1 = \frac{\alpha}{k_e \sqrt{\lambda_1}} e^{-\sqrt{\lambda_1}\,\xi} \qquad \text{(D.12)}$$

where $$\lambda_1 = \left.\frac{d\lambda}{df}\right|_{f_o} = \left.\frac{K}{(K+f)^2}\right|_{f_o} = \frac{1}{K} \qquad (D.13)$$

Therefore, $$f_1 = \frac{\alpha K^{1/2}}{h_e} e^{-\xi/K^{1/2}} \qquad (D.14)$$

Second-Order Solution

$$\frac{d^2 f_2}{d\xi^2} - 2\left(\xi \frac{df_0}{d\xi} + \frac{df_1}{d\xi}\right) = \lambda_1 f_2 + \lambda_2 f_1^2 \qquad (4.68)$$

Setting $\frac{df_0}{d\xi} = 0$ from BC2, substituting for f_1 from Eq. D.14, and rearranging,

$$\frac{d^2 f_2}{d\xi^2} - \frac{1}{K} f_2 = -\frac{\alpha^2}{h_e^2 K} e^{-2\xi/K^{1/2}} - \frac{2\alpha}{h_e} e^{-\xi/K^{1/2}} \qquad (D.15)$$

where

$$\lambda_2 = \frac{1}{2}\left.\frac{d^2\lambda}{df^2}\right|_{f_o} = \frac{1}{2}\left(-\left.\frac{2K}{(K+f)^3}\right|_{f_o}\right) = -\frac{1}{K^2} \qquad (D.16)$$

The particular and complementary solutions for f_2 are, respectively,

$$f_{2p} = B_2 e^{-2\xi/K^{1/2}} + D_2 \xi e^{-\xi/K^{1/2}} \qquad (D.17)$$

$$f_{2c} = A_2 e^{-\xi/K^{1/2}} \qquad (D.18)$$

with the general solution

$$f_2 = f_{2p} + f_{2c} \tag{D.19}$$

We will present the solution herewithout indicating all of the algebra:

$$f_2 = \left[\frac{\alpha K}{k_e} - \frac{2\alpha^2}{3k_e^2} - \frac{k_i \alpha^2 K}{k_e}\right] e^{-\xi/K^{1/2}} - \frac{\alpha^2}{3k_e^2} e^{-2\xi/K^{1/2}} + \frac{\alpha K^{\frac{1}{2}}}{k_e} \xi e^{-\xi/K^{1/2}} \tag{D.20}$$

Therefore, at $\xi = 0$,

$$f_2' = \frac{\alpha K}{k_e} - \frac{\alpha^2}{k_e^2} - \frac{k_i \alpha^2 K}{k_e} \tag{D.21}$$

General Solution

Substituting into Eq. 4.65 at $\xi = 0$ and neglecting terms of order higher than ϵ,

$$f' = f_0' + \epsilon^{\frac{1}{2}} f_1' + \epsilon f_2' \tag{D.22}$$

$$= \frac{\alpha \epsilon^{1/2} K^{1/2}}{k_e} + \epsilon\left[\frac{\alpha K}{k_e} - \frac{\alpha^2}{k_e^2} - \frac{k_i \alpha^2 K}{k_e}\right] \tag{D.23}$$

From Eq. C.13,

$$\rho = 3\gamma\left(\frac{1}{k_e} - k_i f'\right) \tag{C.13}$$

$$= \frac{3\gamma}{k_e}\left[1 - \alpha \epsilon^{1/2} K^{1/2} k_i - \alpha \epsilon K k_i + \alpha^2 \epsilon \left(\frac{k_i}{k_e} + k_i^2 K\right)\right] \tag{D.24}$$

BIBLIOGRAPHY

1. Acrivos, A., Chem. Eng. Educ., Spring, 1968, 62.
2. Alexander, B., A. Rimon, and E. Katchalski, Fed. Proc, Fed. Amer. Soc. Exp. Biol., 24, 804 (1965).
3. Axén, R., P. A. Myrin, and J. C. Janson, Biopolymers, 9, 401 (1970).
4. Axén, R. and J. Porath, Nature, 210, 367 (1966).
5. Baines, N. J., J. B. Baird, and D. T. Elmore, Biochem. J., 90, 470 (1964).
6. Bar-Eli, A., and E. Katchalski, Nature, 188, 856 (1960).
7. Bar-Eli, A., and E. Katchalski, J. Biol. Chem., 238 (5), 1690 (1963).
8. Barman, T. E., Enzyme Handbook, Springer-Verlog New York (1969), entry 3. 4. 4. 4.
9. Bender, M. L., M. L. Begué-Canton, R. L. Blakeley, L. J. Brubacher, J. Feder, C. R. Gunter, F. J. Kézdy, J. V. Killheffer, Jr., T. H. Marshall, C. G. Miller, R. W. Roeske, and J. K. Stoops, J. A. C. S., 88 (24), 5890 (1966).
10. Bender, M. L., J. V. Killheffer, Jr., and R. W. Roeske, Biochem. Biophys. Res. Commun., 19, 161 (1965).
11. Bergman, M., J. S. Fruton, and H. Pollok, J. Biol. Chem., 127, 643 (1939).
12. Bernfeld, P., and J. Wan, Science, 142, 678 (1963).
13. Bernhard, S. A., Biochem. J., 59, 506 (1955).
14. Best, J. B., Int. Rev. Cytology, 9, 129 (1960).
15. Bischoff, K. B., A. I. Ch. E. J., 11 (2), 351 (1965).
16. Blaedel, W. J., and R. G. Boguslaski, Biochem. Biophys. Res. Commun., 47 (1), 284 (1972).
17. Blaedel, W. J., T. R. Kissel, and R. C. Boguslaski, Anal. Chem., 44 (12), 2030 (1972).
18. Blum, J. J., and D. J. Jenden, Arch. Biochem. Biophys., 66, 316 (1957).

19. Boguslaski, R. C., and A. M. Janik, Biochim. Biophys. Acta, 250, 266 (1971).

20. Box, G. E. P., Ann. N. Y. Acad. Sci., 86, 792 (1960).

21. Brown, H. D., A. B. Patel, and S. K. Chattopadhyay, J. Biomed. Mater. Res., 2, 231 (1968).

22. Carbonell, R. G., and M. D. Kostin, AIChE J., 18 (1), 1 (1972).

23. Chang, T. M. S., Science, 146, 524 (1964).

24. Chang, T. M. S., "Semipermeable Aqueous Microcapsules", PhD. Thesis (Physiology), McGill University (1965).

25. Chang, T. M. S., Trans. Amer. Soc. Artif. Intern. Organs, 12, 13 (1966).

26. Chang, T. M. S., Science Tools, 16, 33 (1969).

27. Chang, T. M. S., Fed. Proc., 28, 461 (1969).

28. Chang, T. M. S., Nature, 229, 117 (1971).

29. Chang, T. M. S., Biochem. Biophys. Res. Commun., 44 (6), 1531 (1971).

30. Chang, T. M. S., Biotech. Bioeng. Symp. No. 3, 395 (1972).

31. Chang, T. M. S., L. J. Johnson, and O. Ransome, Can. J. Physiol. Pharmacol., 45, 70 (1967).

32. Chang, T. M. S., and S. K. Lo, Physiologist, 13, 70 (1970).

33. Chang, T. M. S., and F. C. MacIntosh, Pharmacologist, 6, 1968 (1964).

34. Chang, T. M. S., F. C. MacIntosh, and S. G. Mason, Can. J. Physiol. Pharmacol., 44, 115 (1966).

35. Chang, T. M. S., and M. J. Poznansky, J. Biomed. Mater. Res., 2, 187 (1968).

36. Chang, T. M. S., and M. J. Poznansky, Nature, 218, 243 (1968).

37. Chase, T. Jr., and E. Shaw, Biochem. Biophys. Res. Commun., 29, 508 (1967).

38. Cleland, W. W., Adv. Enzymol., 29, 1 (1967).

38a. Crank, J., The Mathematics of Diffusion, Oxford, 1956.

39. Craven, G. R., and V. Gupta, Proc. Nat. Acad. Sci. U.S., 67, 1329 (1970).

40. Desneulle, P., in The Enzymes, Vol. 4, Second Ed., Ed. by P. Boyer, H. Lardy, and K. Myrbäck, Academic Press, New York (1959-63).

41. Desneulle, P., H. Neurath, and M. Ottesen, Editors, Structure-Function Relationships of Proteolytic Enzymes, Academic Press, New York (1970).

42. Draper, N. R., and H. Smith, Applied Regression Analysis, J. Wiley & Sons (1966), esp. chapter 10.

43. Epstein, C. J., and C. B. Anfinsen, J. Biol. Chem., 237, 2175 (1962).

44. Flinn, J. E., and R. H. Cherry, C.E.P. Symp. Series, Vol. 65, No. 91, 90 (1969).

45. Ford, J. R., A. H. Lambert, W. Cohen, and R. P. Chambers, Biotech. Bioeng. Symp. No. 3, 267 (1972).

50. Franks, N. E., Biotech. Bioeng., 14 (6), 1027 (1972).

51. Gabel, D., I. Z. Steinberg, and E. Katchalski, Biochemistry, 10 (25), 4661 (1971).

52. Gabel, D., P. Vretblad, R. Axén, and J. Porath, Biochim. Biophys. Acta, 214, 561 (1970).

53. Gardner, D. L., R. D. Falb, B. C. Kim, and D. C. Emmerling, Trans. Amer. Soc. Artif. Intern. Organs, 17, 239 (1971).

54. Glassmeyer, C. K., and J. D. Ogle, Biochemistry, 10 (5), 786 (1971).

55. Glazer, A. N., A. Bar-Eli, and E. Katchalski, J. Biol. Chem., 237, 1832 (1962).

56. Goddard, J. D., J. S. Schultz, and R. J. Bassett, Chem. Eng. Sci., 25, 665 (1970).

57. Goldberg, D. M., R. Campbell, and A. D. Roy, Biochim. Biophys. Acta, 167, 613 (1968).

58. Goldman, R., L. Goldstein, and E. Katchalski, in Biochemical Aspects of Reactions on Solid Supports, G. R. Stark, Ed., Academic Press, New York (1971).

59. Goldstein, L., Methods Enzymol., 19, 935 (1970).

60. Goldstein, L., and E. Katchalski, Z. Anal. Chem., 243, 375 (1968).

61. Goldstein, L., M. Pecht, S. Blumberg, D. Atlas, and Y. Levin, Biochemistry, 9, 2322 (1970).

62. Green, M., and H. Neurath, J. Biol. Chem., 204, 379 (1953).

63. Gutfreund, H., Trans. Faraday Soc., 51, 441 (1955).

64. Haarhoff, K. N., J. Theoret. Biol., 22, 117 (1969).

65. Habeeb, A. F. S. A., Arch. Biochem. Biophys., 119, 264 (1967).

66. Hamilton, B. K., L. J. Stockmeyer, and C. K. Colton, personal communication to J. S. Schultz (1972).

67. Haynes, R., and K. A. Walsh, Biochem. Biophys. Res. Commun., 36 (2), 235 (1969).

68. Hearon, J. Z., Bull, Math. Biophys., 15, 15 (1953); Bull. Math. Biophys., 15, 23 (1953); Bull. Math. Biophys., 15, 111 (1953).

69. Heineken, F. G., H. M. Tsuchiya, and R. Aris, Math. Biosci., 1, 95 (1967).

70. Heineken, F. G., H. M. Tsuchiya, and R. Aris, Math. Biosci., 1, 115 (1967).

71. Himmelblau, D. M., Process Analysis by Statistical Methods, J. Wiley & Sons (1970).

72. Hornby, W. E., and H. Filippusson, Biochim. Biophys. Acta, 220, 343 (1970).

73. Hornby, W. E., M. D. Lilly, and E. M. Crook, Biochem. J., 107, 669 (1968).

74. Horvath, C., and B. A. Soloman, Biotech. Bioeng., 14 (6), 885 (1972).

75. Howard, S. M., and J. W. Mehl, Biochim. Biophys. Acta, 105, 594 (1965).

76. Hummel, B. C. W., Can. J. Biochem. Physiol., 37 (12), 1393 (1959).

77. Ignagami, T., and J. M. Sturtevant, Biochim. Biophys. Acta, 38, 64 (1960).

78. "Immobilized Enzymes: A Compendium of References From The Recent Literature", Corning Glass Works, Prepared by The New England Research Application Center, University of Connecticut (1972).

79. Inman, J. K., and H. M. Dintzis, Biochemistry, 8, 4074 (1969).

80. Jay, A. W. L., and M. A. Edwards, Can. J. Physiol. Pharm., 46, 731 (1968).

81. Kasche, V., H. Lundqvist, R. Bergman, and R. Axén, Biochem. Biophys. Res. Commun., 45 (3), 615 (1971).

82. Kay, G., Process Biochemistry, August, 1968, 36.

83. Keil, B., in The Enzymes, Vol. III, Third Ed., Ed. by P. D. Boyer, Academic Press, New York (1971).

84. Keller, H. B., Numerical Methods For Two Point Boundary Value Problems, Random House, 1960.

85. Kittrell, J. R., and R. Mezaki, I & EC, 59 (2), 28 (1967).

86. Kobamoto, N., G. Löfroth, P. Camp, G. Van Amburg, and L. Augenstein, Biochem. Biophys. Res. Commun., 24 (5), 622 (1966).

87. Kobayashi, T., and M. Moo-Young, Biotech. Bioeng., 13, 893 (1971).

88. Koch, A. L., and R. Coffman, Biotech. Bioeng., 12, 651 (1970).

89. Koishi, M., N. Fukuhara, and T. Kondo, Chem. Pharm. Bull. (Tokyo), 17, 804 (1969).

90. Kowalik, J., and J. F. Morrison, Math. Biosciences, 2, 57 (1968).

91. Levin, Y., M. Pecht, L. Goldstein, and E. Katchalski, Biochemistry, 3, 1905 (1964).

92. Li, D., "Insolubilized Enzymes on Porous Vycor Glass: A Kinetic Study of Trypsin", M. S. Thesis, Cornell University (1972).

93. Lowey, S., L. Goldstein, C. Cohen, and S. M. Luck, J. Mol. Biol., 23, 287 (1967).

94. Luzzi, L. A., J. Pharm. Sci., 59 (10), 1367 (1970).

95. Marquardt, D. W., J. Soc. Ind. Appl. Math., 11 (2), 431, (1963).

96. McLaren, A. D., and Packer, L., Adv. Enzymol., 33, 245 (1970).

97. Melrose, G. J. H., Rev. Pure and Appl. Chem., 21, 83 (1971).

98. Mezaki, R., and J. R. Kittrell, I & EC, 59 (5), 63 (1967).

99. Mitz, M. A., and R. J. Schlueter, J. Am. Chem. Soc., 81, 4024 (1959).

100. Mitz, M. A., and L. J. Summaria, Nature, 189, 576 (1961).

101. Moo-Young, M., and T. Kobayashi, Can. J. Ch. E., 50, 162 (1972).

102. Morgan, P. W., and S. L. Kwolek, J. Polymer Sci., 40, 299 (1959).

103. Morgensen, A. O., "Mass Transfer and Biochemical Reaction With Semipermeable Microcapsules", Ph. D. Thesis, Rutgers University, 1972.

104. Mori, T., T. Sato, Y. Matuo, T. Tosa, and I. Chibata, Biotech. Bioeng., 14, 517 (1972).

105. Mosbach, K., Acta Chem. Scand., 24, 2084 (1970).

106. Mosbach, K., Scientific American, March, 1971, 26.

107. Mosbach, K., and R. Mosbach, Acta Chem. Scand., 20, 2807 (1966).

108. Murray, J. D., Math. Biosci., 2, 379 (1968).

109. Na, H. S., and T. Y. Na, Math. Biosciences, 6, 25 (1970).

110. Neurath, H., R. A. Bradshaw, and R. Arnon, Structure-Function Relationships of Proteolytic Enzymes, Ed. by P. Desneulle, H. Neurath, and M. Ottesen, Academic Press, New York (1970).

111. Nilsson, H., R. Mosbach, and K. Mosbach, Biochim. Biophys. Acta, 268, 253 (1972).

112. O'Driscoll, K. F., M. Izu, and R. Korus, Biotech. Bioeng., 14 (5), 847 (1972).

113. Ong, E. B., Y. Tsang, and G. E. Perlman, J. Biol. Chem., 241 (23), 5661 (1966).

114. O'Sullivan, D. G., J. Theor. Biol., 2, 117 (1962).

115. Poznansky, M. J., and T. M. S. Chang, Proc. Can. Fed. Biol. Soc., 12, 54 (1969).

116. Rashevsky, N., Mathematical Biophysics: Physico-Mathematical Foundations of Biology, Volume One, Dover Publications, New York (1960).

117. Rhoads, D. G., and M. Pring, J. Theoret. Biol., 20, 297 (1968).

118. Rick, W., in Methods of Enzymatic Analysis, Ed. by H. U. Bergmeyer, Academic Press (1965), 807.

119. Riedel, A., and E. Wünsch, Hoppe-Seyler Z. Physiol. Chem., 316, 61 (1959).

120. Rony, P. R., Biotech. Bioeng., 13, 431 (1971).

121. Ross, L. W., and D. M. Updegraff, Biotech. Bioeng., 13 (1), 99 (1971).

122. Satterfield, C. N., Mass Transfer In Heterogeneous Catalysis, MIT Press, Cambridge, Massachusetts (1970).

123. Schwert, G. W., and M. A. Eisenberg, J. Biol. Chem., 179, 665 (1949).

124. Schwert, G. W., and Y. Takenaka, Biochim. Biophys. Acta, 16, 570 (1955).

125. Selegny, E., G. Brown, and D. Thomas, Physiol. Vég., 9 (1), 25 (1971).

126. Seinfeld, J. H., I & EC, 62 (1), 32 (1970).

127. Shigeri, Y., and T. Kondo, Chem. Pharm. Bull. (Tokyo), 17, 1073 (1969).

128. Shuler, M. L., R. Aris, and H. M. Tsuchiya, J. Theor. Biol., 35, 67 (1972).

129. Sparks, R. E., R. M. Salemme, P. M. Meier, M. H. Litt, and O. Lindan, Trans-Amer. Soc. Artif. Intern. Organs., 15, 353 (1969).

130. Sundaram, P. V., E. K. Pye, T. M. S. Chang, V. H. Edwards, A. E. Humphrey, N. O. Kaplan, E. Katchalski, Y. Levin, M. D. Lilly, G. Manecke, K. Mosbach, A. Patchornik, J. Porath, H. W. Weetall, and L. B. Wingard, Jr., Biotech. Bioeng. Symp. No. 3, 15 (1972).

131. Sundaram, P. V., A. Tweedale, and K. J. Laidler, Can. J. Chem., 48, 1498 (1970).

132. Surinov, B. P., and S. E. Manoilov, Biokhimiya, 31, 387 (1966).

133. Suzuki, S., T. Kondo, and S. G. Mason, Chem. Pharm. Bull. (Tokyo), 16, 1629 (1968).

134. Takahashi, K., M. Koishi, and T. Kondo, Can. J. Chem., 48, 3520 (1970).

135. Takami, T., and T. Ando, Seikagaku, 40, 749 (1968).

136. Taylor, J. B., and H. E. Swaisgood, Biochim. Biophys. Acta, 278, 666 (1972).

137. Trowbridge, C. W., A. Krehbiel, and M. Laskowski, Jr., Biochemistry, 2, 843 (1963).

138. Wagner, T., C. J. Hsu, and G. Kelleher, Biochem. J., 108, 892 (1968).

139. Walsh, K. A., L. L. Houston, and R. A. Kenner, in Structure-Function Relationships of Proteolytic Enzymes, Ed. by P. Desneulle, H. Neurath, and M. Ottesen, Academic Press, New York (1970).

140. Webster's New Collegiate Dictionary, G. & C. Merriam Co., Publishers, Springfield, Mass. (1953).

141. Weetall, H. H., Science, 166, 615 (1969).

142. Weetall, H. H., Biochim. Biophys. Acta, 212, 1 (1970).

143. Wei, J., I & EC, 58 (9), 38 (1966).

144. Wieland, T., H. Determann, and K. Buennig, Z. Naturfursch, B21, 1003 (1966).

145. Wilde, D. J., and C. S. Beightler, Foundations of Optimization, Prentice-Hall (1967).

146. Wingard, L. B., Jr., Editor, Biotech. Bioeng. Symp. No. 3, J. Wiley & Sons, New York (1972).

147. Wiseman, A., and B. Gould, New Scientist, 11 April, 1968, 66.

148. Wittbecker, L. L., and P. W. Morgen, J. Polymer Sci., 40, 289 (1959).

149. Worthington Manual, Worthington Biochemical Corporation, "Enzymes and Enzyme Reagents" (E. C. 3. 4. 4. 4), 1967.